Analysis of Surface Ozone Measurements at Cape Point, SANAE and City of Cape Town

By

Thumeka Mkololo

School of Agricultural, Earth and Environmental Sciences

University of KwaZulu-Natal Durban

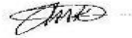Dissertation submitted to the College of Science and Agriculture

For the degree of Master of Science

2013

Declaration

I declare that this dissertation is my own work to fulfill the requirements of a Master of Science degree at the University of KwaZulu-Natal under the supervision of Dr Lisa Frost Ramsay. All people's opinions and work has been referenced and acknowledged.

This work has not been submitted for any degree or examination at any other University.

……………………………………………

(Thumeka Mkololo, student)

……29th…day of…November…2013

……………………………………………

(Lisa Frost Ramsay, supervisor)

…………….day of……………….2013

Acknowledgements

Abstract

This study presents an investigation of surface ozone (O_3) at SANAE (2002 to 2009), Cape Point (1997 to 2009), Molteno (1997 to 2007) and Goodwood (2000 to 2006). The Cape Point data was statistically separated to background and non-background (anthropogenic) contributions. The main aim of the study was to investigate diurnal cycles, seasonal cycles, the weekend effect, and any long term trends in surface O_3, as well as assess meteorological controls on surface O_3 at these stations.

The observed O_3 concentrations were higher during the day than at night at all stations, with urban stations (Molteno and Goodwood) showing more pronounced peak-to-peak variations relative to the marine stations (SANAE and Cape Point). The 'weekend effect' was evident at Molteno and Goodwood with higher O_3 and lower NO_x concentrations on 'weekends relative to weekdays. The weekend effect on O_3 was more pronounced in winter at Goodwood and Molteno. Maximum monthly average concentrations were observed in spring at Goodwood and Molteno, with minimum in winter. The SANAE and Cape Point background O_3 maxima were observed in winter (June to August) with minima in summer (January to February). The Cape Point non-background O_3 maximum was observed in September with a minimum in summer (January). The seasonal cycles at marine sites appear to be driven by O_3 photolysis.

Wind speeds played a critical role in O_3 concentrations, particularly in the continental environment. At Goodwood, high NO_x levels are associated with low wind speeds. At SANAE, no significant O_3 differences were observed between low wind speeds and high wind speeds while at Cape Point, differences were more evident during the winter months. A decreasing O_3 trend in monthly averages was observed from 1997 to 2006 at Molteno while Goodwood demonstrated an increase of O_3 monthly averages with decreasing NO_x monthly averages from 2000 to 2006.

Table of contents

CHAPTER 5

List of plates

List of figures

List of tables

Acronyms and Abbreviations

BG	Background
CH_4	Methane
CO	Carbon monoxide
CO_2	Carbon dioxide
CSIR	Council of Scientific and Industrial Research
EPA	Environmental Protection Agency
$IFB-NO_x$	NO_x from industrial activities (I), fossil fuel combustion (F) and biofuel combustion (B)
LSCE	*Laboratoire des Sciences du Climat et 'Environnement*
MSA	Monosodium acetate
NH_3	Ammonia
NO_2	Nitrogen peroxide
NO_3	Nitrate
NOAA	National Oceanic and Atmospheric Administration
Non-BG	Non-background
NO_x	Oxides of nitrogen
N_2O_5	Dinitrogen pentaoxide
O_3	Ozone
PAN	Peroxyacetyl nitrate
RHUL	Royal Holloway University of London
SANAE	South African National Antarctic Expedition
SAWS	South African Weather Service
SO_2	Sulfur dioxide
SO_x	Oxides of sulfur
UEA	University of East Anglia
VOCs	Volatile organic compounds
WCC	World Calibration Centre

CHAPTER 1

1.1 Introduction

Understanding the physical and chemical dynamics of ozone (O_3) in the troposphere is an important research priority in the context of air pollution and global warming concerns. Surface O_3 is a secondary pollutant which is formed through reactions between oxides of nitrogen (NO_x) such as nitric oxide (NO) and nitrogen dioxide (NO_2), and volatile organic compounds (VOC), including methane, toluene and benzene, in the presence of sunlight. Surface O_3 concentrations have increased in the past century in many urban centres, particularly in the Northern Hemisphere, and O_3 currently is regarded as the third most important contributor to global warming after carbon dioxide (CO_2) and methane (CH_4) due to human development (Intergovernmental Panel on Climate Change (IPCC), 2001). Although O_3 data from the nineteenth century are limited, results suggest that pre-industrial ground level O_3 concentrations were less than 10 ppb (Volz and Kley 1988). According to Vingarzan (2004), present annual average background O_3 concentrations in the mid-latitudes of the Northern Hemisphere range between 20 and 45 ppb, while values range between 23 to 34 ppb at Canadian background stations. In 2008 (Figure 1.1), O_3 annual average concentrations in the Northern Hemisphere varied between 20 to 48 ppb, while in the Southern Hemisphere, values varied between 20.0 to 36.0 ppb (Figure 1.1). According to Ashmore (2005) surface O_3 concentrations are steadily increasing and O_3 is now considered to be the most significant air pollutant affecting vegetation.
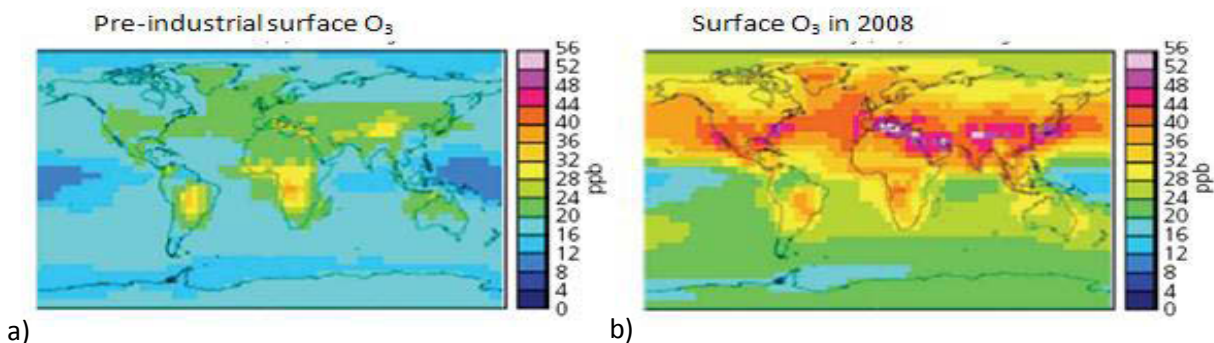
Figure 1.1: (a) Modeled global changes in surface O_3 concentrations between pre-industrial times and (b) surface O_3 in 2008 (Science Policy Report, 2008).

There are two main approaches to understanding surface O_3 increases, namely trend analysis based on long term data, and climatological analysis of long range transport and transformation (Pochanart *et al*, 1999). This study incorporates both approaches to understanding O_3 concentrations measured at SANAE, Cape Point, Molteno and Goodwood, and their relationship with precursor emissions of NO_x and VOCs. This chapter presents the study's aims and objectives, followed by a description of the study sites. Chapter 2 commences with O_3 chemistry in the troposphere, followed by a review of previous studies conducted at the four stations. Chapter 3 describes the measurement techniques at the four stations, data verification, and the filtering method use to separate Cape Point data into background and non-background datasets. The types of data analysis and statistical approaches are also described in this chapter. Chapter 4 presents the study's results and a discussion of diurnal cycles, seasonal cycles, and the influence of meteorology on O_3 concentrations and a description of long term trends. Chapter 5 commences with a summary of the study, followed by conclusion and recommendations.

1.2 Study motivation

The Cape Point station is primarily exposed to air from the South Atlantic Ocean, which provides background concentrations of trace gases as measured at the station. 'Background' refers to air masses arriving at the station without pollutants arising from anthropogenic activities. The Cape Point station, however, also receives polluted air, especially from the Cape Town urban region (Brunke and Scheel, 1998). These air masses contain pollutants from anthropogenic activities and are thus described as 'non-background air'. Such pollution episodes usually last only for a few hours and are easily recognized by simultaneous peaks in carbon monoxide (CO), methane (CH_4) and radon (Rn) concentrations. Non-background pollutant concentrations measured at Cape Point's three intakes (4m, 14m and 30m) from March 2009 until September 2009 previously were analyzed by Brunke *et al.* (2009). Results indicated a significant difference of up to 60 ppb between measurements at these three heights during polluted episodes, while differences between background measurements were as low as 5.0 ppb.

The major focus of the World Meteorological Organization Global Atmosphere Watch (WMO_GAW) is trace gas measurements in clean, background air for the assessment of long-term trends. There is little analysis conducted on non-background data. The analysis of air

derived from the north of Cape Point has received some attention from South African Weather Service (SAWS) but constitutes a largely untapped reservoir of information. The current study provides an excellent opportunity to compare background and non-background air sampled at the three ozone intakes, and to determine whether the diurnal and seasonal cycles affecting background and non-background air differ between sites, and if so, to determine possible reasons for their differences.

1.3 Aims of the study

The primary goals of this study are to analyze surface O_3 from four stations (Cape Point, SANAE, Goodwood and Molteno) and investigate meteorological controls that lead to either enhancement or decreases in tropospheric ozone concentrations at these sites. The study aims to also identify any temporal trends, including diurnal or seasonal variations, at the various sites, and any differences in these patterns between sites.

This study utilizes data from:
- the 30 m Cape Point monitor (1997 to 2009);
- the 4 m Cape Point monitor (1997 to 2009);
- the 14 m Cape Point monitor (2008);
- the City of Cape Town's Molteno (1997 to 2007) and Goodwood (2000 to 2006) monitoring stations;
- SANAE in Antarctica (2002 to 2009).

The study objectives include the following:
1) To develop and compare the background and non-background O_3 concentration roses for Cape Point, the City of Cape Town stations and SANAE;
2) To analyse the temperature, atmospheric pressure, wind speed and wind direction for both background and non-background air masses;
3) To compare the seasonal and diurnal fluctuations of O_3 in the three air intakes at Cape Point (background and non-background), SANAE and the City of Cape Town stations and correlate with ozone concentrations at the study sites;

4) To assess any 'weekend effect' in O_3 measurements at Cape Point, SANAE, and City of Cape Town over the periods of available data.

1.4 Study area

The City of Cape Town is situated to the north of the Cape Peninsular, which lies between the Indian and Atlantic Oceans and ends at Cape Point. Table Mountain (three kilometers from side to side) forms the background to the City.

The Western Cape region is one of the six regions in the world (and the only one in Africa) with a Mediterranean climate (http://www.grabovrat.com). These regions lie between 30° and 45° of latitude (Figure 1.2). Mainly in winter (June to August), but also in late autumn and early spring, well-developed cold fronts move from the Atlantic Ocean towards the Cape coast, bringing heavy precipitation and strong north-westerly winds to the Peninsula. The winter months are cool and wet, with an average minimum temperature of 7.0°C and maximum of 17.5°C. Most of the city's annual rainfall occurs in winter. Due to the mountainous topography of the city, rainfall levels between sites can vary significantly (Wichmann, 2006). During spring, average temperatures range between 20 and 25**°C**. Spring (September to November) is associated with intermittent rainfall episodes (usually associated with the persistence of cold fronts) and mild temperatures. The summer months (December to February) are warm and dry. The Peninsula experiences a strong wind from the south-east, known locally as the Cape Doctor because it dissipates pollution episodes and cleans local air. This south-easterly wind is caused by a high-pressure system that lies over the South Atlantic to the west of Cape Town, known as the South Atlantic High (Kruger *et al*., 2010). Summer temperatures are mild, with an average daily maximum of 28 °C (Wichmann, 2006). During the autumn months (March to May), temperatures are mild with highs averaging in the mid-twenties.
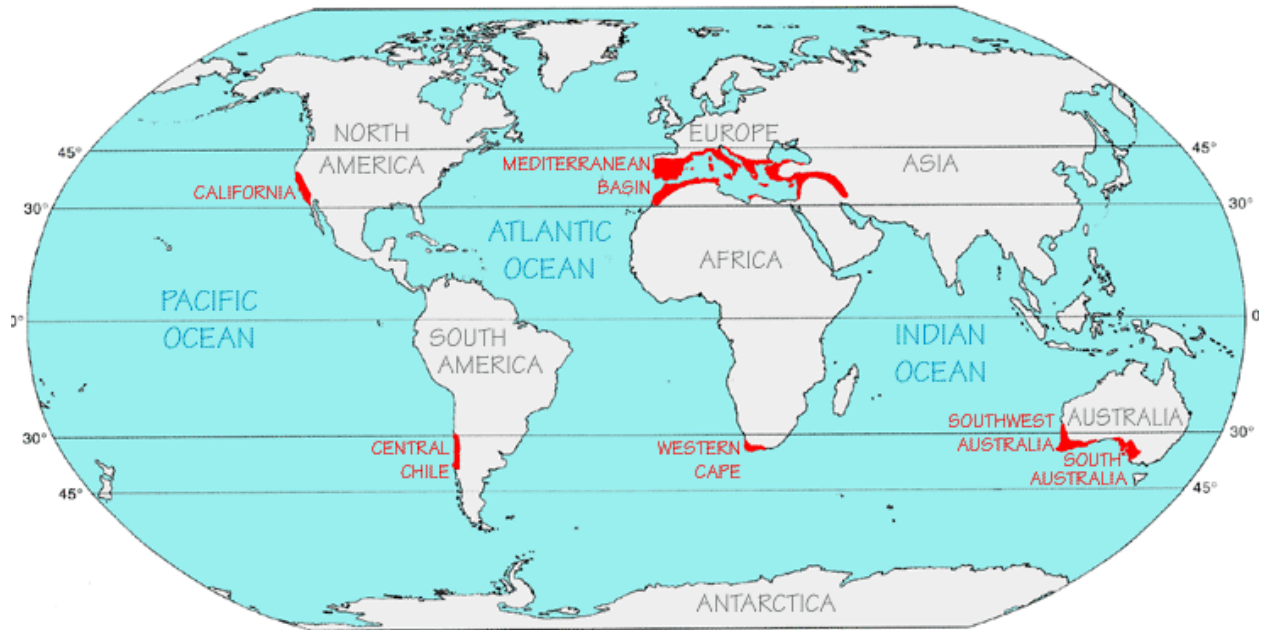
Figure 1.2: Map of the world showing areas with Mediterranean climate in red (http://www.grabovrat.com).

The City of Cape Town's main polluters include:

- traffic, emitting hydrocarbons, CO, NO$_x$, SO$_2$ and particulates; and
- Caltex Refining in Table View, emitting hydrocarbons, SO$_x$ NH$_3$, aldehydes, NO$_x$, cyanides, CO, and particulates;
- domestic fuel burning within townships and informal settlements, with the main pollutants released including CO, NO$_2$, SO$_2$, particulates and polycyclic aromatic hydrocarbons;
- Consol Glass in Bellville, emitting mainly particulates, SO$_X$ and NO$_X$;
- the airport, emitting hydrocarbons, CO, NO$_x$, SO$_2$ and particulates during airport operations, vehicle traffic, aircraft operation and maintenance, and on-site fuel storage facilities (Walton, 2005).

1.4.4 SANAE IV station

SANAE is located 851 m above sea level at 71° 40' 42" S, 2° 49' 44" W. The station is built on solid rock, 170 km inland from the Weddell Sea (Plate 1). Winds blow predominantly from the north-east, east and south-east (Labuschagne *et al.,* 2003).

Temperatures in winter are close to -50˚C and the sun is not observable for more than three months of the year. In 2004, SANAE was one of the 43 stations operating south of 60°S (Figure 1.3) and one of the 60 Antarctic stations. In April 2012, the number of Antarctic stations increased to 101 worldwide (http://www.scar.org).There are four research programs associated with SANAE: Physical Sciences, Earth Sciences, Life Sciences and Oceanographic Sciences. Due to severe weather conditions, only the Physical Science program extends all year round at SANAE IV. The other programs are conducted during summer period when the weather permits fieldwork and the sea ice level is at its minimum (http://www.sanap.org.za).

Plate 1: Outside view of SANAE station (http://www.sanap.org.za).
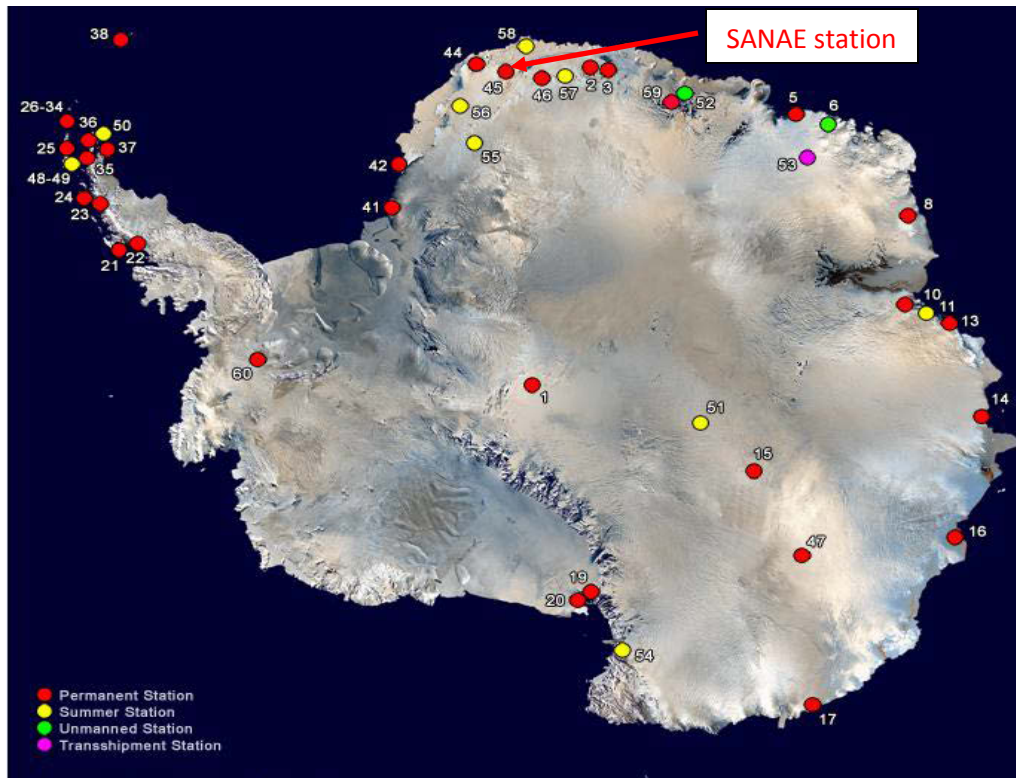
Figure 1.3: location of SANAE IV station in Antarctica (purple arrow) and other stations operating in South of 60° S (www.ecophotoexplorers.com). Red, yellow, green and pink dots indicates permanent, summer, unmanned and transshipment stations respectively.

1.4.2 Molteno and Goodwood

The City of Cape Town monitors air quality at 14 stations (Figure 1.4), measuring particulates (PM$_{10}$ directly), nitrogen dioxide (NO$_2$), sulphur dioxide (SO$_2$), carbon monoxide (CO) and ozone (O$_3$). Ozone measurements commenced in 1992 at Molteno. The City of Cape Town uses instrument caravans for monitoring (Plate 2). The Molteno station is located in Cape Town's city centre at approximately 31º 22' S 26° 22' E. The city bowl is bordered on three sides by mountains, which promotes the accumulation of pollutants throughout the year (Wichmann, 2006).

Figure 1.4: City of Cape Town monitoring stations (http://web1.capetown.gov.za).

Plate 2: Outside view of City of Cape Town monitoring station (City of Cape Town quality monitoring group).

The Goodwood monitoring station is located in a residential area between the southern and the northern suburbs of Cape Town at 33° 55' S, 18° 22' E. It is situated 10 km away from the city centre. The station was located to measure industrial emissions (Wichmann, 2006).

1.4.3 Cape Point

The Cape Point Global Atmosphere Watch (GAW) station, managed and maintained by SAWS, is located on the Cape Peninsula in the South African National Parks (SANParks) nature reserve (34° 35' S; 18° 48' E), which is about 58 km south of the City of Cape Town (Plate 3). The station is located on the top of a cliff (Plate 4). This station provides a record of more than 30 years (beginning 1978) of chlorofluorocarbons [Freon -11 (CF-11)] and CO. Monitoring has expanded over the years and currently includes measurements of carbon dioxide (CO_2), methane (CH_4), ozone (O_3), nitrous oxide (N_2O), sulphur dioxide (SO_2), total gas mercury (TGM) and further chlorofluorocarbons (including Freon-12, Freon-113, methyl chloroform and carbon tetrachloride). In addition, radon (Rn) is measured and used as a tracer for distinguishing background and non-background air masses. Meteorological parameters such as humidity, pressure, temperature, wind direction and wind speed also are measured at the site.

Plate 3: Cape Point GAW station (Courtesy of SAWS).
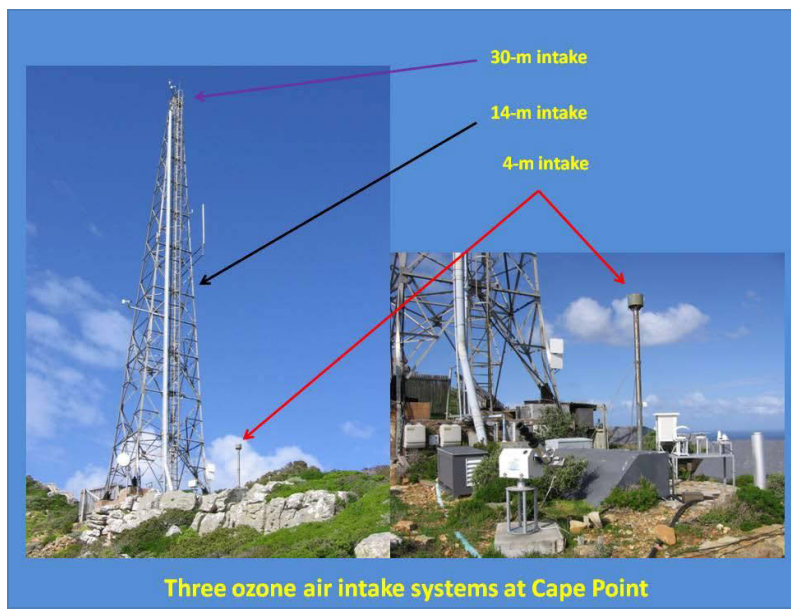
Plate 4: Cape Point GAW station location and three O_3 air intakes (Cape Point GAW station) (Courtesy of SAWS).

Sampling collaborators at the station have included the University of East Anglia (UEA)**,** National Oceanic and Atmospheric Administration (NOAA), Royal University of Holloway (RHUL) and *Laboratoire des Sciences du Climat et 'Environnement* (LSCE). Flask samples are only taken under background conditions and sent back to the respective institutes for analyses. Passive samplers belonging to North West University measure O_3, SO_2, nitrogen dioxide (NO_2) and ammonia (NH_3). Rain water samples are collected for CSIR and the University of North West. Particulate matter sampling has been conducted at Cape Point with filters sent to France for analysis of acetate, propionate, formate, monosodium acetate (MSA), chloride, nitrate, glutarate, succinate, sulphate, oxalate, phosphate, sodium, ammonium, potassium, magnesium and calcium.

1.5 Conclusion

SANAE and Cape Point stations are located far from the anthropogenic activities compared to urban stations (Molteno and Goodwood) which are likely to be affected by human activities. Although background stations are not more affected by anthropogenic emissions, such emissions can be transported from non-background sites to background sites. The available data from SANAE, Cape Point, Molteno and Goodwood will give a better understanding of O_3 in both background and non-background stations.

CHAPTER 2

(Theoretical Framework)

2.1 Introduction

This chapter presents current understandings of ozone chemistry in the troposphere, ozone sources and sinks and the environmental impacts of high ambient ozone concentrations. A review is also conducted of previous studies on diurnal and seasonal cycles, the weekend effect, long-term trends and the effect of meteorology on ambient ozone levels.

2.2 An Introduction to Ozone Chemistry

Prior to the 1940s, stratospheric O_3 was the only known source of tropospheric O_3. Haagen-Smit (1952) suggested that the photochemical smog in the Los Angeles area contained O_3 concentrations that were too high to originate entirely from stratospheric O_3. Since then, further investigations have revealed that O_3 in the troposphere can be caused either by transportation of O_3-rich air from the stratosphere to the troposphere or from photochemical reactions involving O_3 precursors in the troposphere. The chemical formation of O_3 depends on ultraviolet (UV) radiation and O_3 precursors. In 1930, Chapman proposed the photochemical reaction below for O_3 formation.

$$O + O_2 + M \longrightarrow O_3 + M \tag{1}$$

Where M represents any other molecule (usually N_2 or O_2 since these two molecules constitute 99% of the volume of air).

Atomic oxygen is naturally produced when molecular oxygen absorbs UV at wavelengths below 242 nm (Reaction 2), where hν represents ultraviolet radiation. Reaction 2 below shows the photolysis of O_2 molecule by ultraviolet radiation to two oxygen (O) atoms. These O atoms react simultaneously with O_2 molecules to form O_3 molecules (Reactions 3 and 4).

$$O_2 + h\nu \longrightarrow O + O \tag{2}$$
$$O + O_2 \longrightarrow O_3 \tag{3}$$
$$O + O_2 \longrightarrow O_3 \tag{4}$$
Net reaction: $3O_2 + h\nu \longrightarrow 2O_3$ (Chapman, 1930) $\tag{5}$
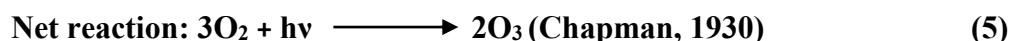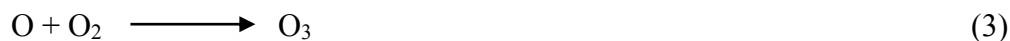
An increase in solar radiation with higher concentrations of NO_2 and VOCs, encourages the formation of O_3 (Seinfeld and Pandis, 1998). Tropospheric O_3 production increases in urban environments due to anthropogenic activities that emit NO_x, CO, and VOCs, which are important O_3 precursors. The ratio of VOCs to NO_x is high in NO_x sensitive environment whereas the VOC to NO_x ratio is low in VOC sensitive environments. Ozone production will increase with increasing VOCs in VOC sensitive environments and decrease with increasing NO_x (Sillman, 1999).

Wavelengths below 310 nm destroy O_3 in the atmosphere, forming an O_2 molecule and O atom (Reaction 6 below). Subsequently the O atom formed reacts with water vapour to form two OH radicals (Levy, 1971).

$$O_3 + h\nu \longrightarrow O_2 + O \qquad\qquad (6)$$
$$O + H_2O \longrightarrow 2OH \qquad\qquad (7)$$

Ozone chemistry at polar sites has been reported to be more complicated (Helmig *et al.*, 2007). Unique photochemical processes at the surface and boundary layer have been reported by Bottenheim *et al.* (1986) and Barrie *et al.* (1988). As a result of these processes, O_3 depletion events (in the range of 20 ppbv/day to 40 ppbv/day) occur during spring time as reported for Barrow in Alaska, Alert in USA, and Neumayer in Antarctica (Kaleschle *et al.*, 2005). On average, however, surface O_3 lifetimes are approximately 100 days in polar regions, which is significantly longer than the average one to two weeks in summer and one to two months during winter in other environments (Liu and Ridley, 1999). The longer lifetime in polar regions is due to weak ozone sinks, low water vapor and low solar radiation. Although lifetimes are generally shorter outside of the polar regions, there is still sufficient time for ambient ozone produced in one polluted region to be transported to another within its lifetime. This can even occur at the scale of continents (Akimoto, 2003). This phenomenon is more likely to occur during winter months when O_3 has a longer lifetime in the atmosphere.

As previously described in this study, there have been significant increases in O_3 concentrations since the commencement of heavy industrial activity. The Intergovernmental Panel on Climate Change (IPCC 2001, 2007) reported a global average radiative forcing of 0.35 W/m^2 in 2005 due to tropospheric O_3. The observed positive radiative forcing was comparable to that of halocarbons, higher than N_2O and lower than CH_4 and CO_2 (Figure 2.1).
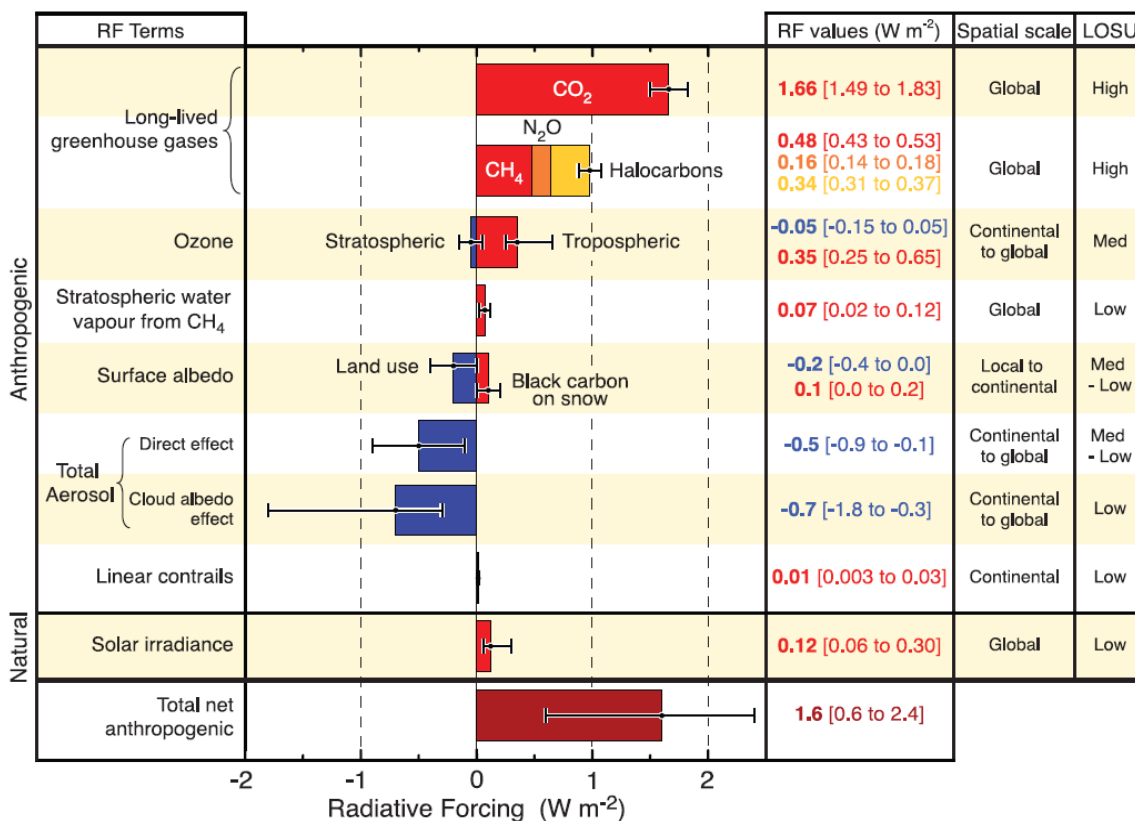
Figure 2.1: Global average radiative forcing in 2005 (IPCC, 2007).

2.3 Sources of Tropospheric O_3

Tropospheric ozone (O_3) levels are controlled by chemical and physical processes, and its precursors originate from both natural and anthropogenic activities. It is a secondary pollutant formed through the reactions of nitrogen oxides (NO_x), volatile organic compounds (VOCs), methane (CH_4), and carbon monoxide (CO) in the presence of sunlight (Seinfeld and Pandis 1998) or through the transportation of O_3-rich air from the stratosphere to the troposphere. Figure 2.2 shows tropospheric O_3 sources according to geographic location. As evident from the diagram, O_3 in the mid-latitudes is strongly influenced by anthropogenic activities (e.g. urban

pollution and biomass burning). In the tropics, NO_x generated during lightning plays an important role in O_3 formation whereas in Arctic and Antarctic regions, snowpack plays a critical role in O_3 formation by releasing NO from the photolysis of nitrate (NO_3^-). Cotter *et al.* (2003) observed that NO_3^- has a strong absorption of ultraviolet light (260-330 nm) and the concentrations of NO_x above the ice surface strong correlates with ultraviolet B-band (UVB; 275-320 nm). At the Neumayer station (Antarctica), high NO concentrations were observed in summer and autumn. The occurrence of the annual maximum strongly correlates with maxima in UVB radiation (Weller *et al.*, 2002). A detailed discussion on the sources of tropospheric O_3 is presented in the following sections.
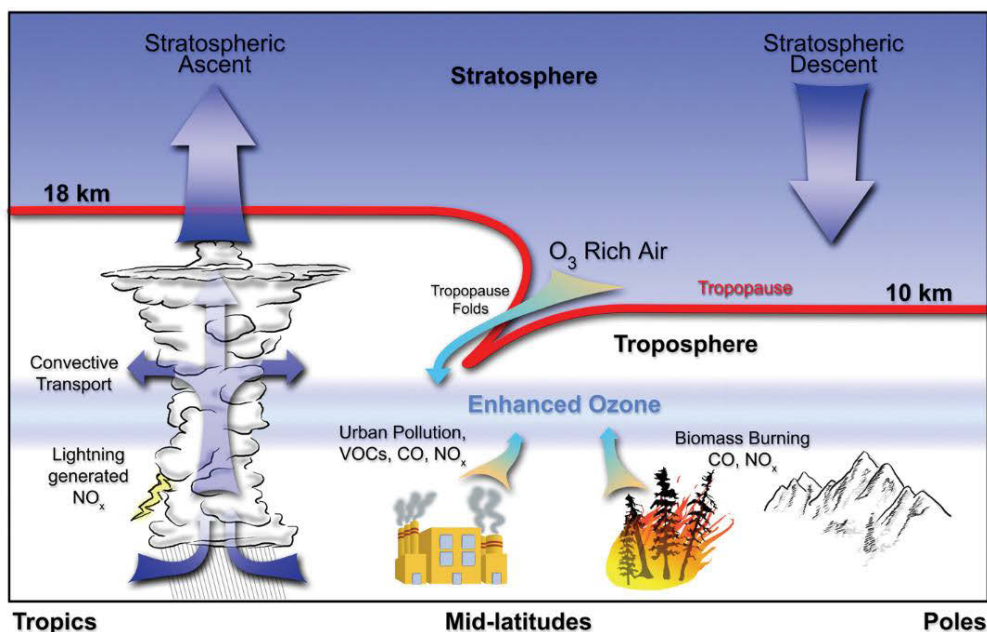
Figure 2.2: Sources of tropospheric O_3 (www.earthobservatory.nasa.gov).

2.3.1 Stratospheric/Tropospheric O₃ Exchange

Although the focus of the current study is on tropospheric O_3, the influence of stratospheric O_3 cannot be ignored and is briefly discussed here. Stratosphere-troposphere exchange is associated with jet streams and tropopause folds (Newell, 1963; Danielsen, 1968) and large-scale overturning of the stratosphere (Brewer, 1949; Holton *et al.*, 1995). Early studies reported two near tropopause jet streams: the subtropical jet streams found at the pole ward edge of the Hardley circulation and polar jet streams found above the polar front zone (Holton, 1992; Bluestein, 1993). Figure 2.3 shows the location of these jet streams in the atmosphere. It is well

known that stratospheric intrusion events can be identified by a rapid decrease of relative humidity and an increase in O_3 concentrations (Cui *et al.*, 2009). Brioude *et al.* (2006) highlighted the importance of understanding these physical transport processes to contextualise any investigation of the chemistry of trace gases.
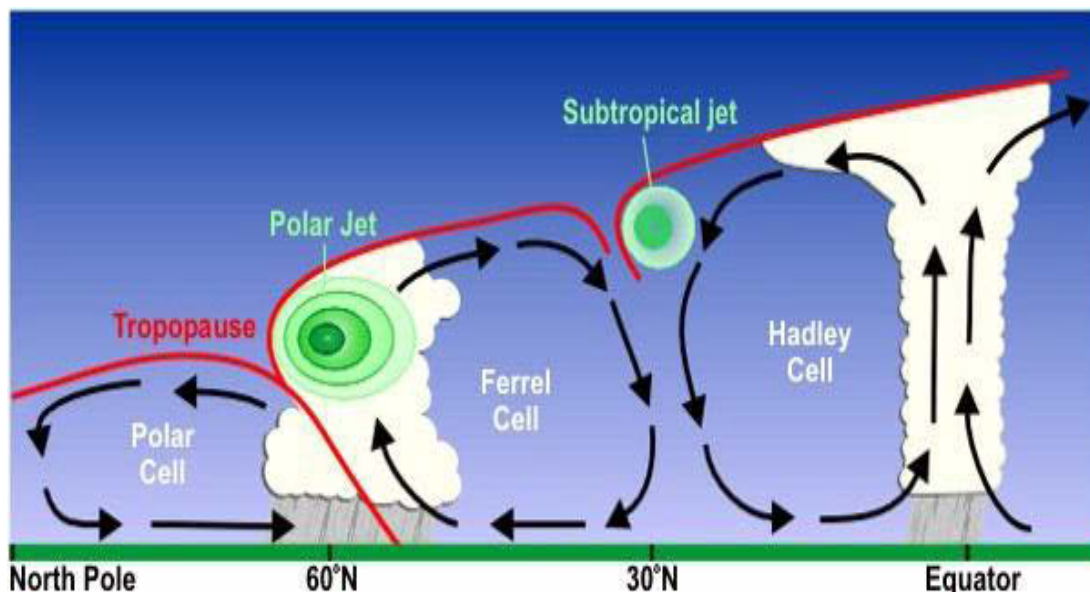
Figure 2.3: Location of jet streams (http://www.srh.noaa.gov).

2.3.2 The Influence of Methane

Tropospheric O_3 is a precursor of the hydroxyl radical (OH) (Reactions 6 and 7 in Section 2.1 above), which controls the chemical composition of the atmosphere through methane (CH_4) and carbon monoxide (CO) reactions (Finnan *et al.*, 1997). Moreover, the hydroxyl radical is known as the major sink of CH_4 and NO_x, with increases in CH_4 concentrations associated with reductions in OH. According to Wild *et al.* (2001) and West *et al.* (2007), increasing CH_4 concentrations cause a long term increase in O_3 concentrations. On the other hand, reductions in global CO emissions cause an increase in OH which causes a reduction in CH_4 concentrations, leading to a long term decrease in O_3.

Sources of atmospheric CH_4 include wetlands, ruminants, energy, rice agriculture, landfills, wastewater, biomass burning, oceans, and termites (Fiore *et al.*, 2008). Anthropogenic emissions are estimated to contribute at least 60% to total CH_4 emissions, with individual studies reporting a range of 500 to 610 Tg^{-1} for total CH_4 emissions (Fiore *et al.*, 2008). Depending on the

availability of NO concentrations, CH_4 oxidation produces O_3 via reactions of peroxy radicals with NO_x. The formation of O_3 from CH_4 involves a sequence of nine reactions which is the longest chain of all the O_3 precursors. These reactions were proposed by Crutzen (1973, 1974):
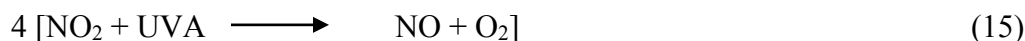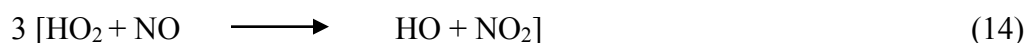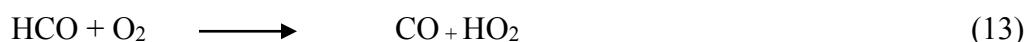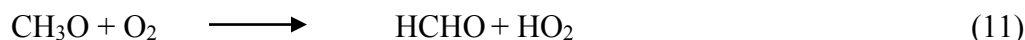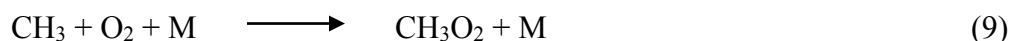
$$OH + CH_4 \longrightarrow H_2O + CH_3 \tag{8}$$

$$CH_3 + O_2 + M \longrightarrow CH_3O_2 + M \tag{9}$$

$$CH_3O_2 + NO \longrightarrow CH_3O + NO_2 \tag{10}$$

$$CH_3O + O_2 \longrightarrow HCHO + HO_2 \tag{11}$$

$$HCHO + UVB \longrightarrow HCO + H \tag{12}$$

$$HCO + O_2 \longrightarrow CO + HO_2 \tag{13}$$

$$3\,[HO_2 + NO \longrightarrow HO + NO_2] \tag{14}$$

$$4\,[NO_2 + UVA \longrightarrow NO + O_2] \tag{15}$$

$$3\,[O + O_2 \longrightarrow O_3] \tag{16}$$

$$\textbf{Net: } CH_4 + 8O_2 + 5\ photons \longrightarrow CO + 4O_3 + 2OH + H_2O \tag{17}$$

Where M represents any other molecule (usually N_2 or O_2 since these two molecules constitute 99% of the volume of air).

2.3.3 The Influence of Volatile Organic Compounds and Carbon Monoxide

Volatile organic compounds (VOCs) are emitted naturally in biogenic processes by vegetation (e.g. pinene and terpene), forest fires, animals and during anthropogenic activities e.g. use of vehicles and industrial processes (Lemieux *et al*., 2004; Buzcu *and Fraser*, 2006). The sequence of O_3 formation from VOCs is initiated by the reaction of a VOC or CO with the OH radical (Haagen-Smit, 1952). Reaction 18 shows the reaction of a VOC with OH and O_2 to form an organic molecule (RO_2) and H_2O. In the absence of VOCs, Reaction 19 takes place with CO reacting with OH and O_2 to form HO_2 and CO_2. These reactions are followed by either Reaction 20 or 21 depending on the availability of RO_2 and HO_2 from Reactions 18 and 19 respectively. In Reaction 22, the NO_2 formed from Reactions 20 or 21 undergoes photolysis to form NO and an O atom. The latter (O atom) is essential to complete O_3 formation through its reaction with an O_2 molecule (Reaction 23).
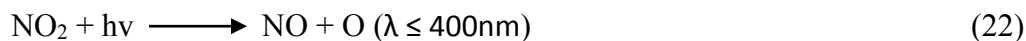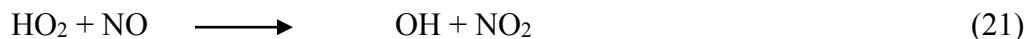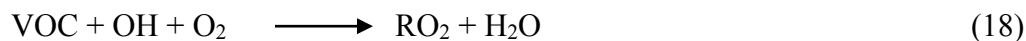
$$VOC + OH + O_2 \longrightarrow RO_2 + H_2O \qquad (18)$$

$$CO + OH + O_2 \longrightarrow HO_2 + CO_2 \qquad (19)$$

$$RO_2 + NO + O_2 \longrightarrow VOC \text{ (secondary)} + HO_2 + NO_2 \qquad (20)$$

$$HO_2 + NO \longrightarrow OH + NO_2 \qquad (21)$$

$$NO_2 + hv \longrightarrow NO + O \ (\lambda \leq 400nm) \qquad (22)$$

$$O + O_2 + M \longrightarrow O_3 + M \qquad (23)$$

Where M represents any other molecule (usually N_2 or O_2 since these two molecules constitute 99% of the volume of air).

RO_2 represents any organic molecule with O_2 attached:

$$C_3H_8 + OH \longrightarrow C_2H_7O_2 \qquad (24)$$

$$C_2H_7O_2 + NO \longrightarrow C_2H_5CHO \qquad (25)$$

These reactions depend on the availability of NO_x. At higher NO_x concentrations, the above reactions will occur (Reactions 21 to 23). These reactions occur at a faster rate (4000 times faster) relative to Reactions 26 to 28. At lower NO_x levels, the sequence of reactions below occurs (Reactions 26 to 28) resulting in the destruction of O_3 (Crutzen, 1973; 1974):

$$OH + CO \longrightarrow CO_2 + H \qquad (26)$$

$$H + O_2 + M \longrightarrow HO_2 + M \qquad (27)$$

$$HO_2 + O_3 \longrightarrow HO + NO_2 \qquad (28)$$

$$\textbf{Net: } CO + O_3 \longrightarrow CO_2 + O_2 \qquad \textbf{(29)}$$

2.3.4 The Influence of Nitrogen Oxides

Nitrogen oxides (NO_x) are produced in urban areas through man-made activities such as fossil fuel combustion and biomass burning (Martin *et al*., 2007; Labrador *et al*., 2005; Boersma *et al*., 2005). Nitrogen oxides also can be emitted naturally from soils, lightning strikes, forest fires started by lightning strikes and oxidation of atmospheric ammonia, NO_x is transported from the stratosphere to the troposphere and can be formed through anthropogenic activities involving complex photochemical reactions.

Reaction 30 below shows the photolysis of NO_2 by UV radiation at wavelengths between 300 nm and 400 nm to form nitric oxide (NO) and an O atom. Atomic oxygen reacts with an O_2 molecule to form an O_3 molecule (Reaction 31). Reaction 31 shows the formation of O_3 molecule whereas reaction 32 shows O_3 titration by NO in the absence of UV radiation (e.g. during night hours). Ozone titration is strong closer to NO-sources and dominates ozone formation and could be the reason why ozone concentrations are lower in the city than in rural areas (Lelieveld and Dentener, 2000). Therefore, NO_x can either generate or destroy O_3, depending on the levels of UV radiation.
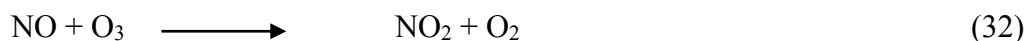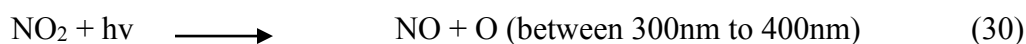
$$NO_2 + hv \longrightarrow NO + O \text{ (between 300nm to 400nm)} \quad (30)$$
$$O + O_2 + M \longrightarrow O_3 + M \quad (31)$$
$$NO + O_3 \longrightarrow NO_2 + O_2 \quad (32)$$

M represents any other molecule (usually N_2 or O_2 since these two molecules constitute 99% of the volume of air) and hv represents ultraviolet radiation.

Other important reactions for tropospheric O_3 chemistry include the formation of gaseous nitric acid (HNO_3) through the oxidation of NO_2 into nitrate (NO_3), dinitrogen pentaoxide (N_2O_5) is formed through the reaction of NO_2 and NO_3, later N_2O_5 reacts with water (H_2O) to form HNO_3. These reactions occur during the night in the absence of NO_x photolysis (Seinfeld and Pandis, 2006).
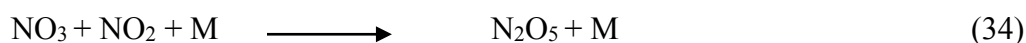
$$O_3 + NO_2 \longrightarrow NO_3 + O_2 \quad (33)$$
$$NO_3 + NO_2 + M \longrightarrow N_2O_5 + M \quad (34)$$
$$N_2O_5 (g) + H_2O (l) \longrightarrow 2HNO_3 (aq) \quad (35)$$

M represents any other molecule (usually N_2 or O_2 since these two molecules constitute 99% of the volume of air).

During the day, HNO_3 is formed directly from the reaction of NO_2 and OH. Reaction 36 below occur when VOC/NO_2 ratio is less than an average of 5.5 in urban areas (Seinfeld and Pandis, 2006).

$$NO_2 + OH + M \longrightarrow HNO_3 + M \qquad\qquad (36)$$

2.4 Sources of Ozone Precursors

2.4.1 Biogenic emissions

The role of biogenic emissions (from soil and vegetation) in tropospheric O_3 chemistry has been studied since the 1970s. In tropical regions, biogenic emissions are particularly important in O_3 chemistry (Aghedo *et al*., 2007). The most important biogenic emission for tropospheric ozone production is the direct emission of NO from recently wetted-soils. Ludwig *et al*. (2001) and Delon *et al*. (2009) reported that NO_x emissions are dependent on precipitation, history of soil type and temperature. Van der *et al*. (2008) used satellite data and reported summer maximum NO_x emissions in both Hemispheres. This maximum was not correlated with the release of NO_x from biomass burning events in winter. These researchers concluded that approximately 40% of surface NO_x in Africa is due to soil emissions.

2.4.2 Lightning

It is well well-known that lightning can lead to increase in NO_x concentrations in the middle and upper troposphere (Choi *et* al., 2005; Zhang *et al*., 2003). Lightning occurrence depends on geographic location with greater frequency in tropical areas relative to mid-latitudes and polar regions due to higher temperatures in the tropics. During the day the land surface is heated, causing convectional currents, cloud formation and potential lightning. These lightning strikes occur frequently in Central Africa (http://www.crh.noaa.gov). The effect of lightning on NO_x production had been extensively studied (e.g. Price *et al*., 1997; Pickering *et al*., 1998) and it has been revealed that NO_x production occurs during the high energy return stroke phase of the flash and about 75% to 95% of the produced NO_x is in the form of NO. Nitric oxide is produced through the Zel'dovich mechanism, which breaks down the N_2 and O_2 molecules (Price *et al*., 1997) at the high temperatures caused by the lightning stroke. Price *et al*. (1997) reported that the nature of clouds plays a critical role in NO formation with cloud to ground (CG) flashes

producing 6.7×10^{26} molecules of NO per flash whereas intracloud (IC) flashes produces 6.7×10^{25} molecules of NO per flash. Pickering *et al*. (1998) observed that clouds with larger volumes above freezing level have more IC flashes than CG flashes and that the ratio of IC/CG is higher in tropics than in the mid-latitudes.

Studies conducted by Tie *et al.* (2002) and Grewe *et al*. (2001) using the Goddard Institute for Space Studies (GISS) model show that lightning contributes about 16% (6.5 TgN/yr) of the total NO_x global budget whereas biomass burning and fossil fuel burning contribute about 70% of the NO_x global budget. These figures were collected from Global Emission Inventory Activity (GEIA) dataset (Benkovitz *et al*., 1996; Olivier *et al*., 1996). According to Martin *et al*. (2007); Labrador *et al*. (2005) and Boersma *et al*. (2005) global estimates of NO_x emissions from lightning vary between 1 to 20 TgN/yr, whereas 5±3 TgN/yr is applied for most modelling (Schumann and Huntrieser, 2007). In 2001 the Intergovernmental Panel on Climate (IPCC, 2001) highlighted the uncertainty on the estimates applied in models for NO_x emissions from lightning, stating that lightning produced NO_x ranges between 2-20 TgN/yr. A further study is required to reduce this uncertainty. Later, Shindell *et al*. (2003) used the NASA GISS global carbon model to study the effect of lightning produced NO_x on tropospheric O_3, and reported a global radiative forcing of 0.35 W/m^2 in June, July and August and 0.26 W/m^2 in December, January and February.

2.4.3 Biomass burning

Biomass burning impacts air quality and the carbon budget due to emissions of aerosols trace gases such as CO, hydrocarbons and NO_x (Andreae and Merlet, 2001; Crutzen and Andreae, 1990; Marufu *et al*., 2000; Thompson *et al*., 2001). These pollutants can be transported many thousands of kilometres downwind. Annual NO_x emissions of 20.9 TgN/yr were reported from biomass burning (Tie *et al.*, 2002 and Grewe *et al*., 2001). Africa has been reported as the continent emitting the largest quantity of biomass burning emissions (Figure 2.4). Several researchers (Andreae, 1991; van der Werf *et al*., 2003; van der Werf *et al.,* 2006) have reported that African fires are responsible for an average of 30 to 50% of the total amount of vegetation burned globally each year, making Africa, on average, the single largest biomass burning emissions source. Tropical countries are affected more by biomass burning compared to mid-latitudes and polar regions because of the greater abundance of vegetation combined with populations reliant of biomass for fuel. It has been estimated that approximately 85% of biomass

burning occurs in tropical countries (Andreae, 1991) and with increasing population the demand for land use is increasing. The main sources of biomass burning reported in previous studies (e.g. Delmas *et al*., 1999; Crutzen and Andreae, 1990) are man-made activities (such as forest clearest, savannah burning, restoration and land management). These sources of biomass burning are particularly evident during dry and hot season, (e.g. Thompson *et al*., 2000; Edwards *et al*., 2003; Jourdain *et al*., 2007) in late November to early March in Northern Hemisphere and July to October in the Southern Hemisphere. However, the frequency and intensity of fires is also dependent on meteorological and climatic conditions (Palacios-Orueta *et al*., 2004). Colour coding on the vertical axis in Figure 2.4 shows the global fire frequency for the period 2000 to 2009.
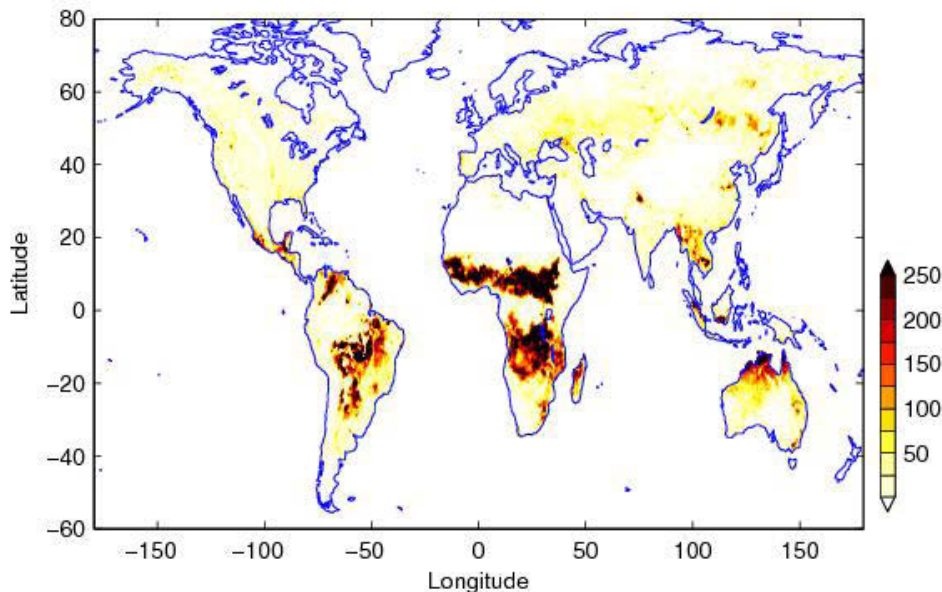
Figure 2.4: Average annual number of fires that occurs from 2000 to 2009 (http://www.gfdl.noaa.gov).

Figure 2.5 shows a biomass burning event that occurred in September 2008 in South Africa, Swaziland and Mozambique. Several studies on biomass burning have been conducted over a long period (e.g. Seiler and Crutzen, 1990; Hao and Liu, 1994) using statistical and inventory data. However these datasets were found to be incomplete and only available for a specific time period. An attempt was made to limit insufficient biomass burning data by starting satellite measurements e.g. Moderate Resolution Imaging Spectroradiometer (MODIS), Global Burned Area (GBA), Global Burn Scar Atlas (GLOBSCAR), Global Fire Emission Database (GFED

3.1) and Global Burn Scar Atlas Lund-Potsdam-Jena Global Dynamic Vegetation model (GLOBSCAR LPJ- DGVM) to improve the estimates of biomass burning emissions.

Seasonal cycles of O_3 can be affected by biomass burning. Zunckel *et al*. (2004) reported O_3 maxima in spring in Africa, and this maximum coincides with biomass burning period. In addition, another study on elevated O_3 events during spring over Johannesburg (Raghunandan *et al*., 2007), revealed the impacts of biomass burning, biogenic emissions and lightning precursors on ozone concentrations in this region.
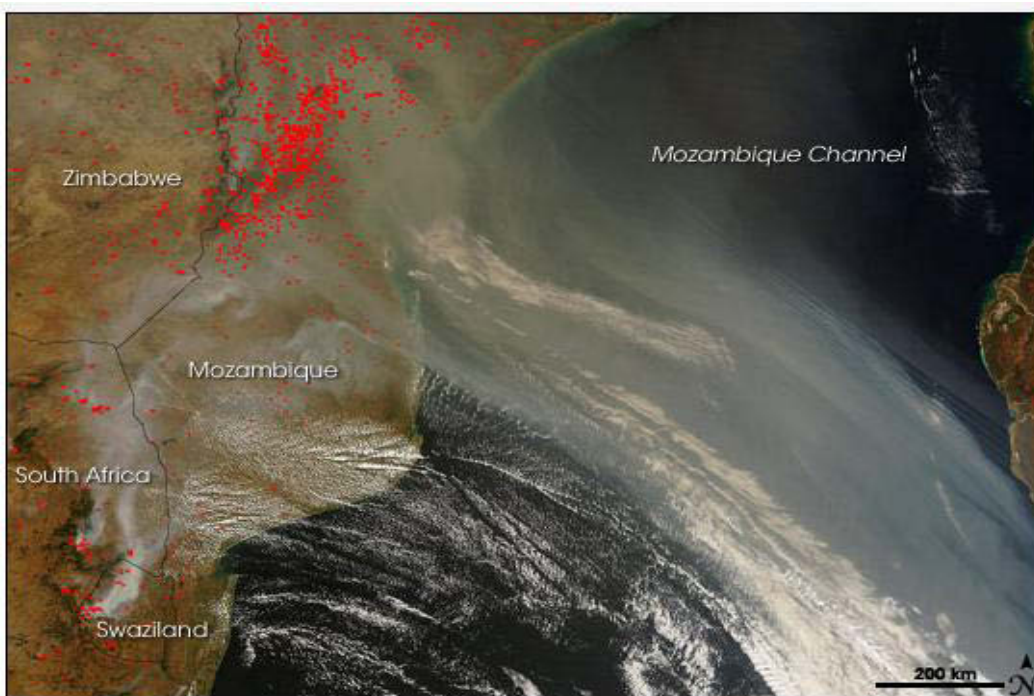
Figure 2.5: Fires burning in Mozambique, South Africa and Swaziland in September 2008 (www.earthobservatory.nasa.gov).

2.4.4 Industrial and Vehicular Emissions

Precursor gases involved in the photochemical O_3 production are at higher concentrations in urban areas due to high traffic (automobile emissions) and industrial activities (Baker *et al*., 2008; Bradley *et al*., 1999; Warneke *et al*., 2007). Fossil fuel combustion is higher in developed countries, notably in the Northern Hemisphere (e.g. Lilieveld and Dentener, 2000). The Southern Hemisphere is considerably less polluted than the Northern Hemisphere because of a lower average population density (Figure 2.6), lower levels of industrialisation and fewer land masses.

Although the sources of industrial emissions are lower in the Southern Hemisphere, they still have a significant influence on the levels of urban smog.

Figure 2.6 shows industrial activities (I), fossil fuels (F) and biofuel combustion (B) (collectively known as IFB-NO$_x$ emissions) for both Hemispheres. Population data used in Figure 2.6 was obtained from United States Central Intelligence Agency (The World Fact Book- CIA, (2007), while emission data was obtained from Olivier and Berdoski (2001). Biofuel burning provides about 15% of the world's primary energy (Bhattacharya and Salam, 2002), with 13% used in developing countries and the remaining 2% in developed and/or industrialized countries. The Southern Hemisphere has a greater proportion of developing countries compared to the Northern Hemisphere.

a)   b)
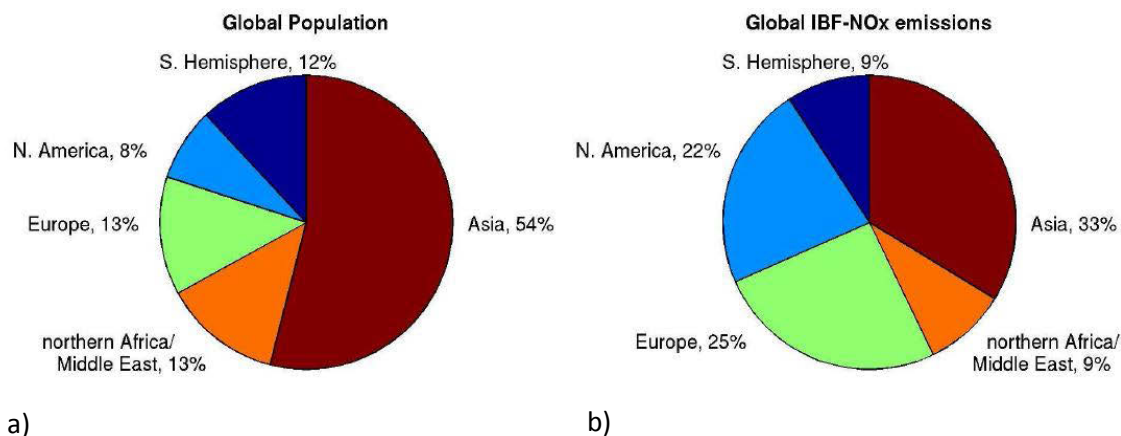
Figure 2.6: (a) Global human population and (b) IFB-NO$_x$ emissions in 2000 (www.unece.org).

Africa is a continent with a number of developing countries with increasing populations, increasing numbers of automobiles and increasing industrial emissions. Previous studies conducted by United States Environmental Protection Agency (http://www.epa.gov) and Wallington et al. (2008) reported that motor cars release high hydrocarbons, CO, carbon dioxide (CO$_2$), NO$_x$, nitrous oxide (N$_2$O), particulate matter (PM), hydrofluorocarbon-134a (HFC-134a) and CH$_4$ from incomplete combustion of petroleum-based fuels in motor car engines. These emissions vary according to the automobile type and primary fuel used (http://www.epa.gov).

In 2005, African fossil fuel emissions contributed about 285 TgC, accounting for 3.7% of the global emissions (Canadell *et al*., 2008). Figure 2.7 shows South Africa as the highest emitter of fossil fuels in Africa with an average of 110.1 TgC/yr from 2000 to 2005 followed by Egypt (38.2 TgC/yr), Nigeria (25.1 TgC/yr) and Algeria (22.4 TgC/yr). In South Africa, coal fired powered stations located in the Highveld and Mpumalanga, timber processing plants, coal and metal mines, smelters, brick factories and petrochemical operations are major sources of carbon emissions (Kirkman *et al*., 2000). As much as 80% of South Africa's electricity is generated by coal–fired power station in Mpumalanga making the Highveld an air pollution 'hotspot' (Tyson *et al*., 1988).
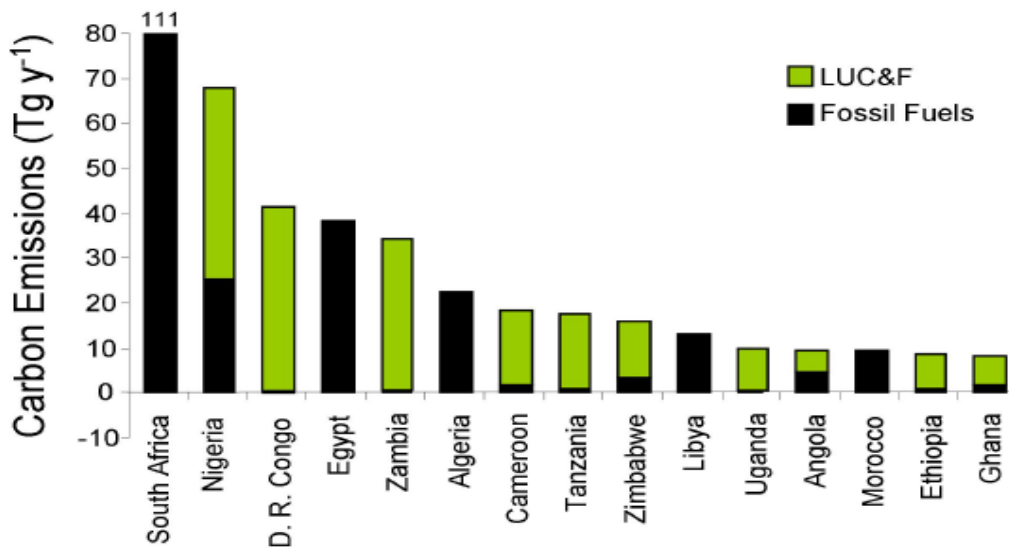
Figure 2.7: Annual emissions of carbon (TgC/yr) from the combustion of fossil fuels and land use change and forestry (LUC&F). Top fifteen African countries averaged for the period 2000–2005 (Canadell *et al*., 2008).

2.5 Ozone Sinks

2.5.1 Dry deposition

Gases and aerosols often adhere to surfaces with which they come into contact. Normally, the rate of dry deposition increases with the reactivity of the gas and depends on the type of surface. Dry deposition on terrestrial and ocean surfaces serves as a physical ozone sink. Ganzeveld *et al.* (2009) estimated that 200 to 300 Tg/yr of O_3 is deposited to the ocean surface. The deposition velocities ranges between 0.01 to 0.15 $cm.s^{-1}$ for ocean water and 0.01 to 0.10 $cm.s^{-1}$ for fresh water. Nightingale and Liss (2003) reported that the deposition velocity is influenced by wind as water turbulence controls the exchange rate. Lower O_3 fluxes are reported for water relative to land surfaces.

2.5.2 Photolysis

Photolysis is another important tropospheric O_3 sink. The destruction of O_3 is caused by short wavelength radiation ($\lambda < 340$ nm).

$$O_3 + hv \longrightarrow O_2 + O \tag{37}$$

The O atom then reacts with water vapour to form two hydroxyl radicals (OH) by Reaction 7 above.

The lifetime of ozone depends on the level of solar radiation and the concentration of water vapour (Zachariasse *et al.,* 2000). In areas with drier atmosphere (middle and upper troposphere), the O_3 lifetime is longer (3 months) relative to the continental or marine boundary layer where ozone molecules survive for 2 to 5 days (Fishman *et al.,* 1990).

2.5.3 HO_2 / OH Catalysed Destruction

Ozone is destroyed by OH and HO_2 (hydroperoxy) radicals (Lelieveld and Dentener, 2000) as shown in Equations 28 above and 38 below:

$$O_3 + HO_2 \longrightarrow 2O_2 + OH \tag{38}$$

2.6 Effect of O_3 on Humans and the Environment

In different parts of the atmosphere, and at specific concentrations, ozone can have benefits or negative impacts on health and environments. In the stratosphere, ozone absorbs incoming ultraviolet solar radiation, and any weakening or thinning of this 'ozone layer' has implications for the health of humans and other animals. On the other hand, ozone in the lower troposphere acts as a strong greenhouse gas and, at concentrations above 60 ppb, O_3 affects the respiratory system, causing lung infections, asthma symptoms and premature mortality (Kinney *et al.*, 1996). According to Lacis *et al.* (1990), Darrall (1989), Bertman and Roberts, (1991) and Derwent (1995), these high O_3 levels can affect human and plants directly or through the formation of poisonous gases such as peroxyacetyl nitrate (PAN). Finkelstein and Johnston (2004) reported that young children are more affected than adults since their lung development is not complete and they tend to have a higher breathing rate than adults. Pulikesi *et al.* (2006) estimated the number of deaths in the Netherlands related to O_3 increased from 990 to 1140 to 1400 people in 2000, 2002 and 2003 respectively.

In addition to the impacts on human health, higher levels of O_3 above 60 ppb are harmful to forests, natural vegetation and agricultural crops (National Research Council, 1999) as ozone has the potential to oxidise plant tissues. According to Wittig *et al*. (2009), present tropospheric O_3 levels and those estimated for later this century are toxic to trees and have potential to reduce the carbon sink. Ambient O_3 enters plant leaves through the stomata during gaseous exchange. Once in the leaves, it limits photosynthesis and other processes necessary for the healthy functioning of the plant (Morgan *et al.,* 2006; Brooker, 2009). Ozone damage to plants was first observed in *Vitis vinifere* in southern California by Richards *et al*. (1958). Since then, O_3 has been reported as the pollutant that most damages vegetation (Gimelo *et al*., 1995; Penuelas *et al*., 1999) and cultivate crops (Treshow and Steward, 1973). Plants affected by O_3 may show severe injuries within palisade tissue (Paoletti *et al*., 2009) with black reddish or brownish spots on branches or stems (Fumagalli *et al*., 2001; Hayes *et al*., 2007).

O_3 has been reported to affect the diameter and size growth relationships in spruce and beech plants (Pretzsch and Dieler, 2011). Delay in flowering and fruit production due to O_3 has also be a concern (Hayes *et al*., 2012). In addition to these impacts, O_3 can form toxic compounds such as hydrogen peroxide (H_2O_2), superoxide (O^{2-}), atomic oxygen (O) and hydroxyl radical.

Calatayud *et al.,* (2011) concluded that the response to O_3 levels is controlled by genotype, competitors and ontogeny. Studies (e.g. Lyons *et al*., 2000; Paakkonen *et al*., 1995) have shown that thick leaves are more tolerant than thinner leaves.

2.7 Cycles and Trends in O_3 Concentrations

Since high concentrations of O_3 in the lower troposphere have implications for the environment (including its inhabitants), it is important to monitor its concentrations so that control measures can be put in place to avoid negative impacts. This section highlights research on these natural cycles and anthropogenic influences on ozone at the sites of focus.

2.7.1 Studies on diurnal cycles at SANAE, Cape Point and City of Cape Town

Ozone levels are at their minimum in the early morning and increase during the day as a result of photochemical processes, reaching their maximum in the early afternoon. During the night, ozone is removed by NO (Reaction 32, section 2.2.4) and remains low until the next morning when sunlight encourages O_3 formation again. Photolysis of ozone results in the formation of oxygen atom (O), which reacts with water vapor to produce the hydroxyl radical (Ramanathan and Dickinson, 1979; Fishman *et al.*, 1979a). This hydroxyl radical (OH) is the most important tropospheric oxidant, removing pollutants and trace gases such as CO, CH_4, other hydrocarbons from the air.

In this study, diurnal cycles of O_3 and NO_x at all four stations (SANAE, Cape Point background, Cape Point non-background, Molteno and Goodwood) and the NO_x diurnal cycle at Goodwood are evaluated. The diurnal cycle at Cape Point has been studied extensively, with authors looking at the combined dataset (unfiltered data meaning background and non-background data not separated) (e.g. Labuschagne *et al*., 2001 and Zunckel *et al.*, 2004) as well as the filtered O_3 background data. According to Zunckel *et al.* (2004) average minimum values (from 1999 to 2001) occur between 06:00 to 08:00 and maximum values at 15:00. An average peak-to-peak difference of approximately 4.0 ppb was reported for all data (all data refers to all data recorded over the study period with no filtering techniques employed) while an average peak-to-peak difference of less than 1.0 ppb was reported for background data (background refers to data filtered according to radon concentrations). The all data peak-to-peak was suspected to reflect

some of the anthropogenic NO_x emissions that lead to O_3 formation during the day and O_3 titration during the night (Zunckel *et al.*, 2004). Smaller diurnal ranges have been observed in polar data relative to non-polar datasets (marine and continental), suggesting cleaner air with low NO_x in the polar regions, most likely due the lack of anthropogenic emissions in these region (Ayers *et al.*, 1997; Monks *et al.*, 1998) sites.

Research conducted by Wichmann (2006) on diurnal cycles in the Cape Town region (Goodwood and Molteno stations specifically) showed higher O_3 concentrations during the day relative to the night and early hours of the day. The same study showed that NO_x concentrations were inversely proportional to O_3 concentrations at these stations. This inverse relationship between O_3 and NO_x suggests NO_x titration.

2.7.2 Ozone Weekend Weekday Variations
Higher ozone levels on weekends relative to weekdays at urban stations have been described by several researchers (e.g. Elkus and Wilson, 1977; Debaje and Kakade, 2006; Swamy *et al.,* 2012). As these studies showed, O_3 concentrations are higher over the weekend despite that ozone precursor concentrations tend to be lower at this time of the week. This phenomenon has been termed the 'weekend effect' (e.g. Debaje and Kakade, 2006), According to Liu *et al.* (1987), ozone production decreases as the NO_x concentration increases during the week. Lower NO_x concentrations on weekends are associated with lower traffic levels. This results in higher O_3 concentrations due to less NO_x titration (Sadananga *et al.*, 2008; Shutters and Balling, Jr., 2006). According to Swamy *et al.* (2012), black carbon (BC) concentrations are lower on weekends and BC has a similar diurnal cycle to NO_x. Less BC on weekends is also associated with high O_3 concentrations due to less absorbance of sunlight by BC particle emissions.

Although many studies have been carried out on diurnal cycles at the four stations of focus in this study (SANAE, Cape Point, Molteno and Goodwood), weekend/weekday variations (and their relationship with NO_x fluctuations) have not been thoroughly investigated before. The effect of other O_3 precursors such as CO and VOCs in O_3 variations over the weekend is not assessed in this study due to the lack of monitoring data in the study areas.

2.7.3 Studies on Seasonal Cycles at SANAE, Cape Point and City of Cape Town

According to Helmig *et al.* (2007) polar stations show maxima during winter months because of the weakness of ozone sinks during the dark hours when there is no solar radiation. Larger seasonal ranges (approximately 5 ppb) in the Southern Hemisphere polar regions compared to the Northern Hemisphere polar regions are most likely due to less summertime photochemical ozone destruction and more transport of ozone rich air to the Arctic during the Northern Hemisphere spring and summer months (Helmig *et al.* 2007).

Seasonal cycles have been studied by several researchers at Cape Point (e.g. Oltmans and Levy II, 1994; Brunke and Scheel, 1998; Labuschagne *et al.*, 2001; Zunckel *et al.*, 2004; Brunke *et al.,* 2009). A continuous seasonal cycle with summer minimum and winter maximum was reported at Cape Point and other Global Atmosphere Watch (GAW) stations (SAMOA, Cape Grim, and South Pole) by Oltmans and Levey II (1994). Further investigations conducted by Brunke and Scheel (1998) revealed a similar seasonal trend with a maximum in July/August and minimum in January for Cape Point. Minima were associated with O_3 photolysis in summer when the intensity of ultraviolet (UV) light reaches its peak. The study conducted by Labuschagne *et al.* (2001) using a 1999 to 2001 dataset shows minima ranging between 14.0 to 17.0 ppb (in summer) and maxima ranging between 31.0 to 32.0 ppb (in winter).

A comparative study was done in 2004 for various ozone monitoring sites in southern Africa (Bosjespruit, 5 km from Secunda, Amersfoort, approximately 90 km from Secunda, Cape Point and Maun in Botswana) by Zunckel *et al.* (2004). Cape Point was the only site experiencing its ozone maximum in winter. Other sites recorded their maxima in late winter or spring (from August to October) and minima in summer months (December and January). Zunckel *et al.* (2004) also reported results from passive samplers deployed at Cape Point (June 2000 to May 2002). This passive sampling formed part of a collaborative program between Cape Point and North West University (NWU). Results showed maxima between May and July and minima between December and January. Monthly averages calculated from passive samples were in good agreement with *in situ* monthly averages from June 2000 to May 2002 at Cape Point. Overall, the seasonal cycle is fairly consistent from year to year and typical of the background Southern Hemispheric marine troposphere.

The current study investigates seasonal cycles at SANAE, Cape Point, Molteno and Goodwood. In addition, Cape Point non-background seasonal cycles are investigated. This allows a comparison between seasonal cycles at SANAE and Cape Point background, and between seasonal cycles at Cape Point non-background and seasonal cycles in the urban Cape Town region.

2.7.4 Effect of Meteorology on Surface Ozone Measurements

Meteorological parameters such as wind direction, wind speed, humidity, solar radiation, cloud cover and temperature are the main forces which drive the reactions of O_3 and its transport to surrounding areas. Winds with low speed, high solar radiation, high temperatures, and low humidity generally promote increased ozone. Contrary to this, wet, rainy weather with high relative humidity is typically associated with the low O_3 concentrations provided by wet ozone deposition on the water droplets (Tarasova and Karpetchko, 2003). Associated with the regular cold fronts traversing the Cape coastline in winter, strong north-easterlies and rainfall clean the urban atmosphere over Cape Town. In-between cold fronts episodes, an anticyclonic ridge bring stable conditions and promote the accumulation of pollutants (Jury *et al.*, 1990), often resulting in a brown haze, consisting of O_3, Peroxyacytyl nitrate (PAN) and other organic compounds, (Wicking–Baird *et al.,* 1997). Stable conditions are further promoted by the onset of surface temperature inversions at night, which only subside when surface temperatures rise after sunrise Pollutants can be trapped within the surface inversion, or below it as it erodes from the surface up after sunrise (fumigation), which increases local pollutant concentrations.

Polar regions experiences snow in winter months and temperatures are very low during this period. Studies conducted by Domine and Shepson (2002) and Shepson *et al.* (2003) in the Arctic and Antarctic have demonstrated that snowpacks release NO_x and there is gaseous exchange between the boundary layer and the atmosphere. This agrees with a previous study by Honrath *et al.* (1999) that revealed that NO_x forms during the photolysis of NO^{-3} in snowpacks and is released to the atmospheric boundary layer (Honrath *et al.*, 1999). According to Domine *et al.* (2008), controls on the release of NO_x from snow packs are temperature, pH and ion content. These factors control the chemical and physical properties of NO_x.

2.7.5 Studies on long term trends in ozone at SANAE, Cape Point and City of Cape Town

Brunke *et al*. (2011) reported a small increase of O_3 at the 30 m intake of approximately 0.17 ppb/year from 1990 to 2009 in SANAE, Cape Point and Cape Town. Brunke *et al*. (2011) also reported changes at 4 m and 30 m from 1990 to 1999 and 2000 to 2009. From 1990 to 1999, the measurements at 30 m showed an increase of approximately 0.30 ppb/yr across seasons. From 2000 to 2009, a non-significant decrease of approximately 0.07 ppb/yr and 0.06 ppb/yr for the 4 m and 30 m intakes respectively was reported. Results showed that long term O_3 trends are not dependent on the intake height. A continuous increase of approximately 0.4 ppb/yr from 1999 to 2001 was reported by Zunckel *et al*. (2004). This study showed that O_3 is not easily linked to an individual source but is the result of photochemical reactions between the products of a number of source types, with precursor gases potentially transported over great distances. These observations highlight the importance of examining meteorological effects in detail so that the atmospheric transport of precursors can be better understood.

2.8 Conclusion

It can be concluded that there are a number of factors affecting the concentrations of O_3. These factors include the influence of industrial and vehicular emissions, lightning, biomass burning, biogenic release, stratospheric-tropospheric exchange, photolytic destruction and dry deposition. These factors can affect both the short and long term trends of O_3. Therefore, it is very important to consider such factors when conducting O_3 studies. High concentrations of O_3 exceeding 60 ppb have a negative effect on human and environment.

CHAPTER 3

(Data and Methodology)

3.1 Introduction

This chapter presents the analytical techniques and calibration methods as applied at SANAE, Cape Point, Molteno and Goodwood. In this chapter, the approach to data analysis is presented for the investigation of diurnal and seasonal cycles, the weekend effect, the effect of meteorology on surface O_3 concentrations, and any long term trends.

3.2 Ozone Measurements at Cape Point, SANAE and City of Cape Town

An intake line mounted from the top of a 30 m mast was established for sampling at Cape Point in 1982. In 1996, measurements commenced from a second air intake (at 4 m above ground level). In September 2008, another intake at 14 m above ground level was installed. The SANAE air intake is approximately 11.5 m above ground level while the stations in the City of Cape Town air intakes are approximately 5 m above ground level.

Measurements are continuous at Cape Point, with one minute samples averaged to 30 minute output values. Measurements are made by three Thermo Electron (Teco) analyzers based on an ultraviolet (UV) detection technique. SANAE employs the same Thermo Electron (Teco) analyzer as Cape Point, while each station in the City of Cape Town utilizes an Ozone Analyzer API (Model 400A) with UV absorption. This model is appropriate for analysing ozone in an urban environment.

3.2.1 Validation procedure

An O_3 calibrator (TEI 49i-PS) is used to verify the three instruments at Cape Point every two months or when there is analytical suspicion. Daily zero and span sensitivity checks are conducted automatically. Monthly zero-calibration levels are factored into the data processing routine, while the span sensitivity values provide information on long-term instrument stability. Calibrations are performed by World Calibration Centre (WCC-Empa) every four years and the last audit at Cape Point was conducted in August 2011. WCC-Empa audits all stations in the Global Atmosphere Watch (GAW) network and the audit reports are sent to the World

Meteorological Organisation (WMO). With the exception of WCC-Empa audits, SANAE follows the same strategy as Cape Point and has a zero and span sensitivity run each day. The instrument is shipped to Cape Point for verifications with their calibrator, normally after a year or immediately if there are concerns of mal-performance. The Molteno and Goodwood instruments are calibrated with a South African National Accreditation Service (SANAS) calibrator every three months while a portable calibrator (O_3 Calibrator, Model 306) is used at the sites every two weeks.

3.2.2 Validation comparison: Cape Point and City of Cape Town

As part of the current study, the City of Cape Town portable calibrator was used to validate one of the instruments (sampling at 4m intake) at Cape Point. It was decided that a comparison of validation results was necessary when the initial analysis of the monitoring datasets showed that the Cape Town O_3 concentrations generally are lower than Cape Point O_3 concentrations yet it was expected that the urban O_3 concentrations would be higher. This comparison exercise was conducted for two days (22nd and 29th of October 2012). After the verifications, results were compared to the verification results obtained when using Cape Point calibrator. Outcomes (Figures 3.1, 3.2 and 3.3 and Table 3.1 and 3.2) achieved from these tests verified the consistency between Cape Point and Cape Town validation approaches and established that the data from these stations are comparable and representative of ambient concentrations if one assumes that the two calibrators do not have the same degree of error and in the same direction. This is a fair assumption.
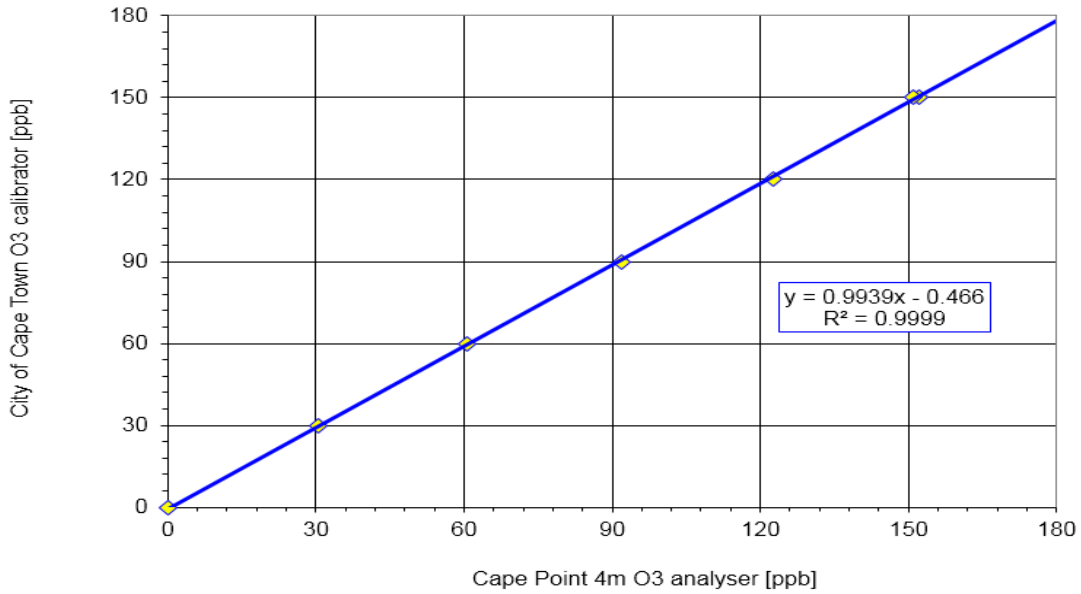
Figure 3.1: Cape Point 4m O_3 analyzer validations using City of Cape Town O_3 calibrator on the 22 of October 2012

Table 3.1 below shows the validation results obtained when verifying the Cape Point analyzer (4 m intake) with the Cape Town calibrator on the 22nd of October 2012. Column 1 shows O_3 concentrations generated from the calibrator (calibrator output to the analyzer), while column 2 shows O_3 readings recorded by the analyzer. During this verification, the Cape Point analyzer reads higher by approximately 7.2 ppb at each level of the calibrator setting (0 ppb to 180 ppb). Column 3 shows actual O_3 concentrations recorded by the analyzer after eliminating the offset (7.17 ppb) of the calibrator. Column 4 shows the difference between the O_3 generated from the calibrator and the O_3 concentrations recorded by the analyzer.

Table 3.1: Validation of Cape Point 4m O$_3$ analyzer using City of Cape Town O$_3$ calibrator on the 22 of October 2012

Column1	Column2	Column3	Column4
Cape Town O$_3$ Calibrator [ppb]	Cape Point O$_3$ analyzer (4m intake)	Cape Point O$_3$ analyzer (4m intake) minus offset (7.17)	Calibrator minus Cape Point analyzer (4m intake)
0.0	7.17		
30.0	37.4	30.2	-0.2
60.0	68.4	61.2	-1.2
90.0	98.8	91.6	-1.6
120.0	129.2	122.0	-2.0
150.0	158.9	151.7	-1.7
180.0	187.9	180.7	-0.7
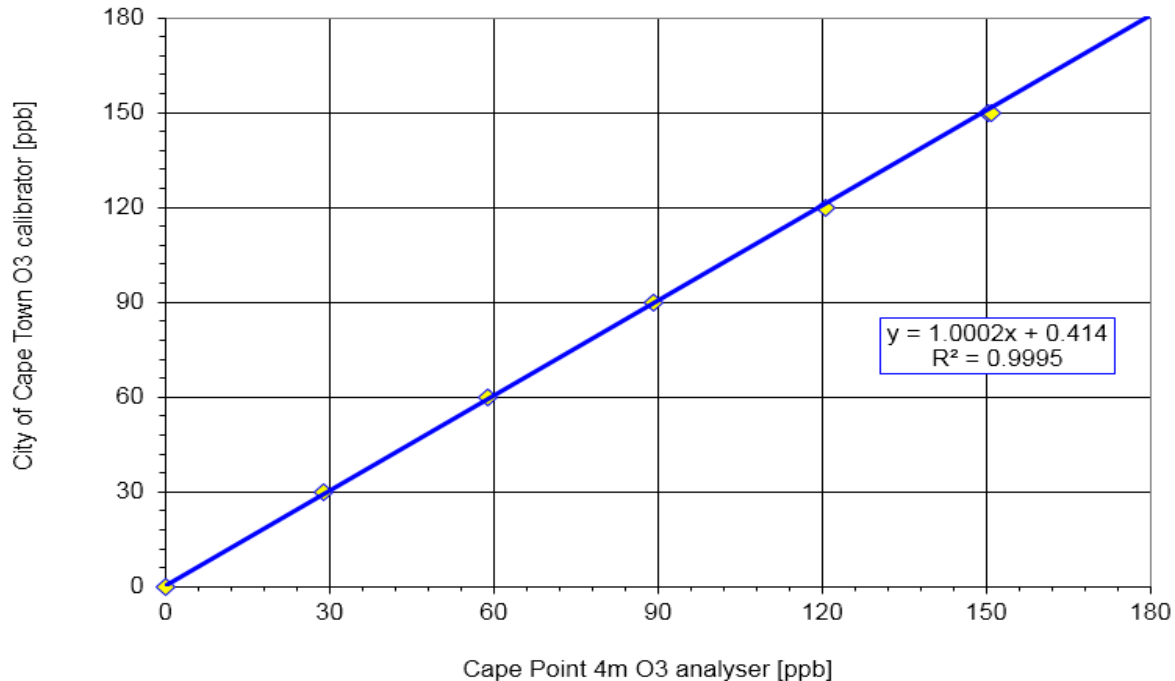
Figure 3.2: Cape Point 4m O$_3$ analyzer validations using City of Cape Town O$_3$ calibrator on the 29 of October 2012

Table 3.2 below shows the validation results obtained when verifying the Cape Point analyzer (4m intake) with the Cape Town calibrator on the 29th of October 2012. Column 1 shows O$_3$ concentrations generated from the calibrator (calibrator output to the analyzer), while column 2 shows O$_3$ readings recorded by the analyzer. During this verification, the Cape Point analyzer read higher by approximately 3.5 ppb at each level of the calibrator setting (0 ppb to 180 ppb).

Column 3 shows actual O_3 concentrations recorded by the analyzer after eliminating the offset (3.50 ppb) of the calibrator. Column 4 shows the difference between the O_3 generated from the calibrator and the O_3 concentrations recorded by the analyzer. With the exception of the offset, the two verification results are in good agreement.

Table 3.2: Validation of Cape Point 4m O_3 analyzer using City of Cape Town O_3 calibrator on the 29 of October 2012

Column1	Column2	Column3	Column4
Cape Town O_3 Calibrator [ppb]	Cape Point O_3 analyzer (4m intake)	Cape Point O_3 analyzer (4m intake) minus offset (3.5)	Calibrator minus Cape Point analyzer (4m intake)
0.0	3.5		
30.0	33.2	29.7	0.3
60.0	62.9	59.4	0.6
90.0	93.0	89.5	0.5
120.0	124.1	120.6	-0.6
150.0	154.2	150.7	-0.7
180.0	183.7	180.2	-0.2
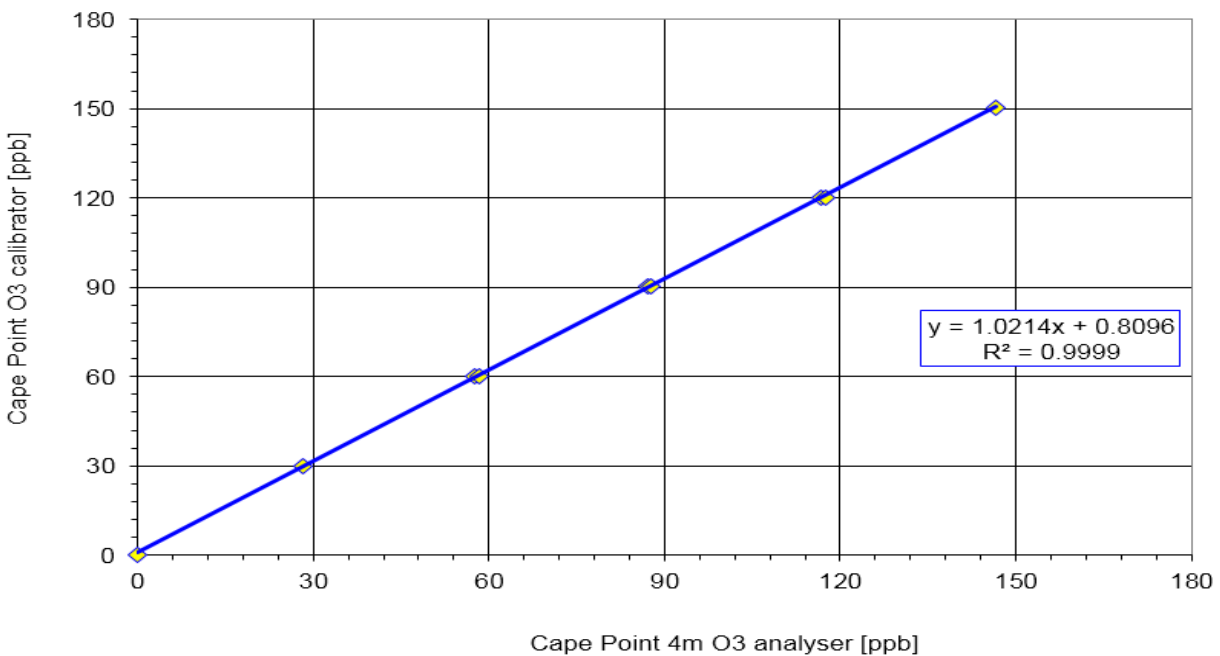
Figure 3.3: Cape Point 4m O_3 analyzer validations using Cape Point calibrator

3.2.3 Filtering of data to background and non-background at Cape Point

Cape Point is regarded as a background station due to its location and dominant southerly winds, which originate from the Atlantic Ocean. When such air masses arrive at the station, they show the following characteristics: low radon (^{222}Rn) concentrations, carbon monoxide (CO) concentration stability over time, and generally low particulate concentrations (measured by a condensation particle counter, CPC), although there are exceptions when particulate measurements are high, possibly due to increased sea salt particulates. Contrary to this, non-background conditions are characterized by higher levels of ^{222}Rn, higher particulate concentrations, and CO levels are more variable, as a result of non-homogenous air masses arriving from terrestrial sources. In non-background conditions, winds generally have lower speeds and the predominant wind direction is northerly.

Cape Point uses two separation techniques for filtering data into background and non-background categories, namely CO filtering technique Brunke *et al*. (2004) and ^{222}Rn filtering technique Brunke *et al*. (2004). The radon technique reported by Brunke *et al*. (2004)to be more sensitive and filter data more adequately relative to the CO filtering technique. Radon occurs naturally as a radioactive gas as part of radioactive decay from radiogenic uranium to stable lead. Sources of radon are minerals rocks rich in potassium, thorium and uranium (e.g. granites) and ground water. Radon has a half life span of 3.8 days and after that decays to stable lead (http://www.epa.gov)). In this study, the ^{222}Rn filtering technique was selected to filter O$_3$ data into background (when ^{222}Rn was less than 250 mBq^{-3}) and non-background (when ^{222}Rn was more than 1200 mBq^{-3}) categories. When an air mass has a ^{222}Rn concentrations between 250 to 1200 mBq^{-3}, it is referred to as a mixed mass (containing both background and non-background masses).

3.3 Data analysis

3.3.1. Diurnal analysis

Averages for each hour of the day (e.g. 1:00 am to 2:00 am, 2:00 am to 3:00 am etc.) were calculated for all the records from Sanae, Cape Point, Molteno and Goodwood. Thirty minute averages also were calculated from one minute data recorded at Cape Point and Sanae. At Cape

Point, hourly O_3 averages were calculated for background and non-background air masses. The background diurnal cycle was compared with the Sanae diurnal cycle while the non-background diurnal cycle was compared with Molteno and Goodwood diurnal cycles. Analysis of diurnal cycles is important for investigating O_3 patterns over the course of a 24-hour period and reflects the influence of local activities if wind data is available.

3.3.2. Weekend/weekday diurnal analysis

The hourly O_3 averages were calculated for weekdays (Monday to Friday) and weekends (Saturday and Sunday) at Sanae, Cape Point, Molteno and Goodwood to study the effect of vehicular emissions on O_3 concentrations. Vehicular emissions of NO_x tends to be higher during the week. As discussed in section 3.1.3, Cape Point data used for this study was categorized into background and non-background categories. For the analysis of weekend and weekday diurnal cycles, hourly O_3 averages were calculated for both background and non-background datasets.

3.3.3. Seasonal analysis

Monthly O_3 averages were calculated from hourly O_3 averages at all four stations (Sanae, Cape Point, Molteno and Goodwood). At Cape Point station, monthly O_3 averages were calculated for both background and non-background categories. The main aim of separating Cape Point data is to study seasonal variations in both background and non-background data and to compare the Cape Point background O_3 seasonal cycle with O_3 seasonal cycle observed at Sanae, and to compare the Cape Point non-background O_3 seasonal cycle with the Molteno and Goodwood O_3 seasonal cycles.

3.3.4. Weekend/weekday seasonal cycle analysis

Weekday (Monday to Friday) and weekend (Saturday and Sunday) monthly O_3 averages were calculated from hourly O_3 averages at all four stations in order to investigate weekday O_3 seasonal cycles and weekend O_3 seasonal cycles. Furthermore, at Cape Point, the weekday and weekend O_3 seasonal cycles were calculated for both background and non-background data. As mentioned earlier in this chapter, the separation of O_3 and NO_x data into weekday and weekend categories assists in the assessment of the influence of vehicular emissions on ambient O_3 concentrations.

3.3.5. Effect of meteorology on surface ozone

The influences of several meteorological parameters on O_3 concentrations at the various stations were assessed. The selected meteorological parameters were as follows: temperature (°C), humidity (%), wind speed (m/s) and wind direction (°). These parameters are monitored at Vesleskarvet weather station (closest meteorological station to SANAE), Cape Point, and Cape Town weather office (approximately 19 km from Molteno and approximately 12 km from Goodwood).

To assess the effect of wind speed on surface O_3, wind speed was categorized into three categories: i) winds less than 5 m/s, ii) winds between 5 to 10 m/s and iii) winds between 10 to 15 m/s. Surface O_3 was filtered according to the wind speed categories mentioned above. Monthly O_3 averages were calculated from hourly O_3 averages for each wind speed category. For the investigation of the influence of wind on O_3 measurements, wind direction was segregated into sixteen azimuth sectors, each being 22.5°, increasing clockwise from N (0°) , Pollution roses were constructed. In addition, monthly O_3 averages were calculated for summer (December-February), autumn (March- May), winter (June-August) and spring (September-November) for each wind sector. These data were used to construct O_3 pollution roses for all seasons at all four stations. Similarly, a NO_x pollution rose was constructed using Goodwood data by following the same procedure as described above. This analysis is critical for relating wind with NOx emissions associated with traffic.

3.3.6. Correlation analysis of surface ozone

Correlation analysis between hourly O_3 averages at SANAE and hourly O_3 averages at Cape Point background were conducted at the 95% confidence level. A similar analysis was done between hourly O_3 averages at Cape Point non-background and hourly O_3 averages at Molteno and hourly O_3 averages at Goodwood. The correlation between hourly NO_x averages and hourly O_3 averages at Goodwood offered a further perspective on the influence of vehicular emissions on O_3 concentrations. Additional correlation analyses were conducted for monthly O_3 averages and monthly averages of meteorological parameters (temperature and humidity).

3.3.7. Long term trends of surface O$_3$

Long term trends in O$_3$ concentrations were assessed by calculating annual O$_3$ averages for all stations and plotting these on a graph. Average trend lines were then added to these graphs and their slopes were calculated for 2002 to 2009 at SANAE, 1997 to 2009 at Cape Point, 1997 to 2007 at Molteno and 2000 to 2006 at Goodwood). The same approach was used to calculate the trend in annual NO$_x$ concentrations at Goodwoood. All the stations used in this study offered more than seven years of data, which allowed for some analysis of changes in annual average O$_3$ concentrations over time. It is critical to know whether surface O$_3$ concentrations are increasing, decreasing or stabilizing. The Cape Town region (Molteno and Goodwood stations) indicates the influence of anthropogenic activities on O$_3$ concentrations over time. The NO$_x$ record from Goodwood helped contextualize this trend analysis with respect to vehicular emissions.

3.4. Conclusion

It is very important to separate Cape Point data into background and non-background dataset because Cape Point is affected by both wind regimes. Although the SANAE dataset is not enough for long term trend analysis, all stations provided enough data for the analysis of diurnal, seasonal and weekend effect. Diurnal analysis are important to determine the effect of local pollution on O$_3$ concentrations. While weekend/weekday analysis gives a better understanding on the effect of vehicular emissions.

CHAPTER 4

Results and Discussion

4.1 Introduction

This chapter presents the results of the analysis of ozone (O_3) concentrations of the three air intakes at Cape Point. Cape Point background and non-background concentrations are compared with O_3 measurements at SANAE, and the Molteno and Goodwood stations respectively. Diurnal and seasonal cycles, weekend effects and long term O_3 trends are also discussed for all stations.

4.2 Diurnal Cycles

This analysis focuses on the averages for each hour of the day across the records. These averages show that O_3 levels increase once solar radiation increases in the morning with sunrise, reaching a maximum in the afternoon. This can be explained by the increase in photolysis reactions as well as the emission of oxides of nitrogen (NO_x) by traffic and industry as the daytime progresses. The photolysis of ozone precursors to form ozone (Equations 30 and 31) occurs as UV radiation increases and the temperature rises in the morning, peaking in the afternoon. As UV radiation decreases, O_3 production decreases and more O_3 is destructed by NO titration (Equation 32) than produced. O_3 levels remain low until the next morning (Seinfeld and Padis, 2006).

Zunckel *et al.* (2004) reported O_3 minima occurring between 06:00 to 08:00 and maxima at 15:00 at Cape Point under background conditions. Current findings agree with these results with diurnal minima experienced between 08:00 and 09:00 for all three air intakes (Figure 4.1). Peak-to-peak values (i.e. difference between maxima and minima) for the 4 m, 14 m and 30 m background intakes are 1.81 ppb, 2.44 and 1.26 ppb respectively.
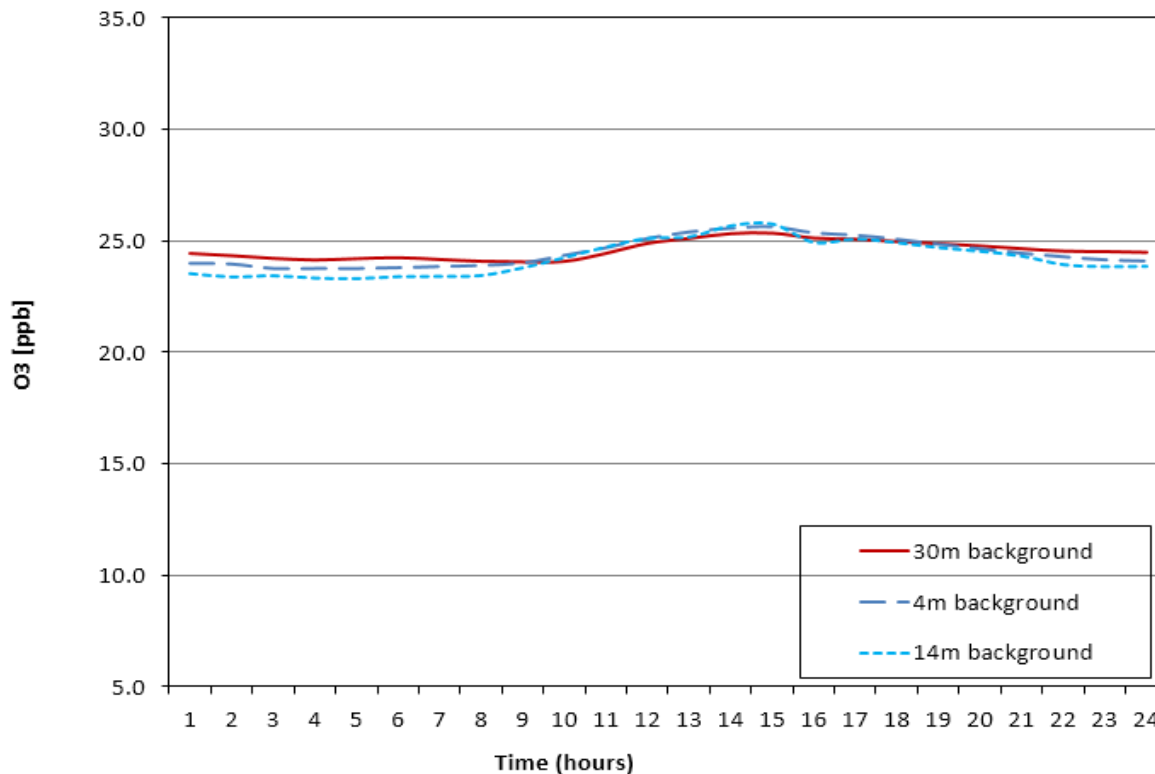
Figure 4.1: Diurnal cycle of background O_3 for three intakes at Cape Point (1997 – 2009).

The non-background diurnal cycle (Figure 4.2) shows minima and maxima at similar times to the background diurnal cycle, but with different peak-to-peak values. Non-background peak-to-peak values for 4 m, 14 m and 30 m are 6.00 ppb, 6.13 ppb and 4.73 ppb respectively. Labuschagne *et al.* (2001) reported a peak-to-peak value of 4.00 ppb at Cape Point for the period of 1999 to 2001 when conducting a similar study. This value incorporated both background and non-background concentrations and it is expected that the non-background concentrations would have a higher peak-to-peak value because of greater NO_x variations relative to background air.
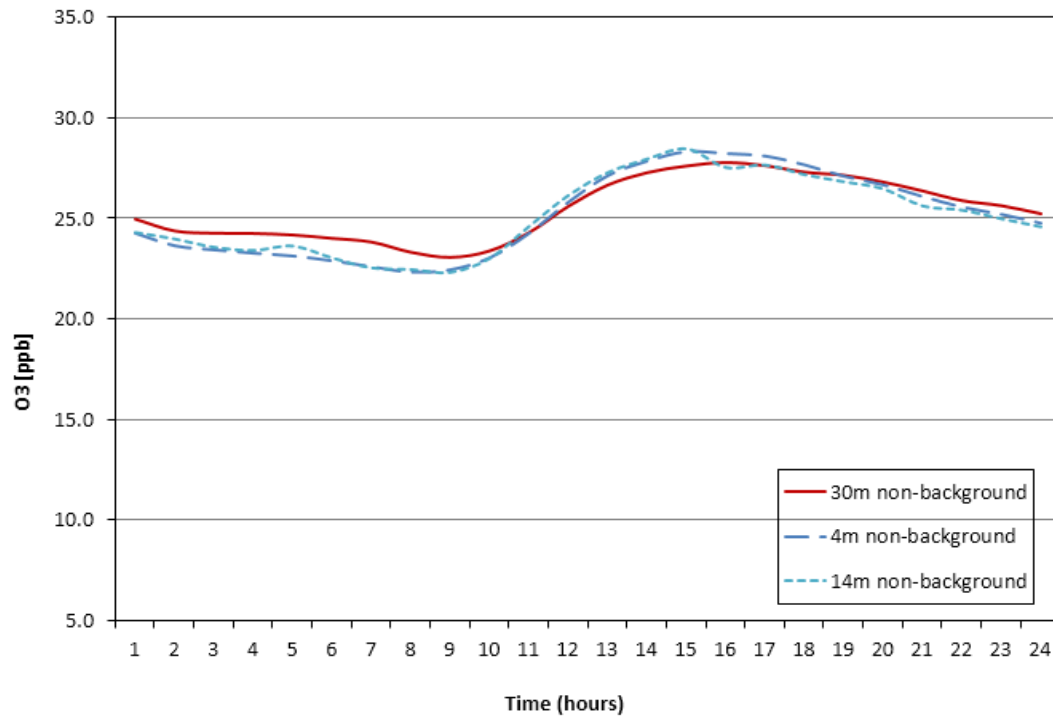
Figure 4.2: Diurnal cycle of O_3 for three intakes at Cape Point non-background (1997 – 2009).

Figure 4.3a illustrates a weak diurnal cycle in the Cape Point background data. There is small peak observed at 15:00 for Cape Point background. The peak-to-peak value of this cycle (1.81 ppb) is low but greater than that at SANAE (0.2 ppb). As Figure 4.3a reveals, there is no distinct diurnal cycle at SANAE over this period of study. This amplitude of 0.2 ppb at SANAE falls within the range of 0.00 to 1.5 ppb reported by Helmig *et al.* (2007) for polar regions. The strong correlation between the SANAE and Cape Point records (Figure 4.3b bottom) is not significant at the 95% confidence level (p = 0.124, r = 0.7678, r^2 = 0.5896).
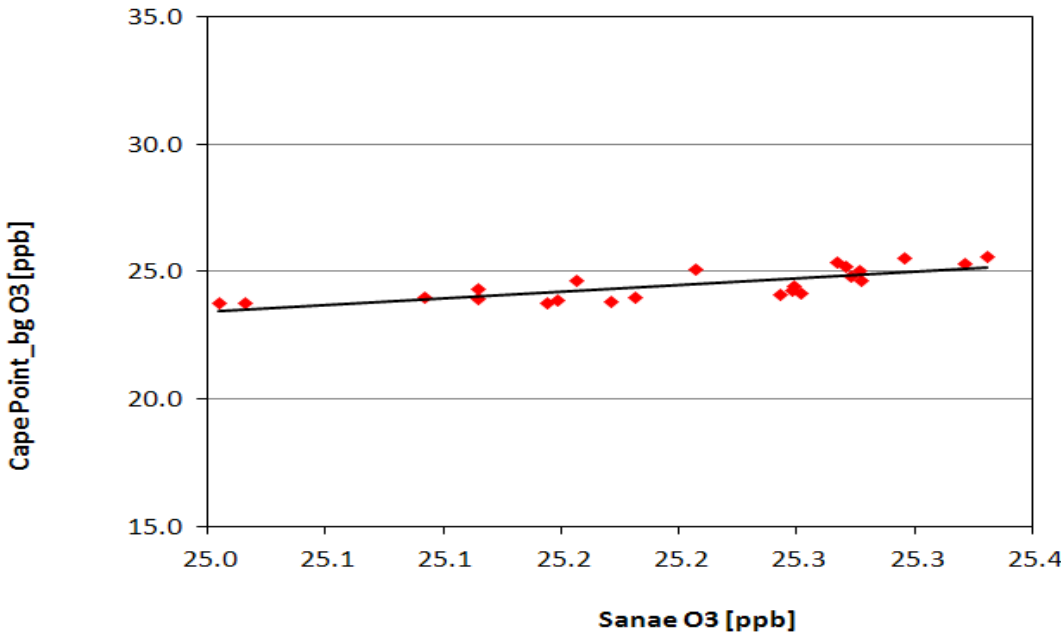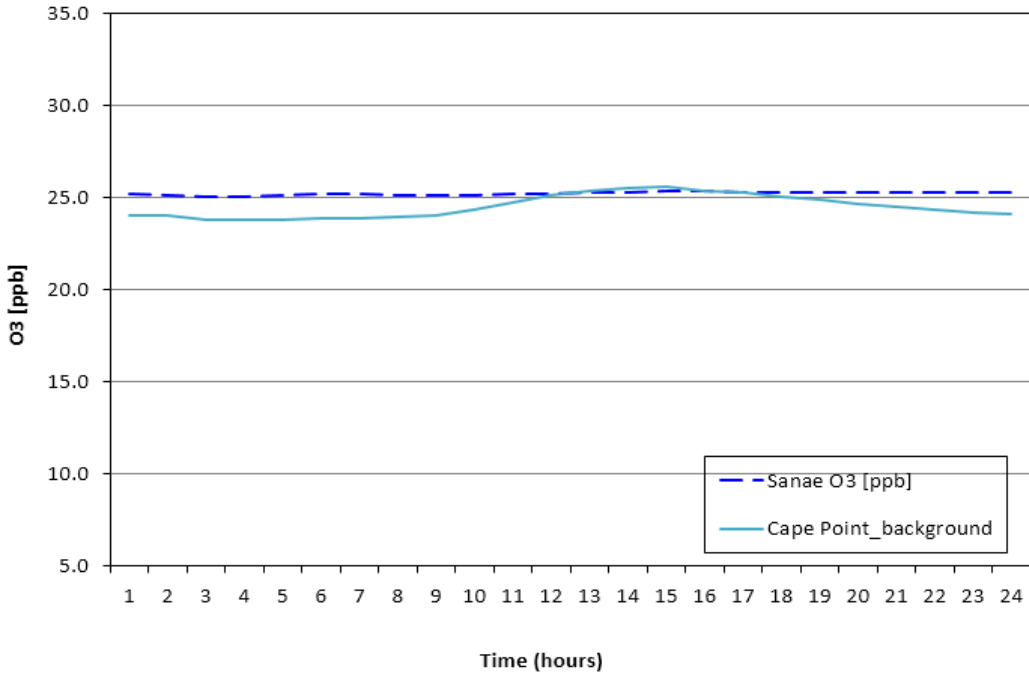
Figure 4.3: (a) Average background O_3 diurnal cycles at SANAE and Cape Point from 2002 – 2009 and (b) Correlations between the background O_3 diurnal cycles at SANAE and Cape Point from 2002 – 2009.

The Cape Point non-background diurnal cycle resembles those of Molteno and Goodwood with the exception that cycles at the latter stations are more pronounced than at Cape Point, with a peak-to-peak value of 6.00 ppb at Cape Point in contrast to 12.16 ppb and 16.80 ppb for Molteno

and Goodwood respectively (Figure 4.4). Maxima occur between 14:00 and 15:00 and minima between 08:00 and 09:00 at Cape Point, Molteno and Goodwood. The morning peak between 04:00 and 08:00 is not visible in the Cape Point non-background record. A previous study (Wichmann, 2006) associated the morning peak with traffic emissions and this could explain its absence at Cape Point since this is not an urban station.

Figure 4.4 illustrates the O_3 and NO_x diurnal cycles. The O_3 trend lags by five to six hours relative to the NO_x trend. This delay has been observed by Pudasainee *et al.* (2006) for sites in the Northern Hemisphere. Figure 4.4 reveals an inverse relationship between NO_x and O_3 concentrations at Goodwood. At Goodwood the diurnal range in O_3 and NO_x is greater relative to non-industrial sites. Molteno and Goodwood diurnal trend is comparable with peak-to-peak values of 12.16 ppb and 15.02 ppb respectively. These results illustrate a greater variation in O_3 at Molteno and Goodwood, where more anthropogenic activities occur such that more NO_x and other O_3 precursors are produced.
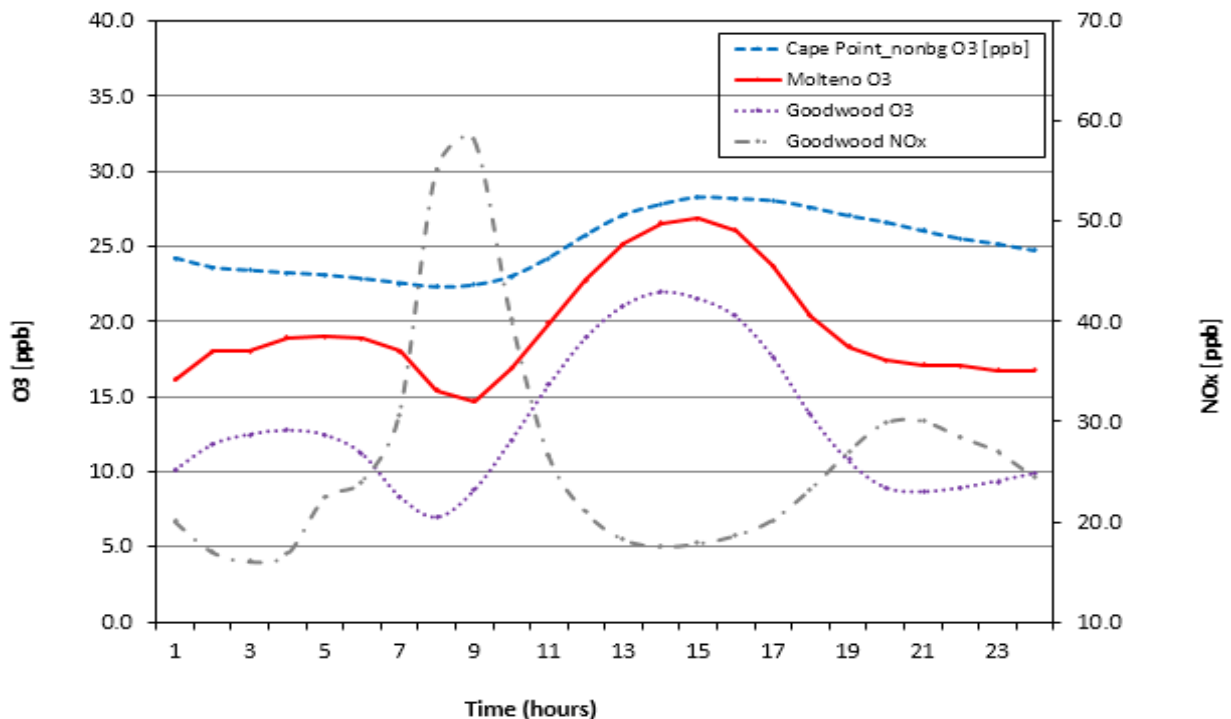
Figure 4.4: Average O_3 diurnal cycles for Cape Point non-background, Goodwood, Molteno and NO_x diurnal cycle for Goodwood (2000 – 2006).

Figure 4.5a illustrates the positive correlation between average hourly non-background O_3 at Molteno and Cape Point from 2000 to 2006. The strong correlation is not significant at the 95% confidence level (p = 0.061, r = 0.7322, r^2 = 0.5361). Figure 4.5b demonstrates a positive correlation between average diurnal O_3 experienced at non-background Goodwood and Cape Point from 2000 to 2006. The relationship, however, is not significant at the 95% confidence level (p = 0.1161, r = 0.6472, r^2 = 0.4189).

a)

Molteno O3 [ppb]
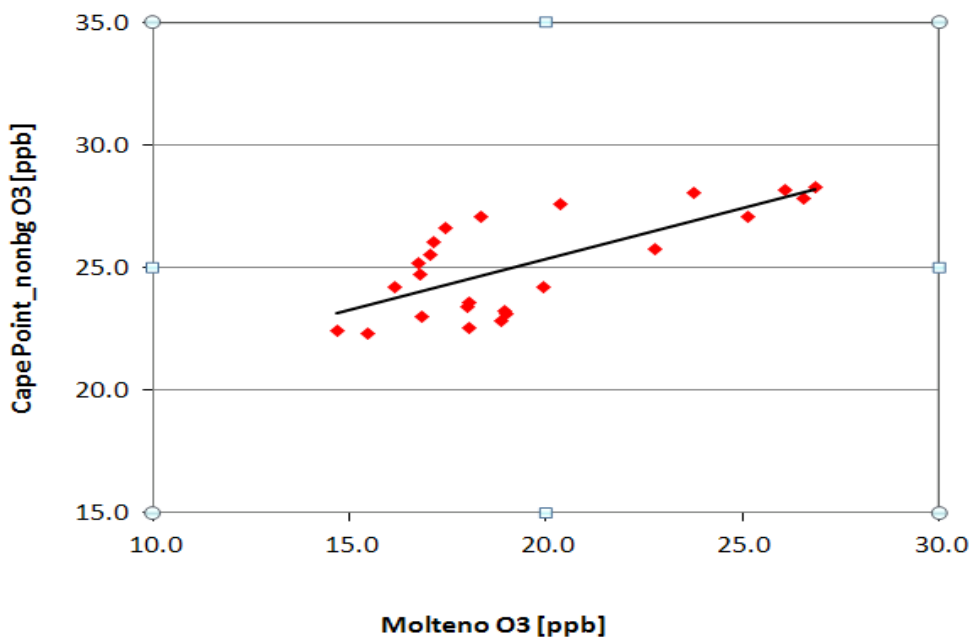
b)
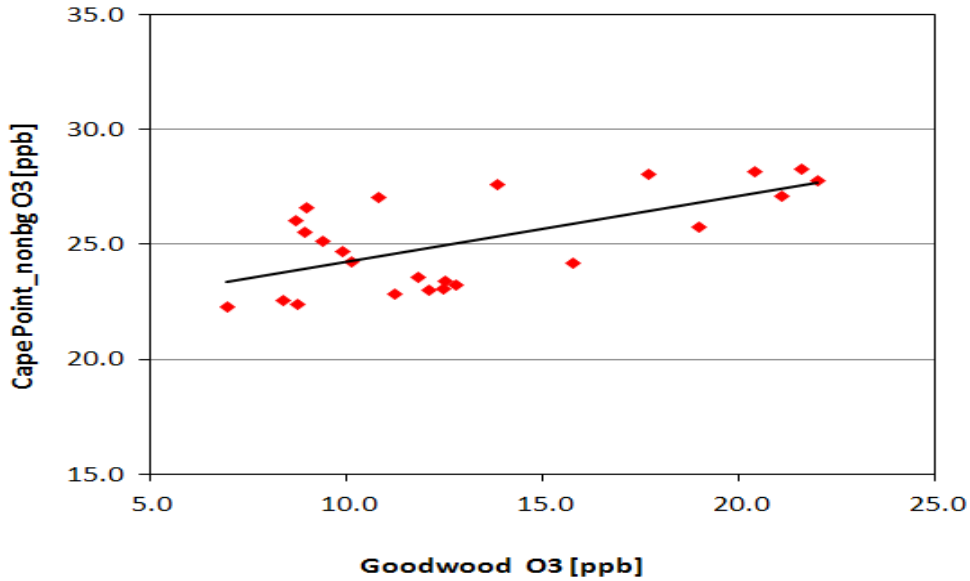
Figure 4.5: (a) Correlations between the non-background O_3 diurnal cycles at Molteno and Cape Point from 2000 – 2006 (b) and correlation between the non-background O_3 diurnal cycles at Goodwood and Cape Point from 2000 – 2006.

Figure 4.6 reflects the inverse relationship between NOx and O_3 widely documented in literature. Although there is a relationship between the two variables in Goodwood from 2000 to 2006 hourly average data (Figure 4.6), the correlation is not significant at 95% confidence level ($p = 0.182$, $r = -0.57$, $r^2 = 0.32$).
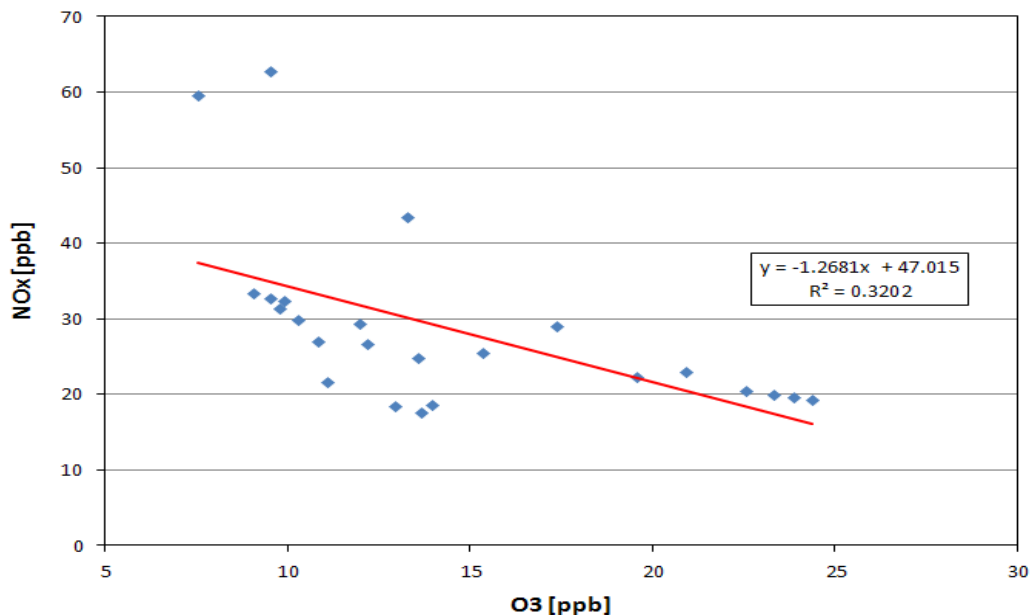
Figure 4.6: Correlation of O_3 and NO_x averaged for each hour of the day at Goodwood (2000 – 2006).

4.3 Weekday and Weekend Diurnal Cycles

Weekday and weekend surface O_3 diurnal cycles were analysed using data for 2002 to 2009 at SANAE and Cape Point, and for 2002 to 2007 at Molteno and Goodwood. Surface ozone concentrations are higher over weekends at Molteno and Goodwood. This is most likely due to lower NO_x emissions. Lower NO_x promotes accumulation of O_3 because NO titration is limited.

Figure 4.7 illustrates the weekday and weekend diurnal cycles at SANAE. The O_3 trend cycle is similar for both weekdays and weekends although peak-to-peak values are slightly lower during the week (0.85 ppb) relative to weekends (0.94 ppb). Peak-to-peak values increase by only 0.09 ppb on the weekends. It can be concluded that there is no significant weekend effect at SANAE over the study period.
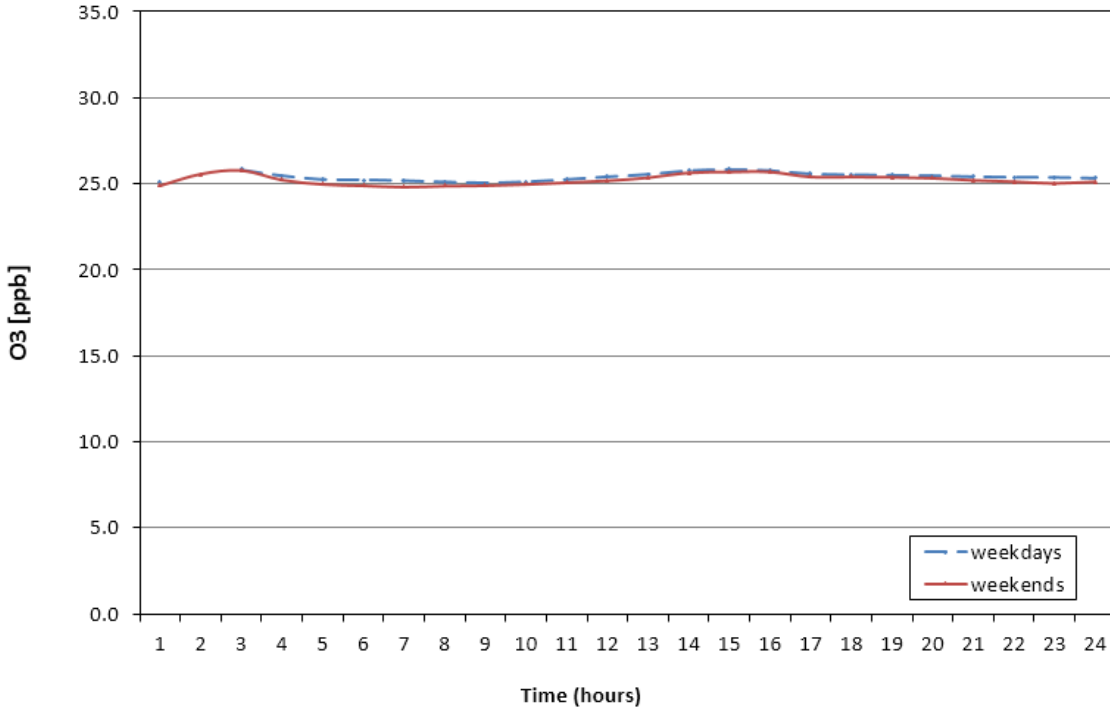
Figure 4.7: Average O_3 diurnal cycle for weekends and weekdays at SANAE (2002 – 2009).

A weekend effect is also not obvious for the Cape Point background data (Figure 4.8). The O_3 trend at Cape Point background is similar for both weekdays and weekends. Peak-to-peak values are slightly lower during the week (1.52 ppb) relative to weekends (1.66 ppb). The peak-to-peak difference is thus 0.14 ppb.
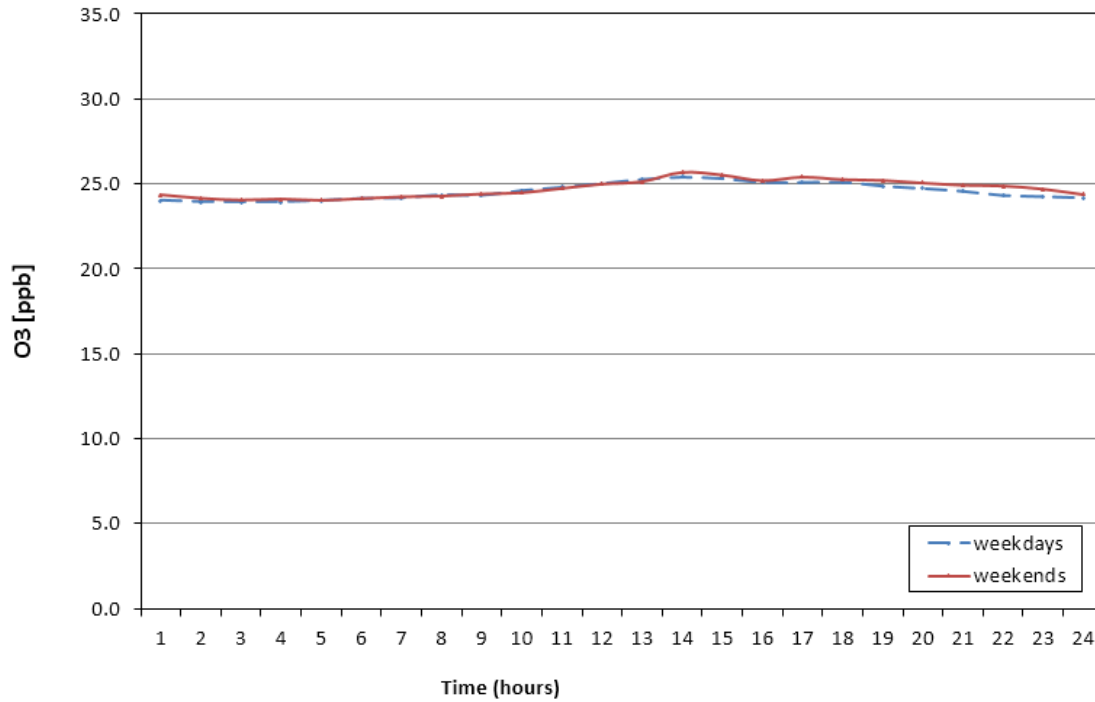
Figure 4.8: Average O$_3$ diurnal cycle for weekends and weekdays at Cape Point background station (1997 – 2009).

A weekend effect is not clear for the Cape Point non-background data (Figure 4.9). The O$_3$ trend at Cape Point non-background is similar for both weekdays and weekends although peak-to-peak values are slightly higher during the week (5.88 ppb) relative to weekends (5.52 ppb). Peak-to-peak difference thus decreases by 0.36 ppb. It can be concluded that Cape Point is not significantly impacted by the weekend effect. This is expected because the Cape Point station is not proximate to vehicular emission sources.
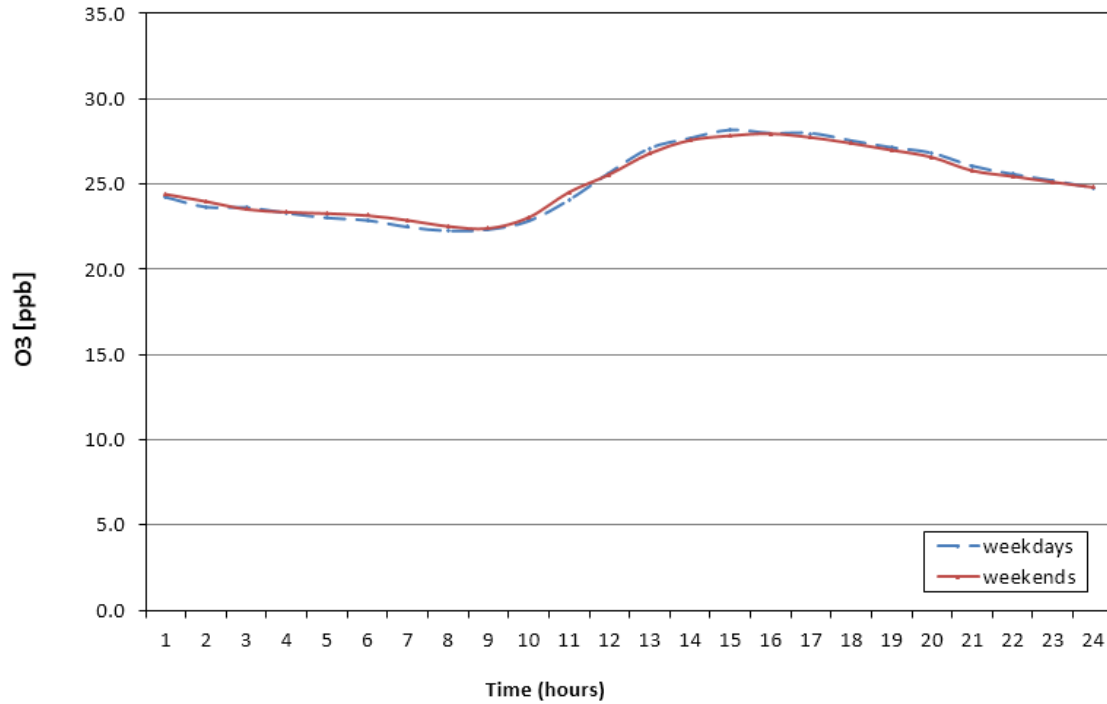
Figure 4.9: Average non-background O$_3$ diurnal cycle for weekends and weekdays at Cape Point (1997 – 2009).

Figure 4.10   shows the O$_3$ trend at Molteno. The minimum increases by 2.84 ppb while the maximum increases by 0.84 ppb on weekends. As such, peak-to-peak values are higher during the week (12.10 ppb) relative to weekends (11.56 ppb). Peak-to-peak difference decreases by 0.54 ppb on the weekends.
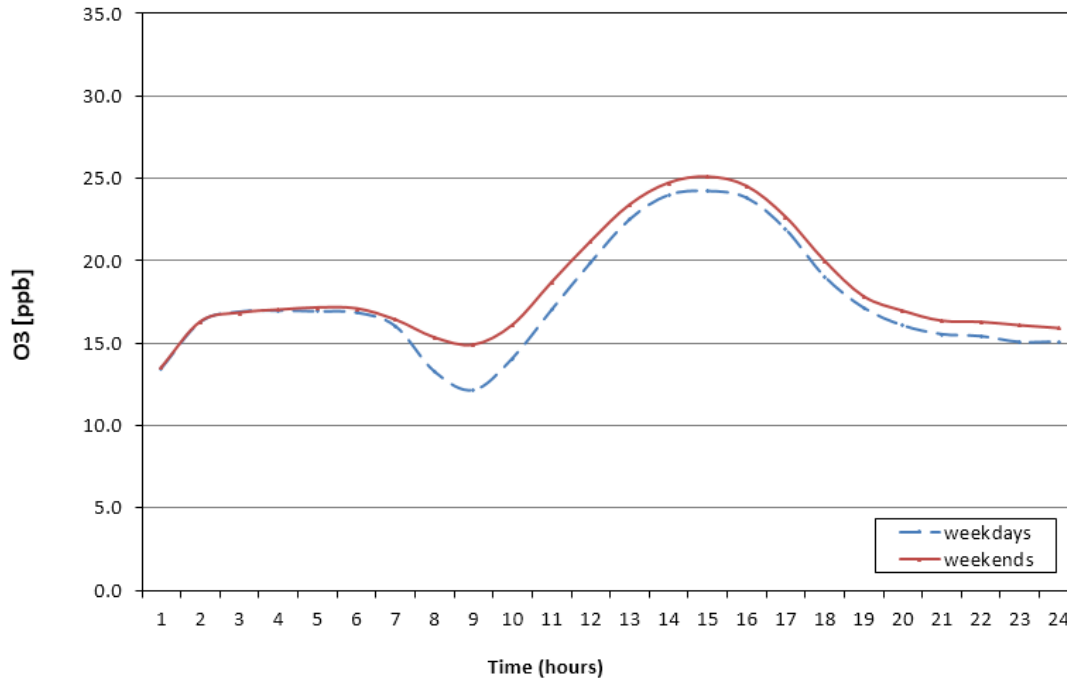
Figure 4.10: Average O_3 diurnal cycle for weekends and weekdays at Molteno (1997 – 2007).

Goodwood shows a clearer variation between weekdays and weekends (Figure 4.11). Here morning levels of O_3 are low, decreasing from around 05:00 until 09:00 before increasing to the afternoon peak. The minimum increases by 2.86 ppb and the maximum increases by 0.70 ppb on weekends. The peak-to-peak values decreases from 17.56 ppb during the week to 15.41 ppb for weekends. The peak-to-peak difference thus decreases by 2.15 ppb on weekends. The observed weekend effect is most likely related to the decreased number of automobiles on roads on weekends relative to weekdays resulting in lower NO_x emissions on weekends. Therefore, there is less O_3 titration by NO_x in the mornings on weekends.
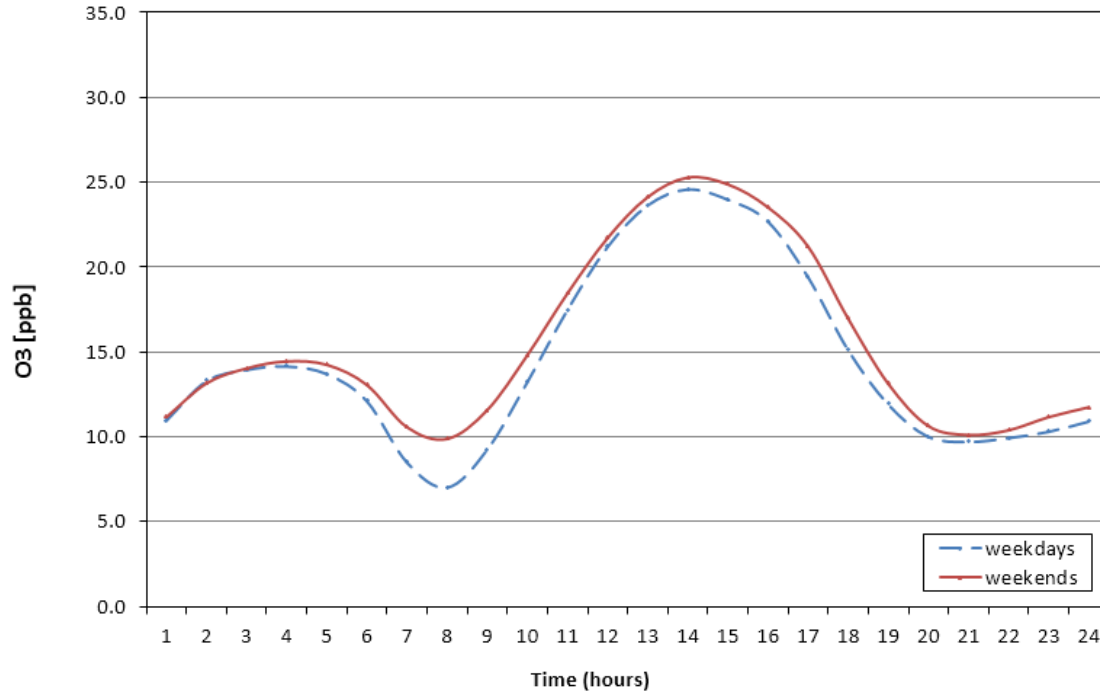
Figure 4.11: Average O_3 diurnal cycle for weekends and weekdays at Goodwood (2000 – 2006).

Figure 4.12 illustrates NO_x concentrations on weekends and weekdays at Goodwood. The times when NO_x levels are low coincide with high O_3 levels and vice versa, suggesting O_3 titration by NO_x. The trend is similar to that found by researchers at stations where NO_x is the main control on the weekend effect (e.g. Sadanaga *et al.* 2008). According to Debaje and Kakade (2006) higher O_3 on weekends is due to decreased NO_x emissions resulting in less NO_x titration of O_3. Jenkin *et al.* (2002), Palombo *et al.* (2006) and Sadanaga *et al.* (2012) reported that the VOC/NO_x ratio plays a critical role in weekend effect. On weekends O_3 concentrations are higher while NO_x and VOC emissions are lower, however it is hypothesised that there is more NO_x reduction than VOC reduction on weekends and the ratio of VOC to NO_x in the ambient air is likely to be greater on weekends relative to weekdays.
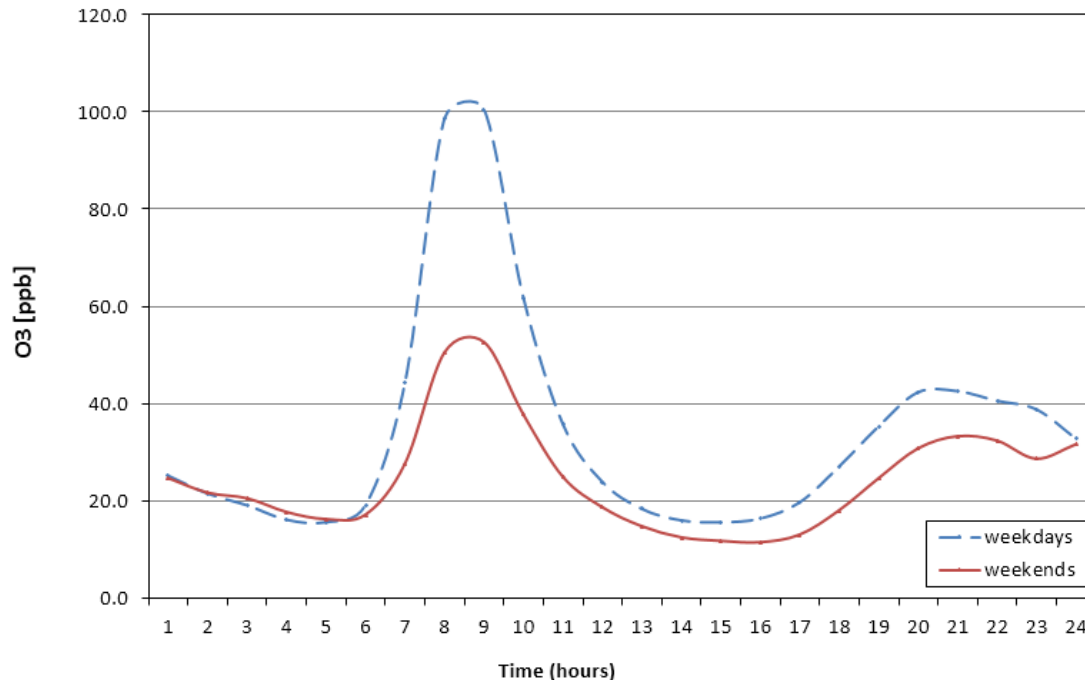
Figure 4.12: Average NO$_x$ diurnal cycle for weekends and weekdays at Goodwood (2000 – 2006).

4.4 Seasonal Cycles

This analysis is based on monthly average concentrations across the records. Three air intakes at Cape Point (Figure 4.13) demonstrate similar seasonal cycles with minima occurring between January and February and maxima between July and August for background measurements. This pattern of summer minima and winter maxima is seen in many locations both in the Northern and Southern Hemispheres, e.g. Barbados (13°N; 59°W) (Oltmans and Levy III, 1994) and Cape Grim (41°S; 145°E) (Ayers *et al.*, 1997). Other studies confirming this pattern include Logan (1985; 1999), Oltmans and Komhyr (1986) and Janach (1989).

The 14 m intake shows lower O$_3$ levels (by approximately 1 ppb relative to the 4 m and 30 m air intakes) in June (Figure 4.13a). In July 2009, the 14 m intake recorded approximately 1 ppb higher than the other two intakes. The 14 m intake data is for 2009 only, whereas the data for the other two intakes covers the period from 1997 to 2009, and this could explain the observed variations. Figure 4.13b shows a similar trend for all three intakes with an average deviation of 0.24 ppb between the 4 m and 14 m intake and 0.05 ppb between the 4 m and 30 m intakes when analyzing only the 2009 datasets for each intake height.

(a)
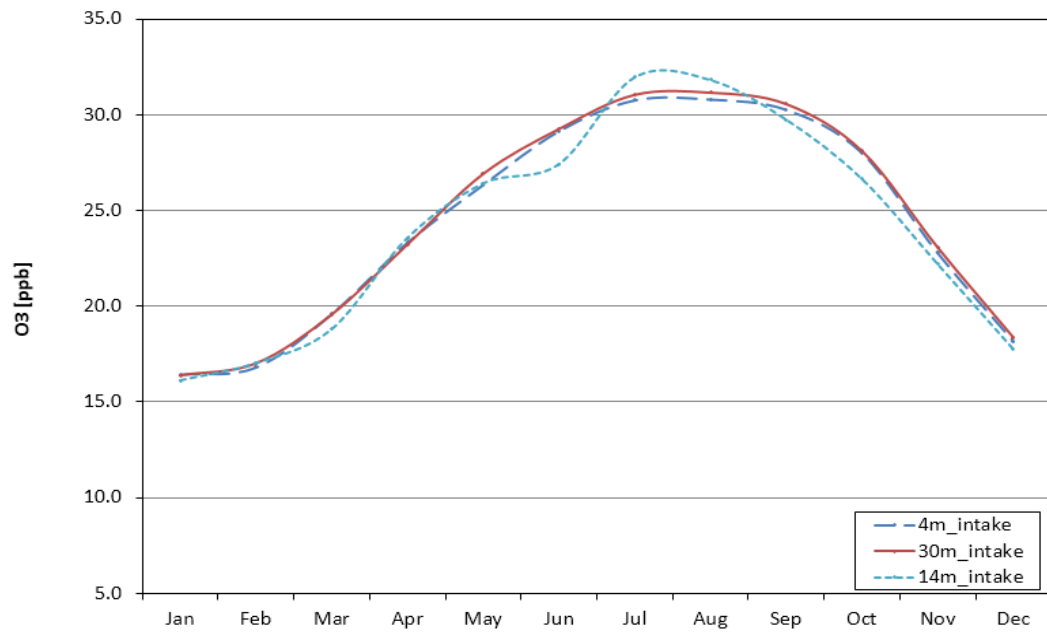
(b)
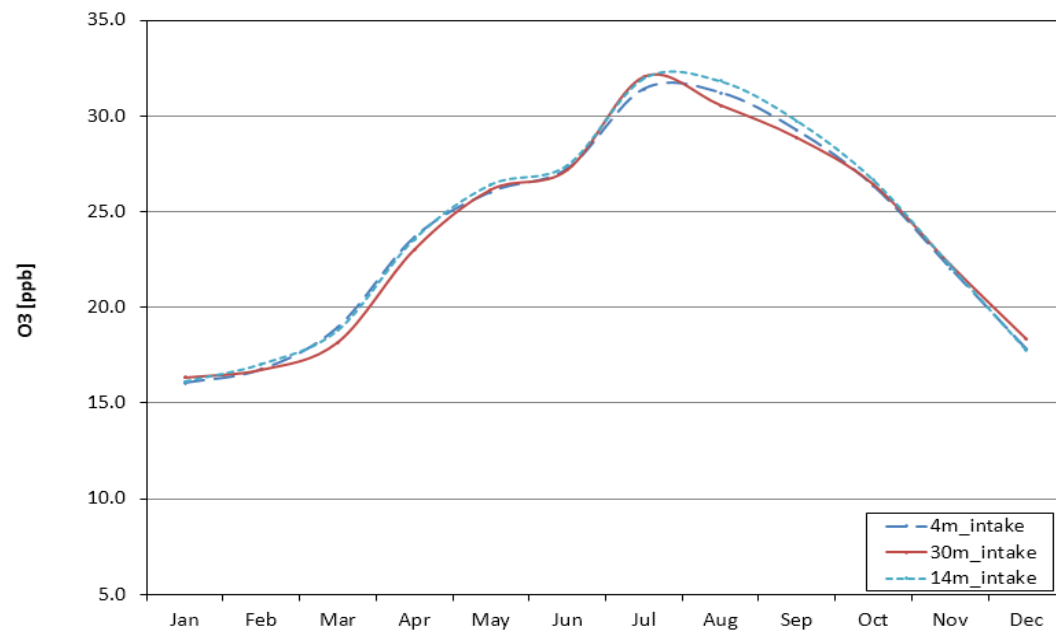
Figure 4.13: Average background O₃ monthly values at (a) 4 m, 30 m (1997 to 2009) and 14 m (2009) at Cape Point and (b) average O₃ monthly values at 4 m, 14 m and 30 m (2009) at Cape Point.

Figure 4.14 illustrates non-background O₃ monthly averages observed from the three air intakes at Cape Point. As reported for the Cape Point background data, the 14 m dataset shows some differences to the 4 m and 30 m intakes. Higher O₃ values of approximately 3 ppb in March are

observed for the 14 m intake relative to other two intakes while in May, the 14 m intake reads lower by approximately 3 ppb relative to other intakes (Figure 4.14a). When analysing only 2009 data (Figure 4.14b), all three intakes show a similar trend. It is thus suggested that these differences are a result of the differences in the lengths of the records (i.e. 14 m is only one year long while the others are thirteen years long allowing for greater variation).

The analysis below is based on the 2009 data where all intakes show a similar seasonal trend. An increase of 8.57 ppb, 11.15 ppb and 8.57 ppb from January to March observed for the 4 m, 14 m and 30 m intakes respectively. A decrease in O_3 levels is observed for all three intakes in April, followed by a sustained increase of 7.43 ppb, 7.72 ppb and 8.53 ppb to July for the 4 m, 14 m and 30 m intakes respectively (Figure 4.14b).

(a)
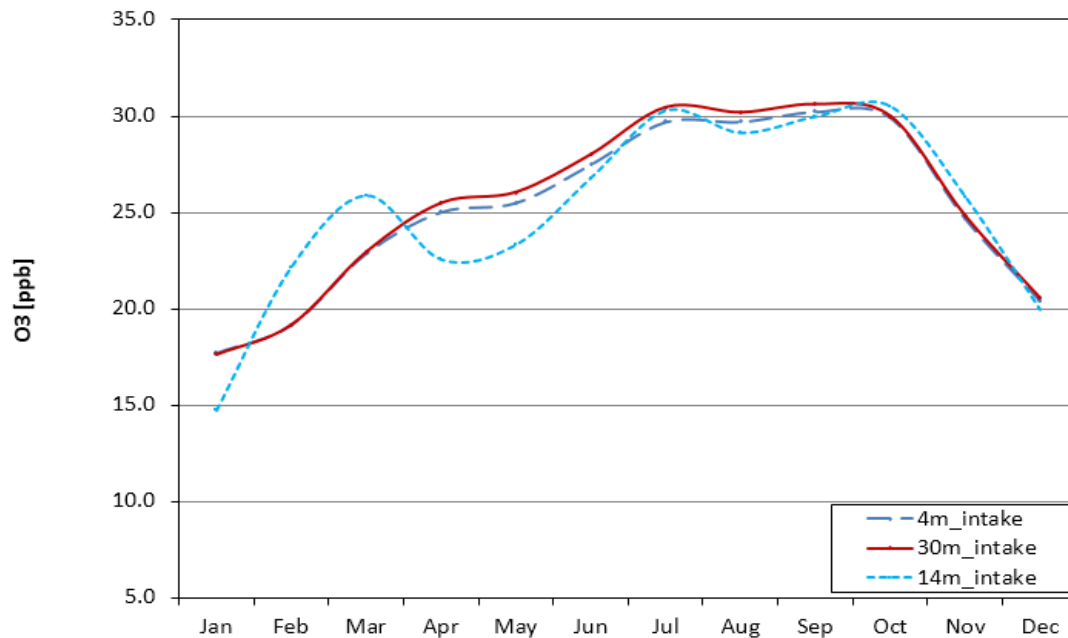
(b)
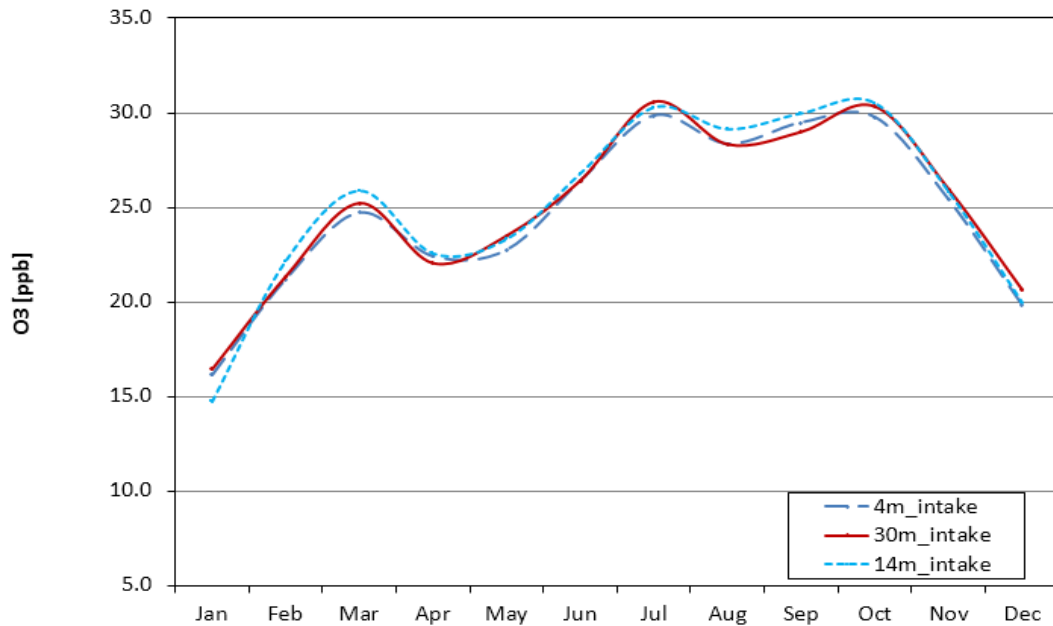
Figure 4.14: Average non-background O_3 monthly values at Cape Point (a) 4 m, 30 m (1997 to 2009) and 14 m (2009) and (b) at 4 m, 14 m and 30 m (2009).

Figure 4.15 illustrates monthly NO_x concentrations at Goodwood. A minimum of 27.5 ppb is observed in summer (January) while a maximum of 148.6 ppb is observed in winter (June). The effect of vehicular traffic and cold weather could be the reason of winter NO_x maxima although a narrower atmospheric mixing depth over this time is likely to play a significant role in increasing concentrations.
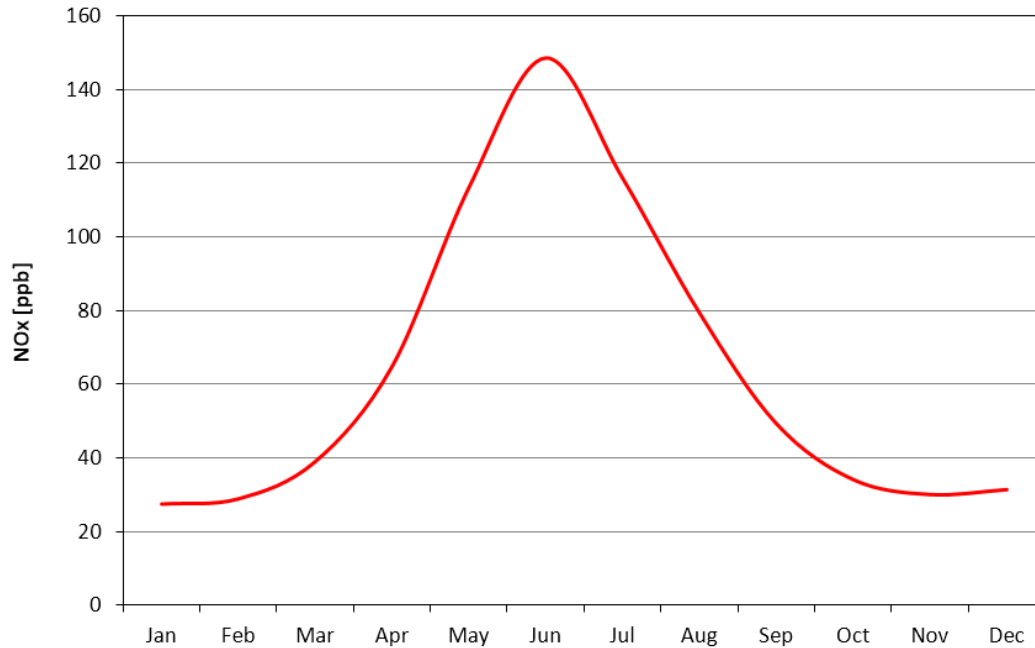
Figure 4.15: Average NO$_x$ monthly values at Goodwood (2000 – 2006).

Cape Point background station and SANAE experience their minima in summer (January) and maxima in winter (July or August). In late spring and winter months (April to August), concentrations at SANAE are higher by an average of approximately 2 ppb relative to Cape Point background concentrations (Figure 4.16). A minimum of 16.32 ppb is observed at SANAE and 16.70 ppb at Cape Point background, while the maximum at SANAE is 33.20 ppb and 31.05 ppb at Cape Point background. These result in peak-to-peak values of 16.88 ppb at SANAE and 14.36 ppb for Cape Point background. The SANAE peak-to-peak value falls within the range of 9 to 20 ppb as reported by Helmig *et al.* (2007) for polar stations in the Southern Hemisphere.
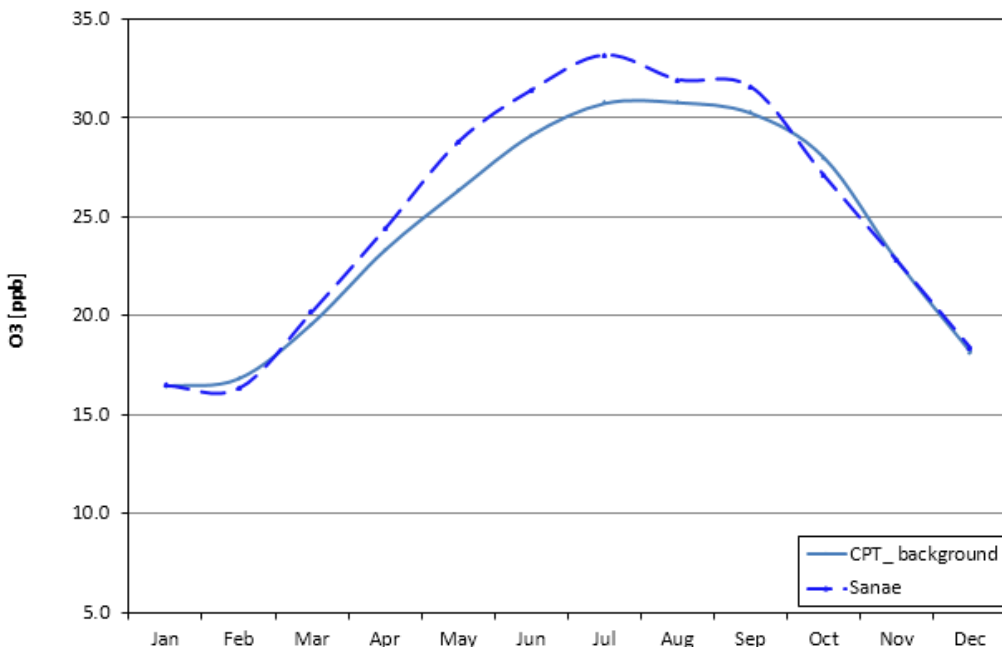
Figure 4.16: Average O_3 monthly values at Cape Point and SANAE (2002 – 2009).

The urban sites show maxima in October, and minima in May and June for Molteno and Goodwood respectively (Figure 4.17). The Cape Point non-background seasonal cycle is comparable to the Molteno and Goodwood sites except that the minimum occurs in summer with a peak-to-peak value of 12.31 ppb compared to 8.79 ppb for Molteno and 6.11 ppb for Goodwood. Results thus reveal lower O_3 peak-to-peak values for the Cape Town region relative to Cape Point. These results highlight the importance of NO_x in O_3 formation. At Molteno and Goodwood O_3 levels decrease during the autumn/winter months (April to June) but this trend is not clearly visible in the Cape Point non-background data. During this period, NO_x levels are at their highest at Goodwood (Figure 4.15 above). A spring O_3 maximum (October) is evident in all three records (Figure 4.17). The reason for this maximum is not clear. There is debate on the causes of this peak but various studies have suggested that PAN and NO_x also peak at this time (e.g. Bottenheim *et al.*, 1994; Sirois and Bottenheim, 1995; Sorteberg *et al.*, 1998; Solberg *et al.*, 1997; Fenneteaux *et al.*, 1999). At Goodwood, a NO_x maximum is not linked to the O_3 spring maximum as NO_x shows its maximum in winter. Liu *et al.* (1987) proposed that the observed O_3 spring maximum is due to the long O_3 winter lifespan of 200 days and he concluded that the observed spring amplitude could be the result of O_3 accumulation during the winter months.

Other studies (e.g. Wang *et al*., 1998; Jaffe *et al*., 2003) in the Northern Hemisphere have associated spring maxima with the intercontinental transport of pollution.
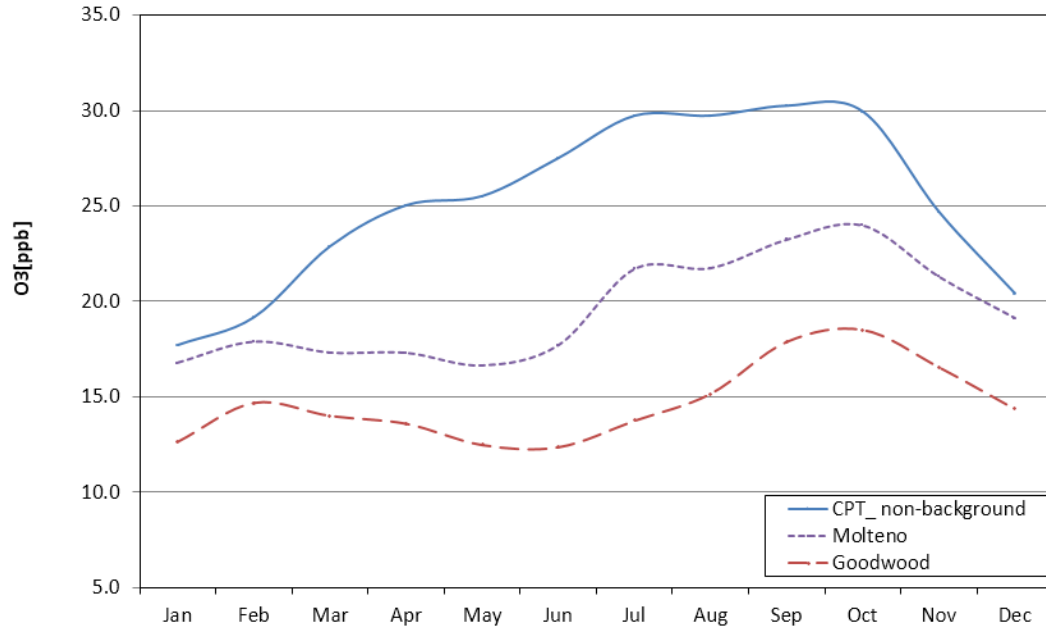
Figure 4.17: Average O_3 monthly values at Cape Point, Molteno and Goodwood (2000 – 2006).

4.5 Weekday and Weekend Seasonal Cycles

Average monthly O_3 levels at SANAE (Figure 4.18) are similar on weekends and weekdays with insignificant differences occurring in late summer and springtime (Feb-May) when average weekend values are slightly higher that weekday values. The 'weekend effect' thus does not have a significant influence on this record.
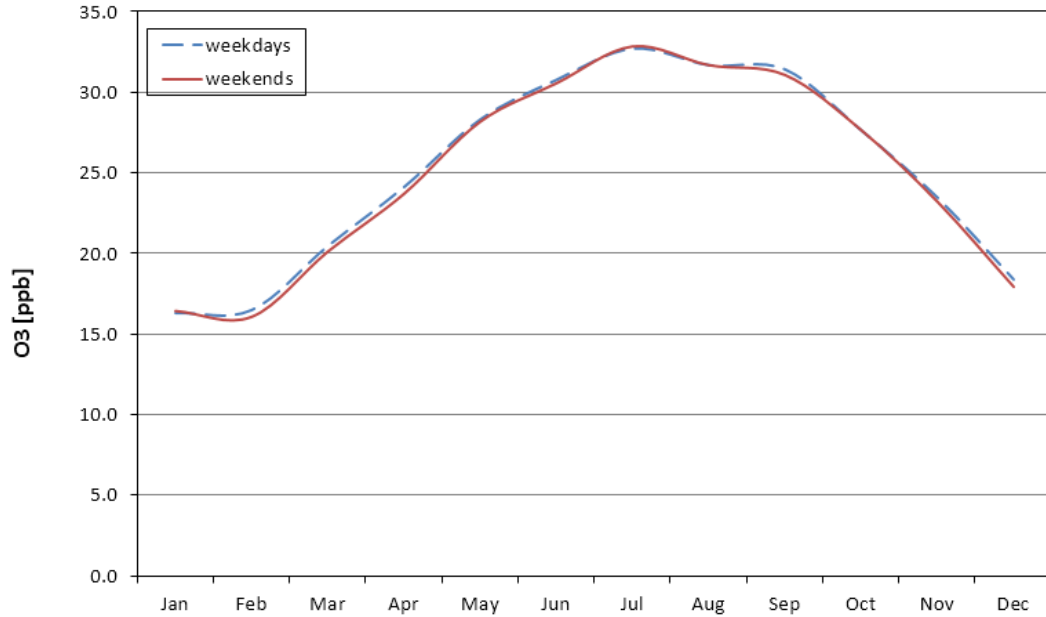
Figure 4.18: Monthly O$_3$ concentrations for weekdays and weekends at SANAE (2002 – 2006).

Cape Point background monthly average concentrations (Figure 4.19) on the weekend are either similar or higher than average weekday concentrations for most months of the year, expect for August, October and December when average weekday concentrations are higher. It is suspected that some of the higher weekend concentration months are an artifact of the separation process into background and non-background values rather than indicators of the influence of the 'weekend effect'.
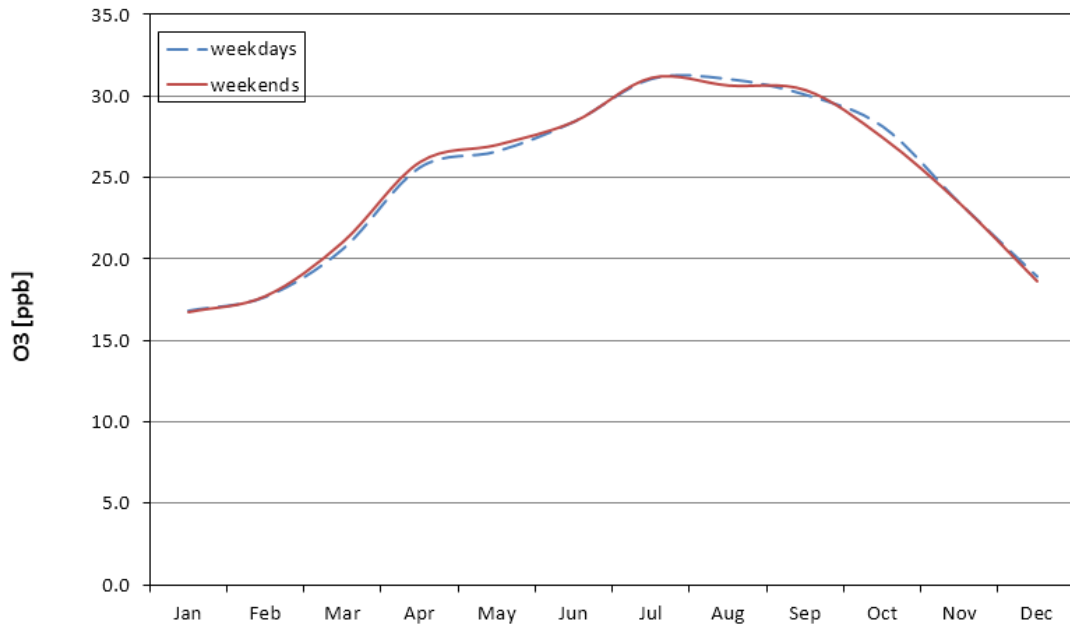
Figure 4.19: Monthly background O_3 concentrations for weekdays and weekends at Cape Point (2002 – 2006).

At Cape Point non-background (Figure 4.20), average weekend concentrations of O_3 are higher than weekdays during January, February, June, July and August, while average weekday concentrations are higher during the rest of the year. The 'weekend effect' may explain elevated weekend concentrations in the winter months of June to August. The differences between weekend and weekday concentrations are less pronounced during the summer months of January and February. NO_x is the driving factor for the weekend effect. At Goodwood (Figure 4.21), average monthly weekday NO_x concentrations are higher than average weekend concentrations throughout the year. In winter months, however, the difference between weekends and weekday concentrations can reach more than 20 ppb. This is likely to be related to two key factors. First, and most importantly, increased temperatures during summer increases atmospheric turbulence and the dilution of pollutants, thereby decreasing their concentrations. Thus vehicular emissions of NO_x will be more diluted and have less effect. Second, the average number of vehicles on the roads are likely to be lower during the warmer (and drier) months as conditions are more conducive to walking, cycling or waiting outside for public transport. A further investigation is required with vehicular statistics in summer and winter.
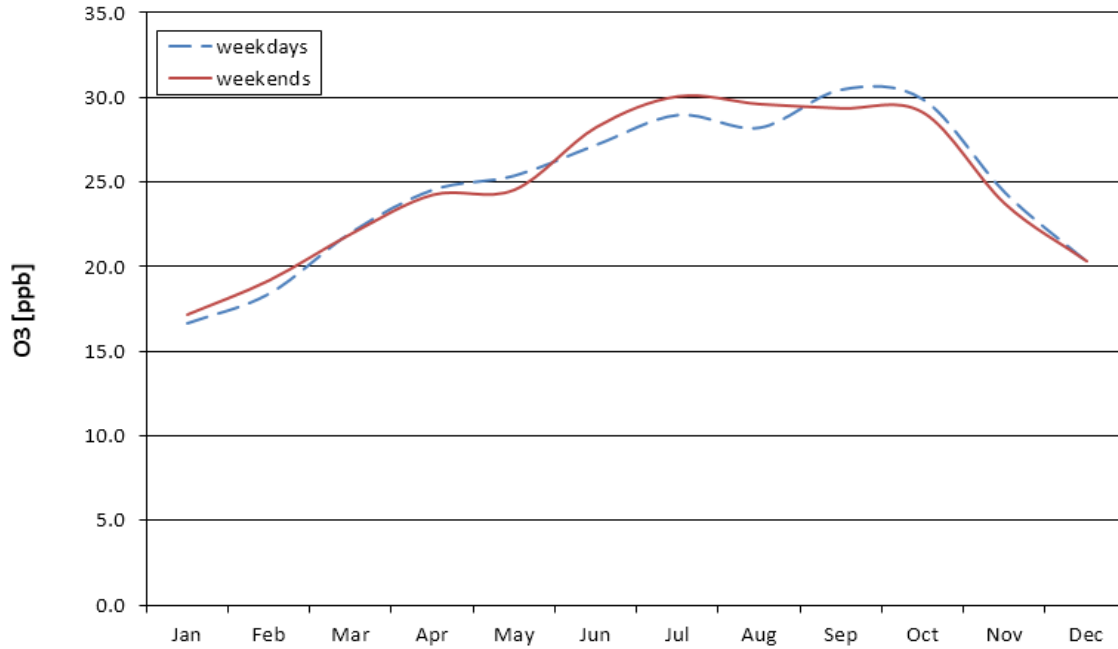
Figure 4.20: Monthly O_3 non-background concentrations for weekdays and weekends Cape Point (2002 – 2006).
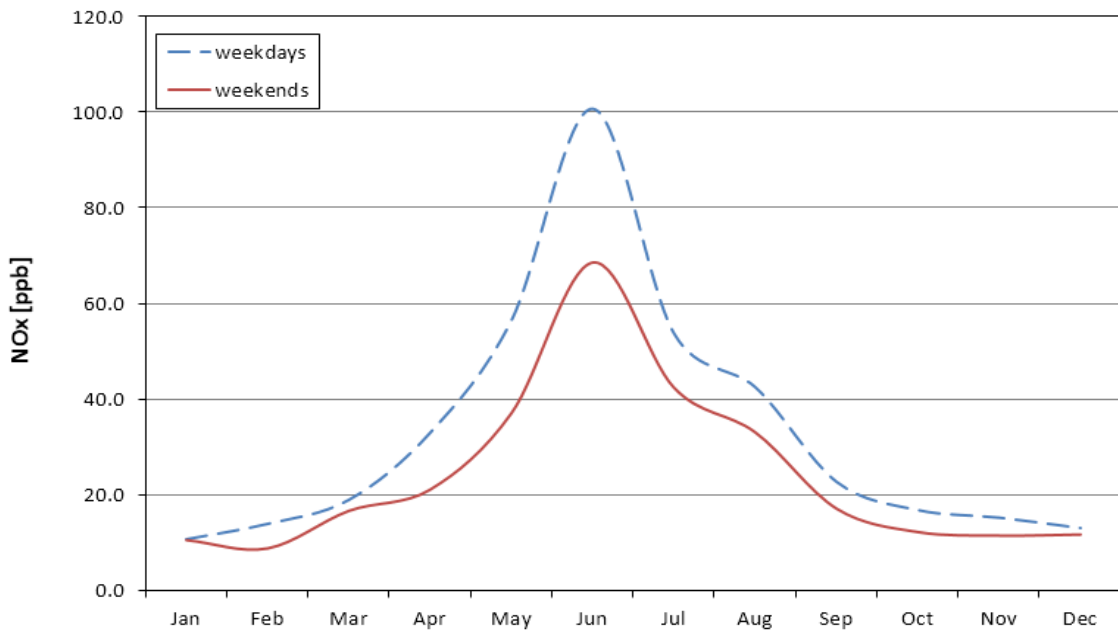
Figure 4.21: Monthly NO_x concentrations for weekdays and weekends in Goodwood (2000 – 2006).

At Molteno, average monthly weekday concentrations are lower than average monthly weekend concentrations except during July and December (Figure 4.22). The weekend effect may explain the more pronounced differences between higher weekend and lower weekday values during

March, April, June and September. The weekend effect is least evident during the summer months (December to February) due to the seasonal pattern in weekday and weekend NO_x described above with greater differences between weekday and weekend NO_x concentrations during winter.
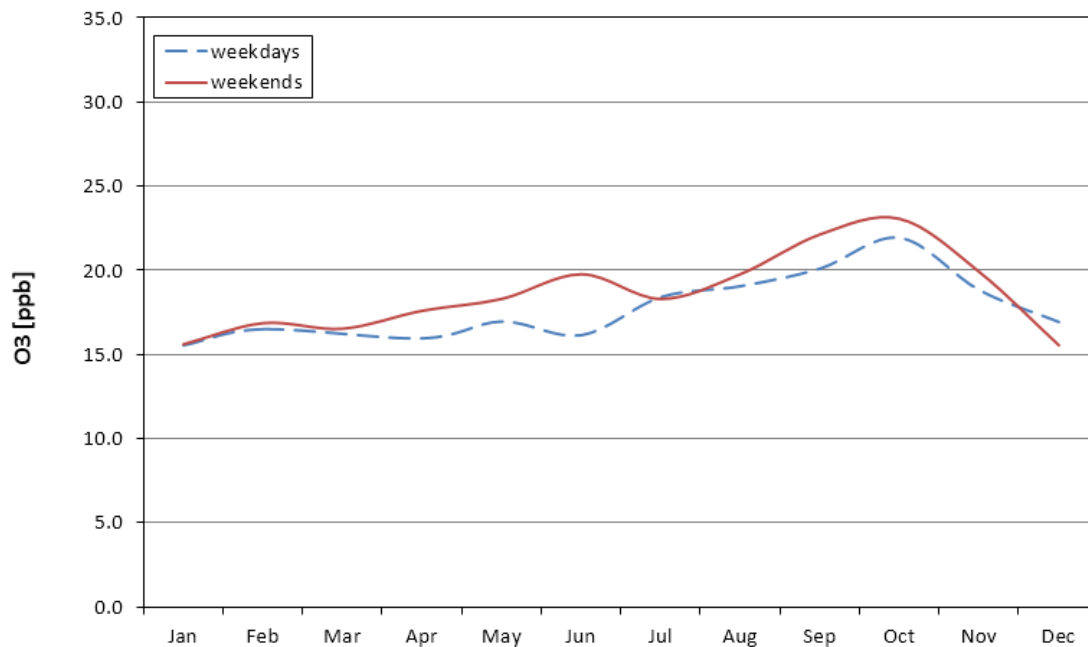
Figure 4.22: Monthly O_3 concentrations for weekdays and weekends in Molteno (2002 – 2006).

At Goodwood (Figure 4.23), average monthly weekday concentrations are lower than average weekend concentrations during all months except for January, September, October and December. The weekend effect may explain the particularly pronounced differences between higher weekend concentrations and lower weekday concentrations for April, June and August. The weekend effect is least apparent during some spring and summer months (September, October, December and January). It is suggested that the reasons for this follow the explanation described for Molteno above.
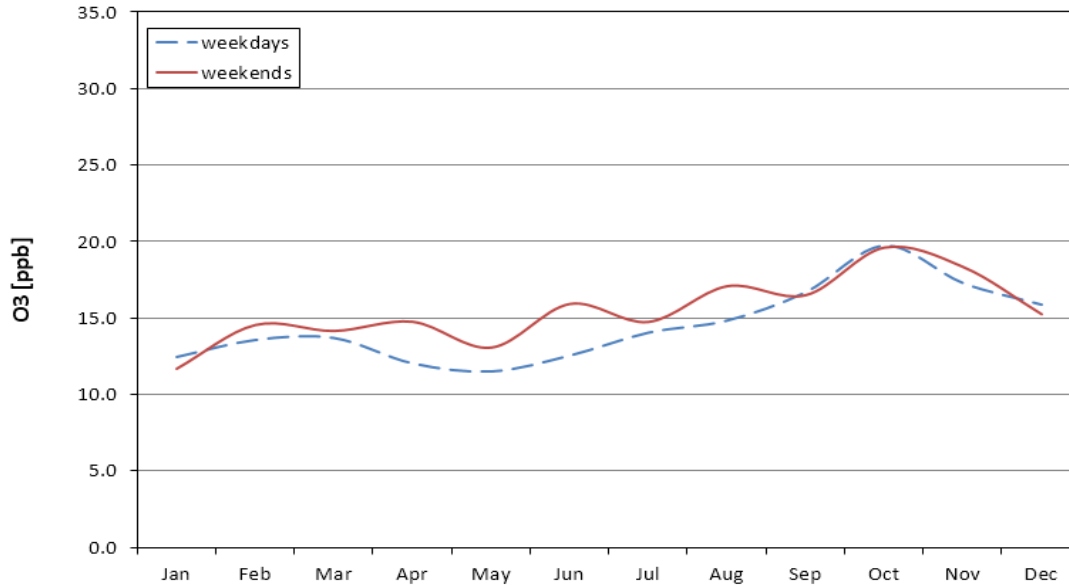
Figure 4.23: Monthly O$_3$ concentrations for weekdays and weekends in Goodwood (2000 – 2006).

Figure 4.24a illustrates the positive correlation between the weekday monthly averages at Cape Point non-background and Molteno. The relationship is significant at the 95% confidence level ($p = 0.01$, $r = 0.62$, $r^2 = 0.38$). Figure 4.24b shows the positive correlation between the weekday monthly averages at Cape Point non-background and Goodwood. The relationship is not significant at the 95% confidence level ($p = 0.191$, $r = 0.41$, $r^2 = 0.16$).

(a)

(b)
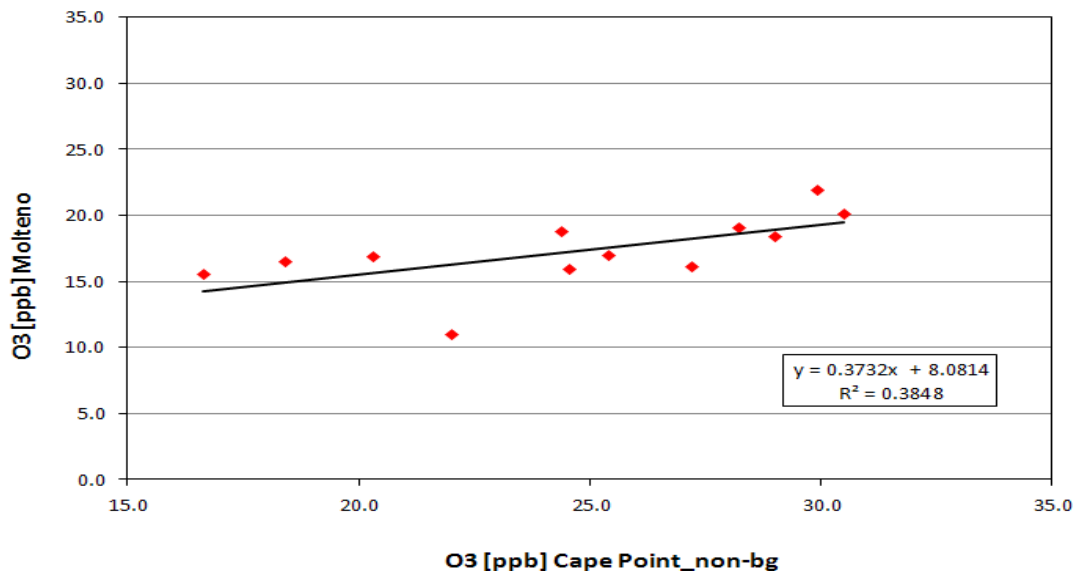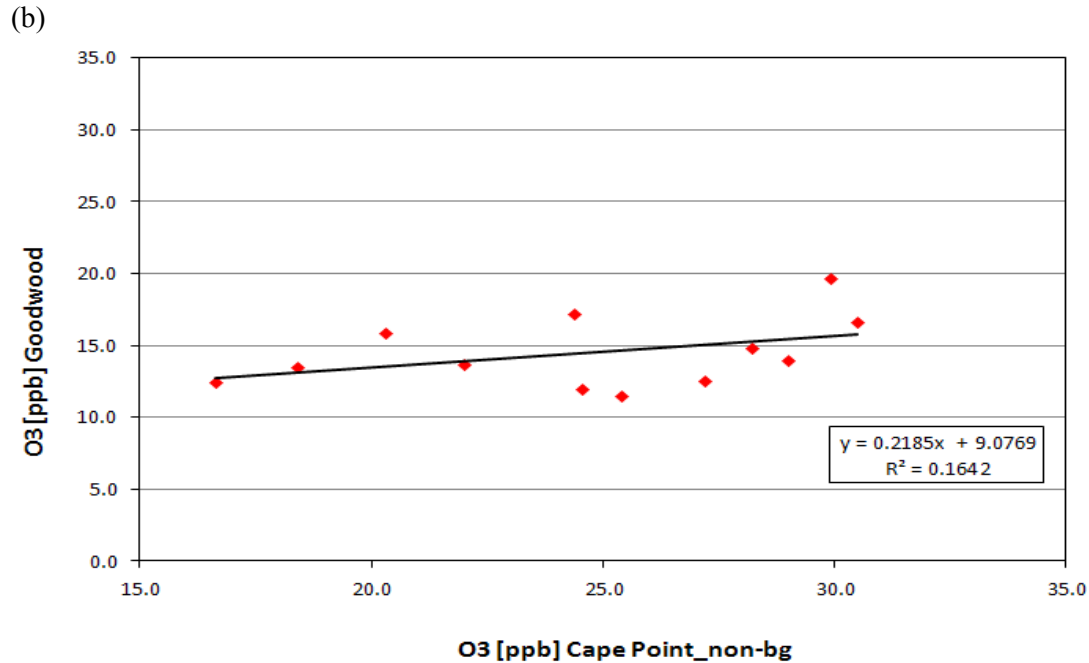
Figure 4.24: Correlations between average weekday concentrations of non-background O_3 at (i) Cape Point and Molteno and at (b) Cape Point and Goodwood from 2000 – 2006.

Figure 4.25a illustrates the strong positive correlation between the weekend monthly averages at Cape Point non-background station and Molteno. The relationship is significant at the 95% confidence level (p = 0.00, r = 0.80, r^2 = 0.64). Figure 4.25b shows the positive correlation between the weekend monthly averages at Cape Point non-background and Goodwood. The relationship is significant at the 95% confidence level (p = 0.04, r = 0.60, r^2 = 0.36). The correlation is higher for weekends than weekdays at Molteno and Goodwood. This observation can be explained by the higher concentrations of NO_x during the week at the urban stations, which influences levels of O_3 at Molteno and Goodwood. On weekends, lower NO_x at Molteno and Goodwood means that these stations show an increasing similarity with the Cape Point Station (non-background data), which is located some distance from traffic sources.

(a)
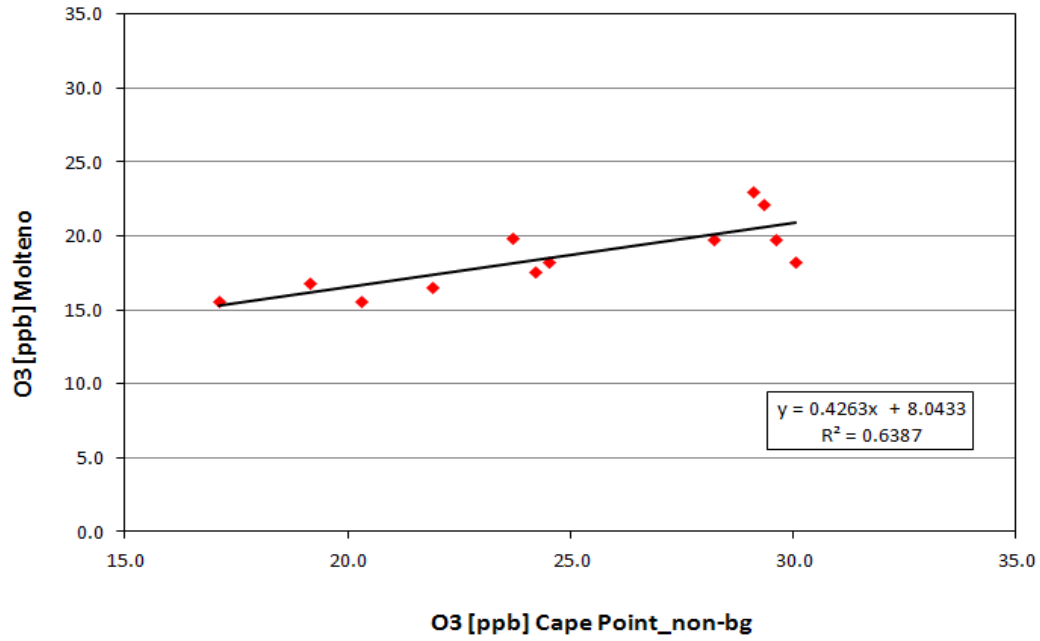
(b)
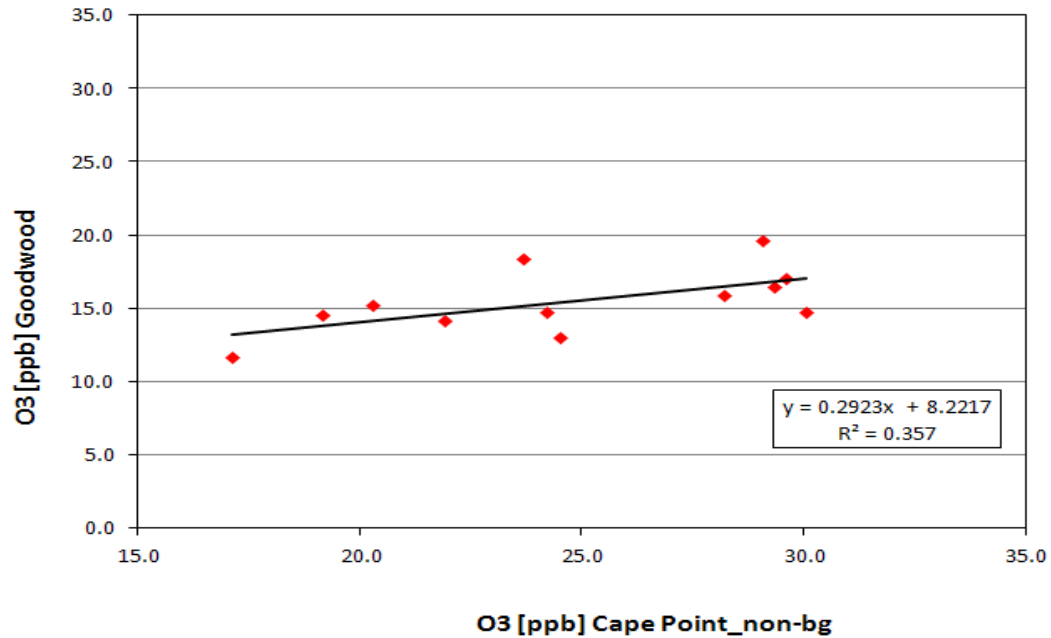
Figure 4.25: Correlations between average weekday concentrations of O_3 at (a) Cape Point non-background data and Molteno from 1997 – 2007 and at (b) Cape Point non-background and Goodwood from 2000 – 2006.

4.6 Angular Distribution of O₃

Angular distribution of ozone was worked out in this study as a function of wind direction. The closest station to SANAE that measures wind direction is Vesleskarvet station. Figure 4.26 illustrates the seasonal angular distribution of O_3 at SANAE as a function of wind direction measurements at Vesleskavet. Each sectoral component is the average ozone concentration measured during winds from that sector over the season of focus. SANAE is dominated by winds originating from the east with lowest frequencies from the north and north-east.

In summer (Fig. 4.26a), average O_3 levels are lower relative to other seasons. A somewhat uniform O_3 distribution is observed during this season with a maximum sectoral average concentration of 17.43 ppb from south-west and a minimum sectoral average of 16.06 ppb from the north-north-east. A difference of 1.37 ppb between maximum and minimum sectoral averages is recorded in summer.

Autumn is the season with the second lowest seasonal average (Fig. 4.26b). During this season, highest average concentrations are observed from the north with an average of 26.71 ppb while the sectoral minimum (22.46 ppb) is from the south. A difference of 4.26 ppb between maximum and minimum sectoral averages is recorded in autumn.

In winter, a more uniform O_3 distribution is observed with the lowest sectoral average of 30.20 ppb from the west and the highest sectoral average average levels of 33.00 ppb from the south-east (Fig. 4.26c). A difference of 2.80 ppb between maximum and minimum sectoral averages is recorded during this season.

Minimum concentrations observed in spring (22.48 ppb) (Fig. 4.26d) are similar to those recorded in autumn but are from the north. The maximum sectoral average of 30.79 ppb is observed from south-south-east. A difference of 8.30 ppb between maximum and minimum sectoral averages is recorded in spring. This sudden decrease of O_3 from the north (with an average of 8 ppb) was reported previously by Labuschagne *et al.* (2003).

Figure 4.26: Seasonal angular distribution of O$_3$ (ppb) as a function of wind direction at SANAE (2002 – 2009).

Figure 4.27 illustrates seasonal angular distribution of O$_3$ as a function of wind at Cape Point background.

In summer (Figure 4.27a), a somewhat uniform distribution of O$_3$ concentrations is evident, with a maximum sectoral average of 17.00 ppb from the south-east and a minimum sectoral average of 16.21 ppb from the north-north-west. A difference of 0.80 ppb between maximum and minimum sectoral averages is recorded during this season.

In autumn, a maximum sectoral average of 22.88 ppb is recorded from the west-north-west with and a minimum sectoral average of 21.40 ppb is observed from the south-south-east (Figure

4.27b). A difference of 1.47 ppb between maximum and minimum sectoral averages is recorded during this season.

In winter, minimum sectoral average concentrations (29.88 ppb) are observed from the north-north-west with a maximum sectoral average of 31.06 ppb from the west (Figure 4.27c). A difference of 1.18 ppb between maximum and minimum sectoral averages is recorded during this season.

Higher concentrations are observed in spring from the west and west-north-west with a maximum sectoral average of 27.32 ppb. The lowest sectoral average of 26.00 ppb is recorded from the east (Figure 4.27d). A difference of 1.33 ppb between maximum and minimum sectoral averages is recorded during this season.

(a)

(b)

(c)

(d)

Figure 4.27: Seasonal angular distribution of O_3 (ppb) as a function of wind direction in Cape Point background (1997 – 2009).

Figure 4.28 illustrates seasonal angular distribution of O_3 as a function of wind at Cape Point non-background.

In summer (Figure 4.28a), a somewhat uniform distribution of O_3 concentrations is evident, with a maximum sectoral average of 19.58 ppb from the west-north-west and a minimum sectoral average of 17.83 ppb from the east. A difference of 1.75 ppb between maximum and minimum sectoral averages is recorded during this season.

In autumn, a maximum sectoral average of 25.02 ppb is recorded from the west-north-west and a minimum sectoral average of 22.95 ppb is observed from the south-south-east (Figure 4.28b). A difference of 2.07 ppb between maximum and minimum sectoral averages is recorded during this season.

In winter, the minimum sectoral average concentration (26.22 ppb) is observed from the north-north-east while a maximum sectoral average of 31.38 ppb is observed from the west-south-west to west (Figure 4.28c). A difference of 5.17 ppb between maximum and minimum sectoral averages is recorded during this season.

Higher concentrations are observed in spring from the west and west-north-west with a maximum sectoral average of 31.03 ppb (Figure 4.28d). The lowest sectoral average of 26.98 ppb is recorded from the east. A difference of 4.04 ppb between maximum and minimum sectoral averages is recorded during this season.

(a)

(b)

(c)

(d)
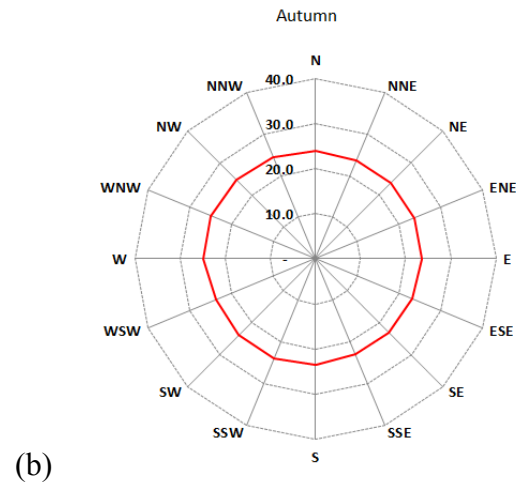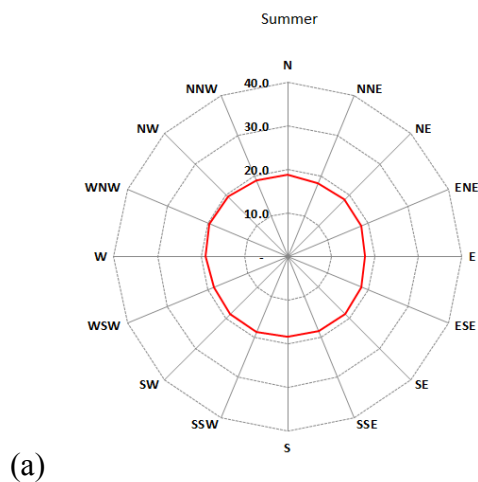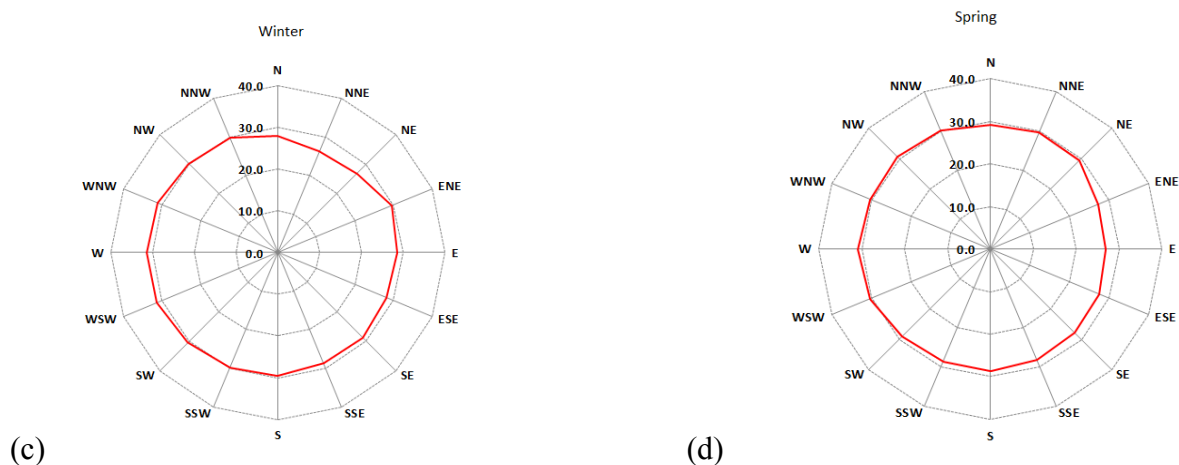
Figure 4.28: Seasonal angular distribution of O_3 (ppb) as a function of wind direction in Cape Point non-background (1997 – 2009).

Figure 4.29 illustrates seasonal angular distribution of O_3 at Molteno as a function of wind direction measurements at Cape Town weather office.

In summer (Figure 4.29a), the maximum sectoral average of 19.42 ppb occurs from the south-south-east while the minimum sectoral average of 11.29 ppb is observed from the north-north-east and south-east. A difference of 8.13 ppb between maximum and minimum sectoral averages is recorded during this season.

In autumn, a maximum sectoral average of 19.52 ppb is recorded from the south and a minimum sectoral average of 11.15 ppb is observed from the east-south-east (Figure 4.29b). A difference of 8.37 ppb between maximum and minimum sectoral averages is recorded during this season.

In winter, minimum sectoral average concentrations (15.61 ppb) are observed from the north-east with a maximum sectoral average of 23.84 ppb from the north-west (Figure 4.29c). A difference of 8.23 ppb between maximum and minimum sectoral averages is recorded during this season.

Higher concentrations are observed in spring from the west with a maximum sectoral average of 24.38 ppb (Figure 4.29d). The lowest sectoral average of 16.67 ppb is recorded from the north-east. A difference of 7.71 ppb between maximum and minimum sectoral averages is recorded during this season.
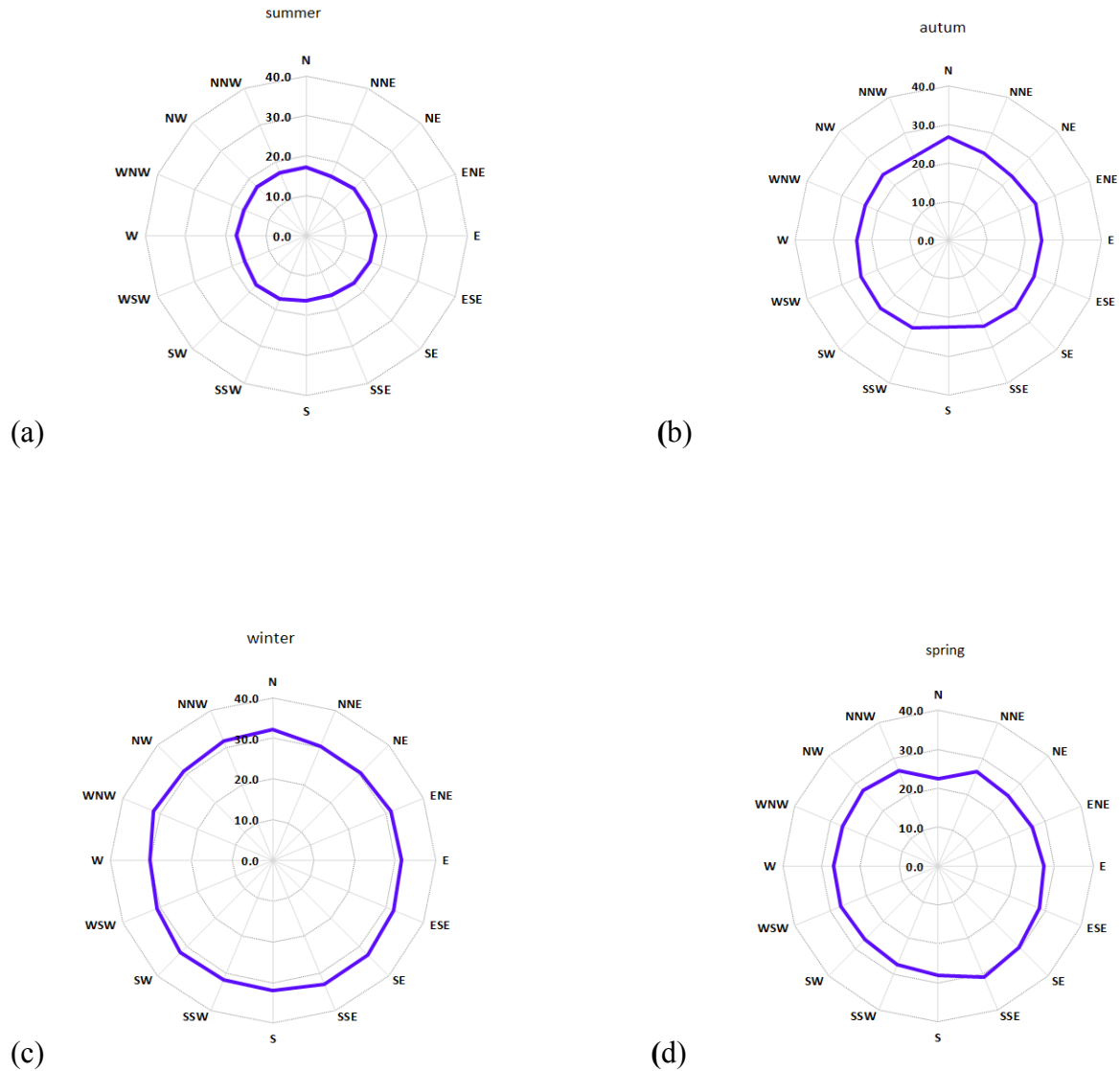
(a)

(b)

(c)

(d)
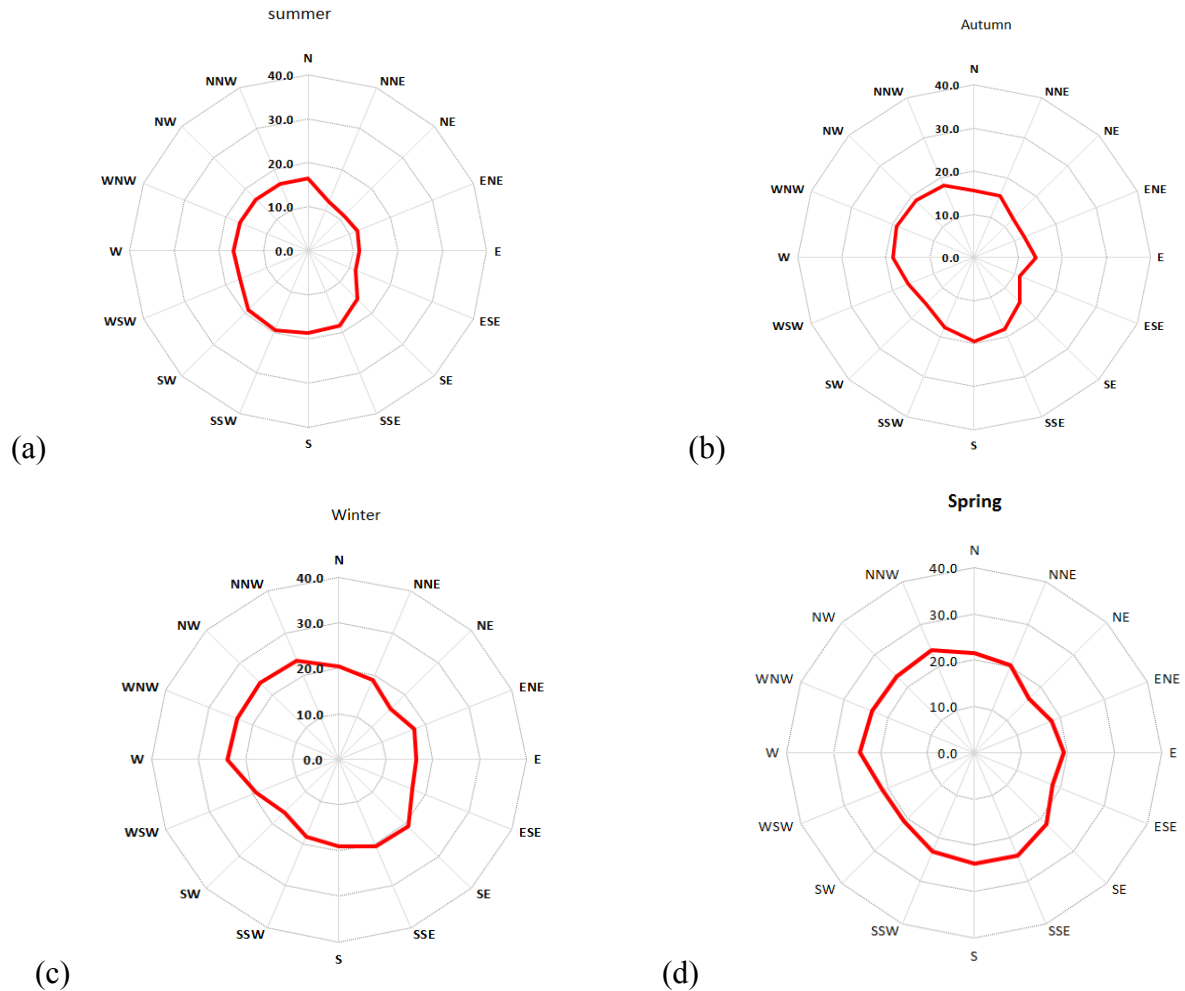
Figure 4.29: Seasonal angular distribution of O_3 as a function of wind direction in Molteno (1997 – 2007).

Figure 4.30 illustrates seasonal angular distribution of O_3 and NO_x at Goodwood as a function of wind direction measurements at Cape Town weather office.

In summer (Figure 4.30a), a maximum sectoral average of 15.49 ppb is observed from the south-south-east and a minimum sectoral average of 6.30 ppb is observed from the north-east. A difference of 9.20 ppb between maximum and minimum sectoral averages is recorded during this season.

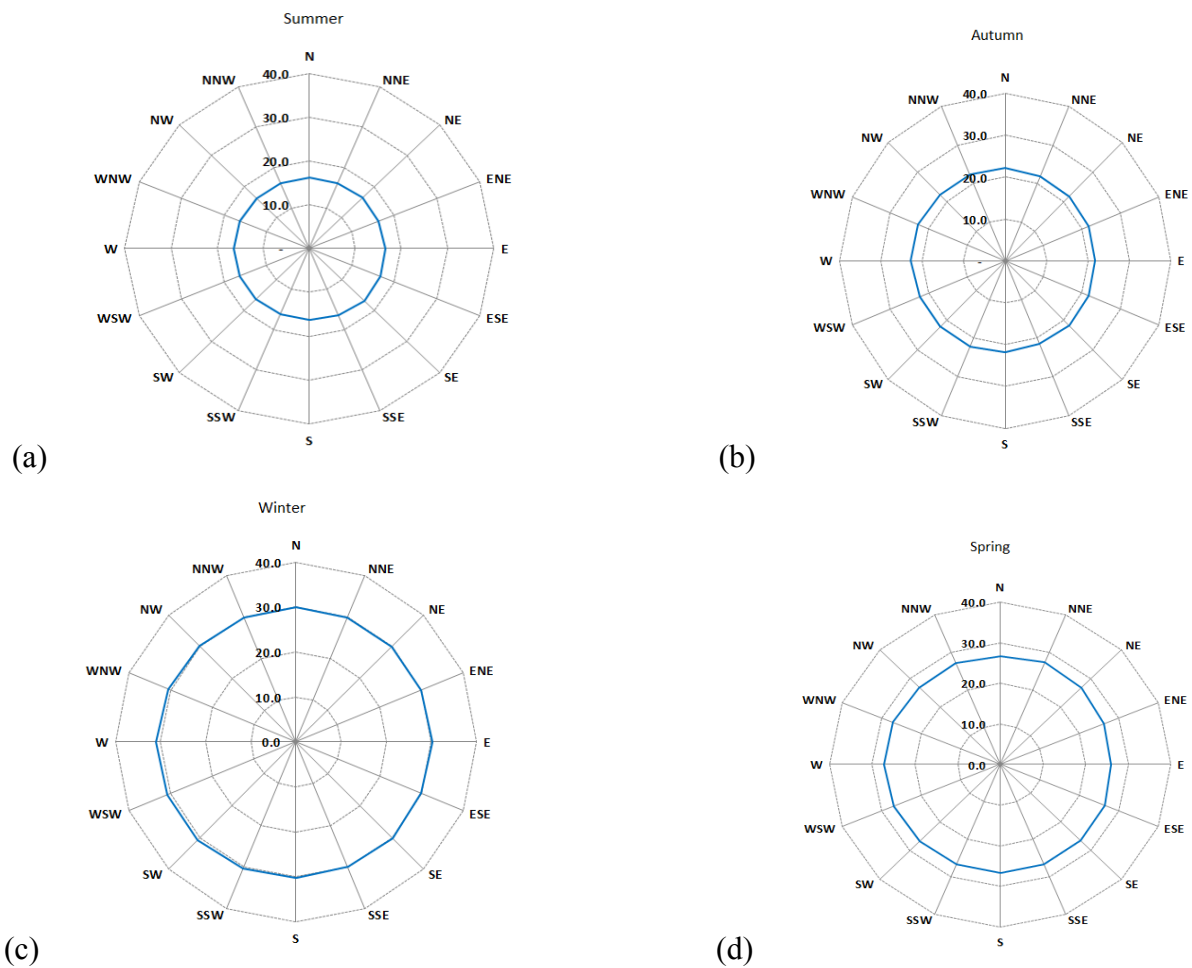In autumn, a maximum sectoral average of 16.10 ppb is recorded from the south and a minimum sectoral average of 6.20 ppb is recorded from the east-south-east (Figure 4.30b). A difference of 9.89 ppb between maximum and minimum sectoral averages is recorded during this season.

In winter, minimum sectoral average concentrations (5.74 ppb) are observed from the east while the maximum sectoral average of 17.60 ppb is observed from the west-north-west (Figure 4.30c). A difference of 11.86 ppb between maximum and minimum sectoral averages is recorded during this season.

Higher concentrations are observed in spring from the west-north-west with a maximum sectoral average of 19.72 ppb. The lowest sectoral average of 6.43 ppb is recorded from the east-north-east (Figure 4.30d). A difference of 13.29 ppb between maximum and minimum sectoral averages is recorded during this season.

Sectors with higher O_3 concentrations coincide with lower NO_x concentrations and vice versa. Thus stations with greater differences between sectoral maxima and minima values indicate the influence of NO_x sources in the direction of the O_3 minima. These observations are a reflection of theory (Section 4.1, Equation 3). Equation 3 shows O_3 titration by NO_x, with higher levels of NO_x causing decreases in O_3 concentrations. Higher NO_x levels from north-east to east can be related to traffic peaks from surrounding areas. Neighbourhood sources of NO_x in Goodwood include traffic at the Shell Petrol Station, traffic on Hugo Street, traffic on the corner of Milton Street, traffic at neighbouring schools (Fairbarn College, Hoerskool President), traffic at the proximate vehicle testing station, traffic at the Municipal buildings on Hugo Street, traffic on the N1, traffic on Giel Basson Road, and traffic on Frans Conradie Road. These sources of NO_x are listed in order of proximity to the Goodwood station.

(a)

(b)

(c)

(d)
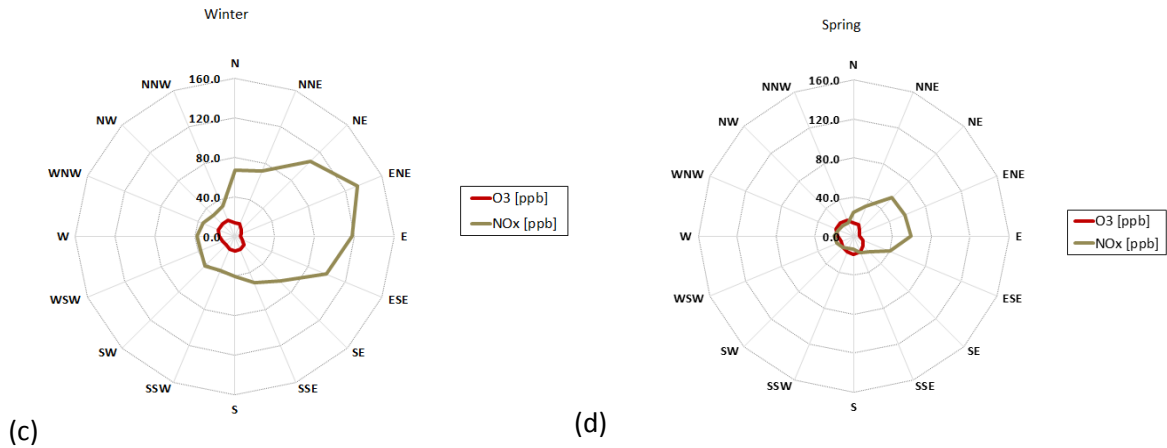
Figure 4.30: Seasonal angular distribution of O_3 and NO_x as a function of wind direction in Goodwood (2000 – 2006).

Figure 4.31 illustrates the angular distribution of NO_x at Goodwood as a function of wind direction measurements at the Cape Town weather office. Data was filtered according to time, specifically morning traffic hours (06:00 to 09:00) and other times (20:00 to 05:00 and 10:00 to 15:00). During morning traffic hours, higher values of NO_x are observed in all sectors relative to other times. These high values are related to a number of factors including increased traffic emissions and the persistence of an early morning inversion layer. The inversion layer is more evident in the morning hours and in winter months. The morning traffic maximum is much higher (by 133.95 ppb) than the other times. Outside of the traffic period, NO_x levels decrease due to fewer vehicular sources. Atmospheric instability also generally increases during the course of the day after the morning inversion is lifted.
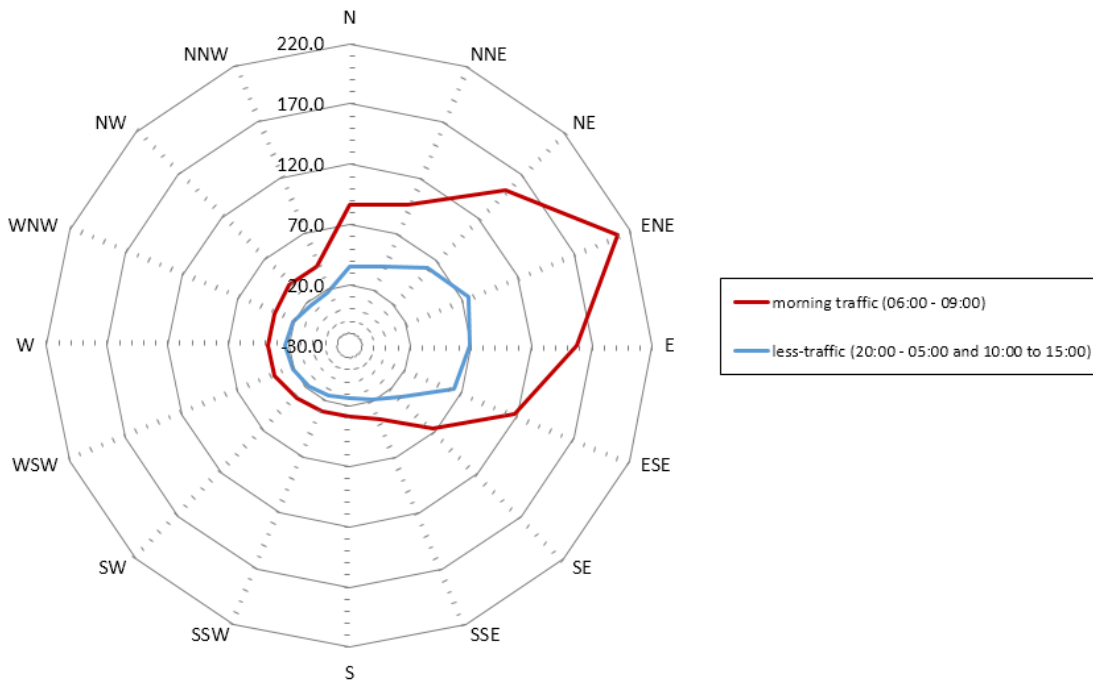
Figure 4.31: Angular distribution of NO_x at Goodwood as a function of wind direction for morning traffic and other times (2000 – 2006).

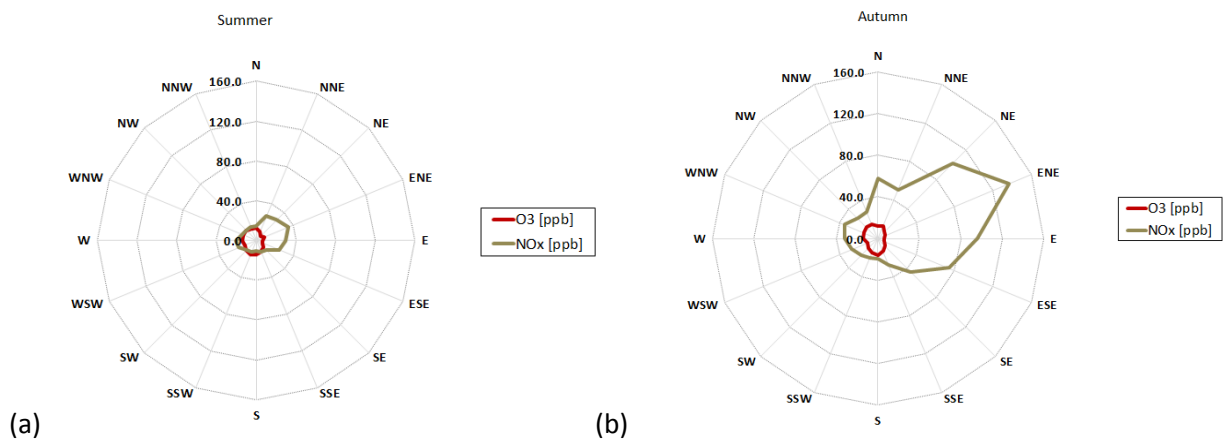Figure 4.32 illustrates the angular distribution of NO_x at Goodwood as a function of wind direction measurements at Cape Town weather office. Data was filtered according to time, afternoon traffic hours (16:00 to 19:00) and other times (20:00 to 05:00 and 10:00 to 15:00). During the afternoon traffic hours, higher values of NO_x are observed. The difference between afternoon maximum NO_x and the maximum at other times is 32.16 ppb. The afternoon maximum is much lower (by 101.79 ppb) than the morning traffic maximum. One possible explanation for this is that the afternoon peak traffic period occurs after much of the school traffic whereas in the mornings, school traffic occurs at the same time with other traffic. A more pertinent explanation is that atmospheric instability and thus dispersion and dilution is stronger in the afternoons relative to the mornings.
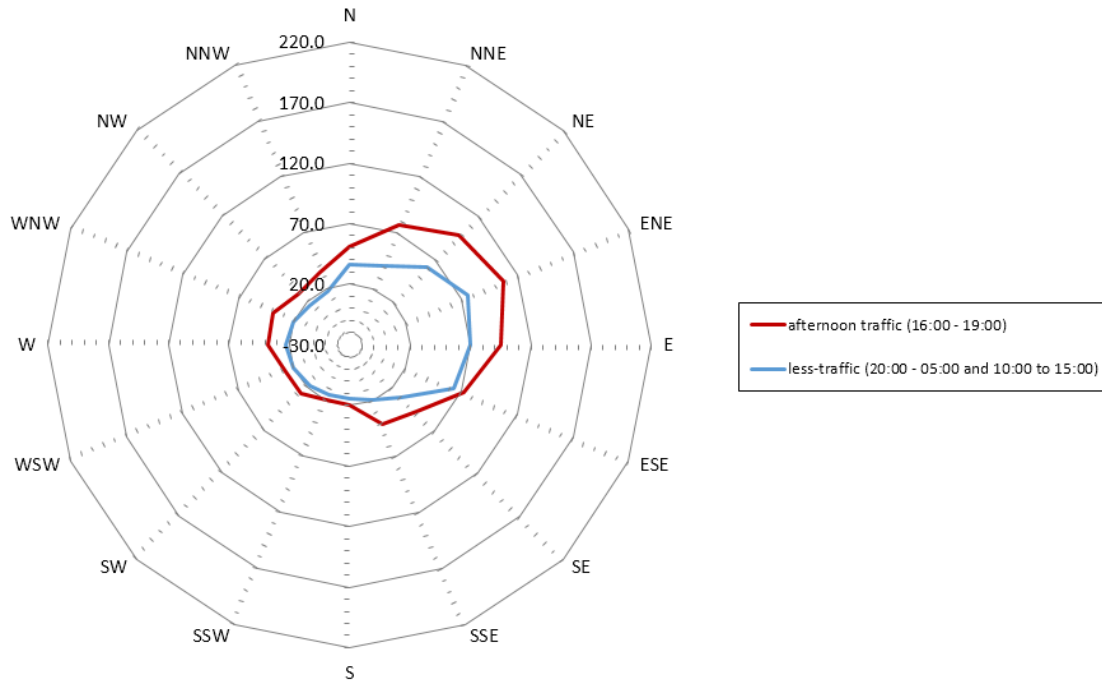
Figure 4.32: Angular distribution of NO_x at Goodwood as a function of wind direction for afternoon traffic and other times (2000 – 2006).

4.7 Effect of Meteorology on Seasonal Cycles

Global radiation tends to be lower at Cape Point during the winter months because of higher cloud cover. Ozone is limited by UV (Figure 4.33) since surface O_3 is broken down by photolysis as described in equation 6 above:

Figure 4.33 shows the relationship between monthly average O_3 and global radiation at Cape Point background. The monthly average O_3 maximum is recorded in winter months when global radiation is at minimum. The global radiation maximum at Cape Point is observed in December (monthly average of 272.02 W/m^2) while the minimum occurs in June (85.28 W/m^2). The monthly average peak-to-peak value of global radiation is 186.79 W/m^2 from 1997 to 2009.
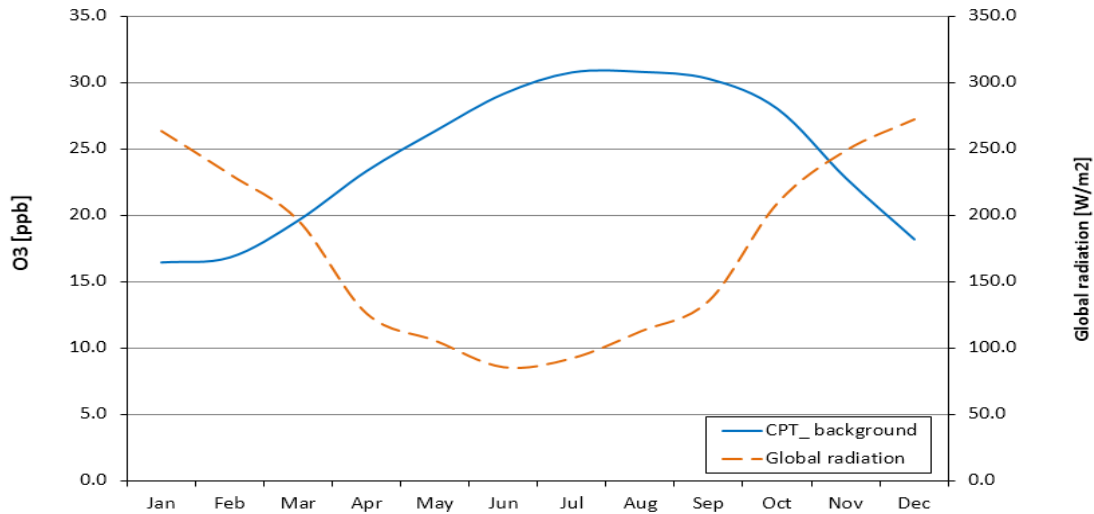
Figure 4.33: Monthly average global radiation at Cape Point and monthly average background O_3 Cape Point station (1997 to 2009).

Figure 4.34 illustrates negative relationship between monthly average O_3 at Cape Point background and monthly average global radiation experienced at Cape Point from 1997 to 2009. The strong negative correlation is significant at a 95% confidence level ($p = 0.00079$, $r = -0.81$, $r^2 = 0.65$). Global radiation decreases from January and reaches its minimum in June before increasing to December. On the other hand, O_3 increases from January to July and decreases from August to December. At Cape Point, global radiation is inversely related to O_3.
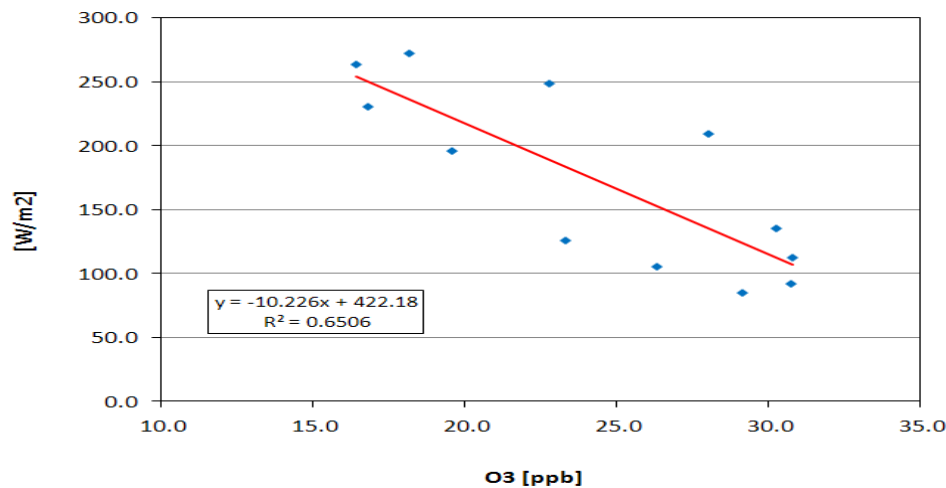
Figure 4.34: Relationship between monthly average O_3 concentrations and global radiation at Cape Point (1997 - 2009).

At SANAE, minimum monthly average temperatures occur in late winter and early spring (Figure 4.35) with temperatures falling below -20°C. Monthly average temperature maxima are observed during summer months; these maxima are, however, still below 0°C. The monthly average temperature and O_3 at SANAE reveal that O_3 and temperature are inversely related. However, the temperature minimum occurs in September while the O_3 maximum occurs in July.
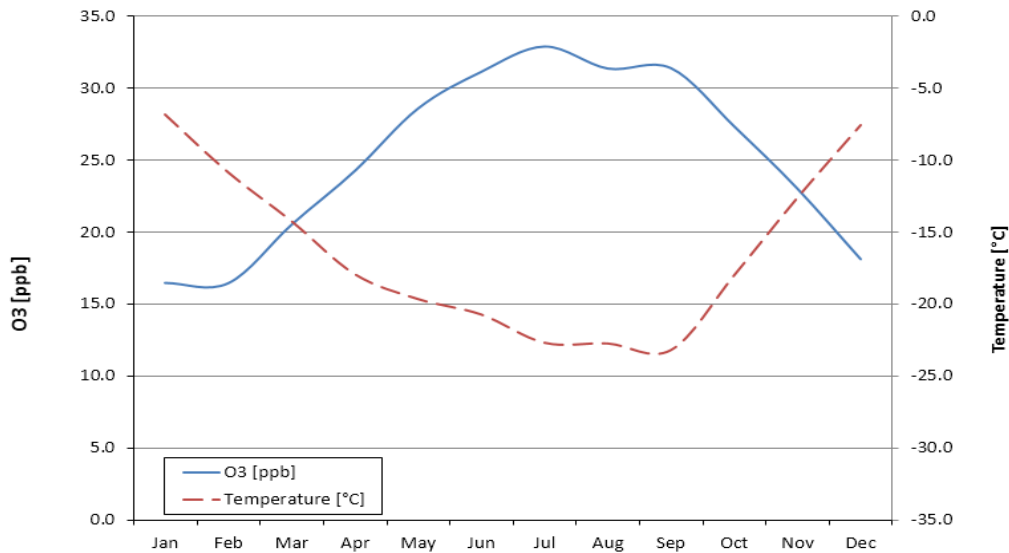
Figure 4.35: Relationship between monthly average temperature at SANAE and monthly average SANAE (2002 – 2009).

Figure 4.36 illustrates the strong negative correlation between monthly average O_3 at SANAE and monthly average temperature experienced at SANAE from 2002 to 2009, significant at the 95% confidence level (p = 0.00018, r = -0.958, r^2 = 0.918). The relationship between O_3 and temperature at SANAE is negative because temperature minima are recorded in winter and maxima in summer while SANAE experience O_3 maxima in winter and minima in summer. The observed inverse relationship is evident in Figure 4.36.
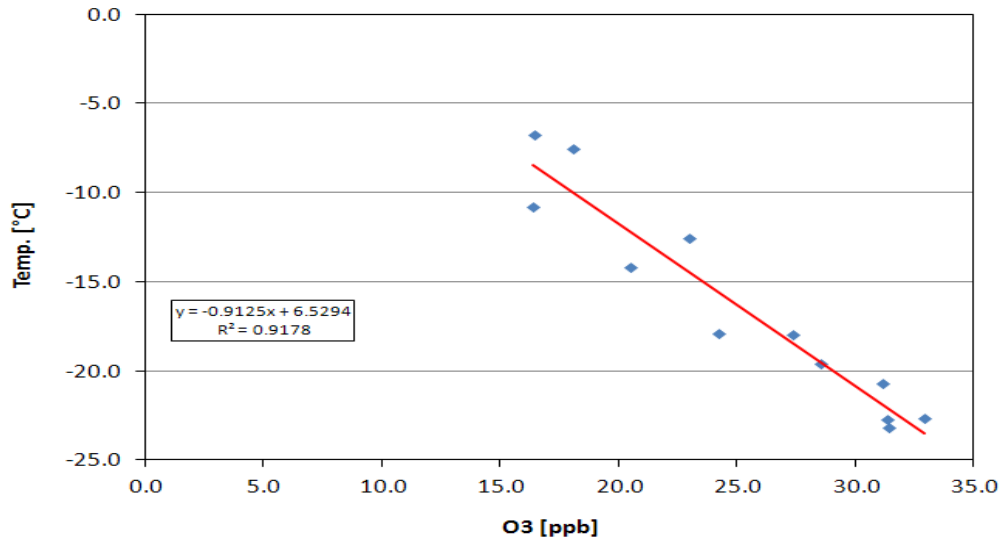
Figure 4.36: Correlation between monthly average O₃ concentrations and temperature at SANAE (2002 – 2009)

Mean monthly atmospheric pressure and monthly average O_3 at SANAE (Figure 4.37) are not clearly related. Atmospheric pressure increased from January (884.24 hPa) to February (894.52 hPa) while a small decrease of 0.56 hPa was observed in March. Average monthly values are 892.66, 892.47 and 893.17 hPa from April to June respectively, followed by a decrease of 18.32 hPa in August. From August to December there is an increasing pressure trend of 8.85 hPa.
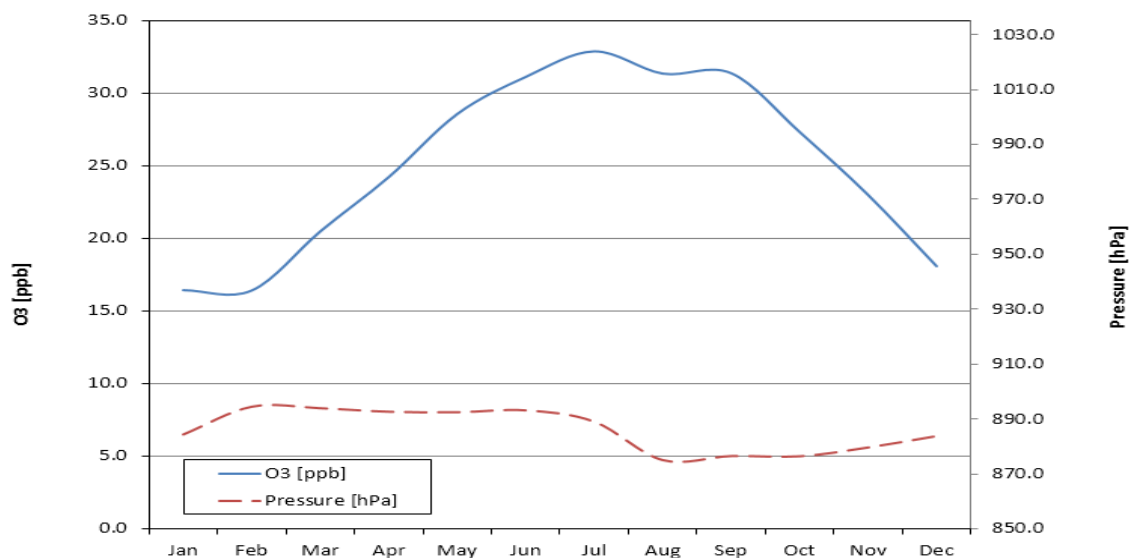
Figure 4.37: Monthly average atmospheric pressure at SANAE and monthly average SANAE ozone averages (2002 – 2009).

Figure 4.38 illustrates the negative relationship between monthly average O_3 at SANAE and monthly average pressure experienced at SANAE from 2002 to 2009. The correlation is not significant at the 95% confidence level (p = 0.536, r = -0.259, r^2 = 0.067).   According to Simpson *et al.* (1995), elevated levels of O_3 are found in high pressure systems. At SANAE, however, pressure variation is low, and this could explain the lack of any clear relationship between the two variables.
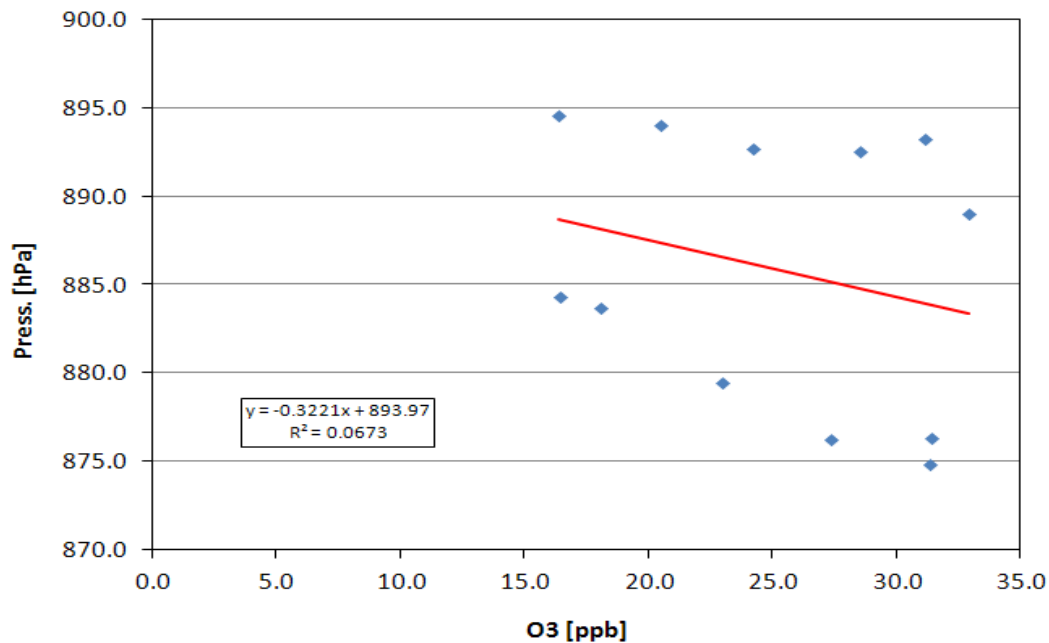
Figure 4.38: Correlation between monthly average O_3 and pressure at SANAE (2002 – 2009).

Figure 4.39 shows the relationship between monthly average O_3 and atmospheric pressure at Cape Point background. The monthly average O_3 maximum is recorded in winter months for both variables. Atmospheric pressure at Cape Point is at its maximum in July (monthly average of 993.99 hPa) and decreases from August to January (987.00 hPa). The monthly average peak-to-peak value is 6.99 hPa over this period while a maximum of 30.80 ppb and a minimum of 16.43 ppb are recorded for O_3.
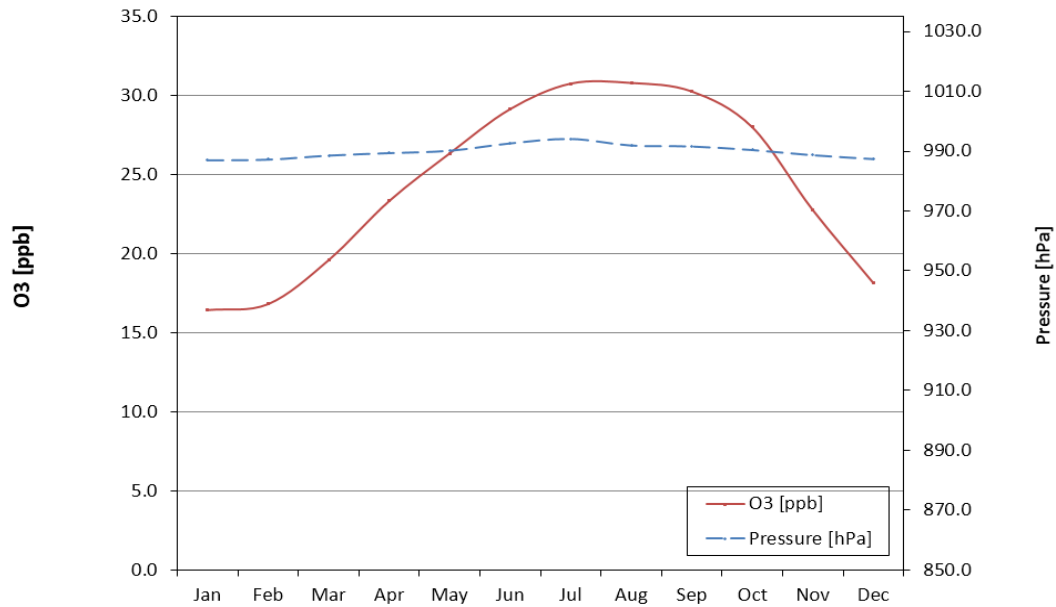
Figure 4.39: Monthly average atmospheric pressure at Cape Point (background) and monthly average O_3 at Cape Point (background) from 1997 – 2009.

Figure 4.40 illustrates positive relationship between average monthly O_3 concentrations at Cape Point background station and average monthly pressure experienced at Cape Point from 1997 to 2009. The relationship is significant at 95% confidence level (p = 0.0000018, r = 0.94, r^2 = 0.89). It is in agreement with observations by Simpson *et al.* (1995) that elevated levels of O_3 are found in high pressure meteorological conditions. Ozone formation is driven by photochemical initiated reactions and these correlate with high atmospheric pressure because of the prevalence of clear (cloudless) skies under high pressure conditions. Thus a positive relationship between pressure and O_3 is observed. Higher levels of O_3 and pressure are recorded in winter while lower levels of O_3 and pressure are observed in summer.
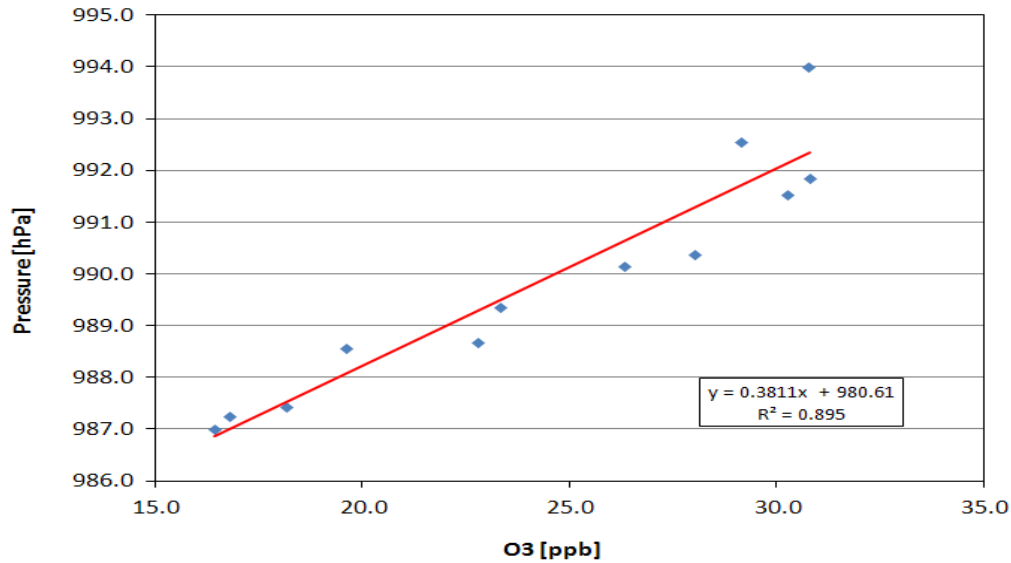
Figure 4.40: Correlation between monthly average O_3 and pressure at Cape Point background station (1997 – 2009).

Figure 4.41 illustrates monthly average temperature and O_3 at Molteno and Goodwood. Temperature decreases from January and reaches a monthly average minimum of 12.53 °C in July, followed by an increase to 20.29 °C in December. A decrease of O_3 for both stations (Molteno and Goodwood) is observed from January to June. In July, O_3 increases and reaches a peak in October of 23.99 ppb and 18.48 ppb at Molteno and Goodwood respectively. Monthly average O_3 concentrations are not clearly related to atmospheric temperature at these stations.
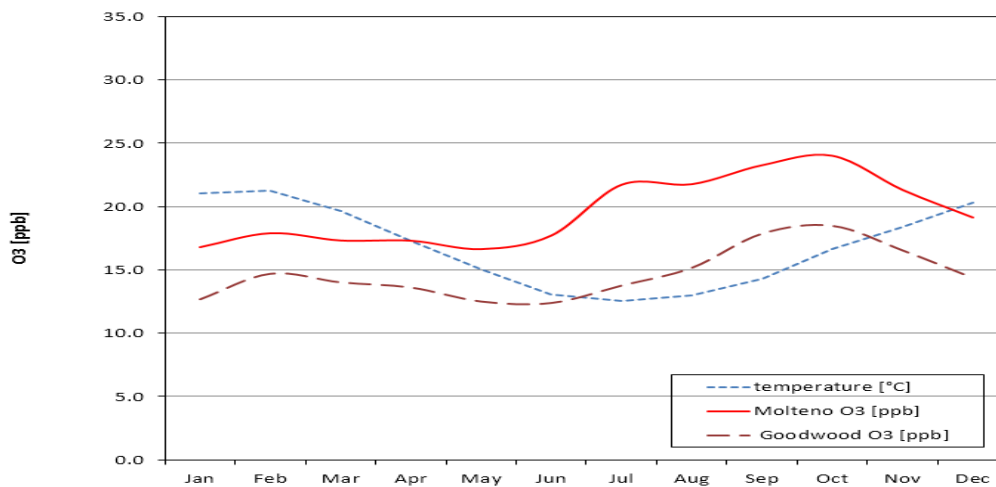
Figure 4.41: Monthly average temperature at Cape Town and monthly average O_3 concentrations at Molteno and Goodwood (2000 – 2006).

Figure 4.42 illustrates an inverse relationship between monthly average O_3 emissions and monthly average temperature recorded in Molteno from 2002 to 2007. The relationship is not significant at 95% confidence level (p = 0.407, r = -0.42, r^2 = 0.18) at this station. Temperature minima occur in winter months whereas maxima are recorded in summer months. On the other hand, O_3 maxima are observed in spring and minima occur in summer. Hence, the relationship between monthly O_3 averages and monthly average temperature is not significant at 95% confidence level. Further investigation of the seasonal cycles is recommended at Molteno. The relationship between O_3 and temperature is not significant at the 95% confidence level. It can be suggested that the observed O_3 maxima at Molteno is not related to monthly average temperatures.
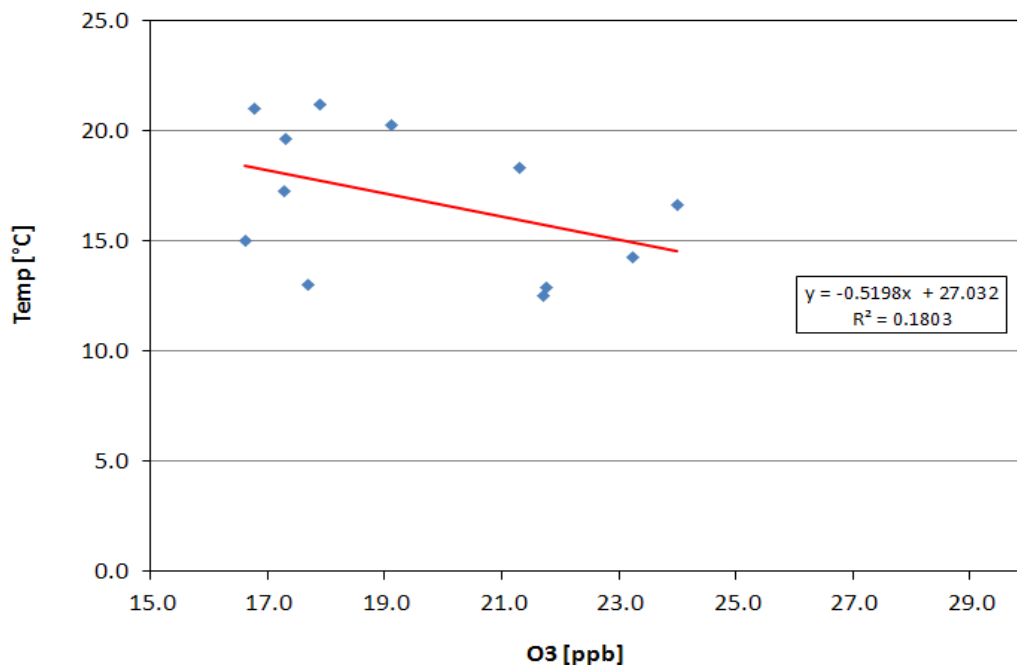
Figure 4.42: Correlation between monthly average O_3 and temperature at Molteno (1997 – 2007).

Figure 4.43 shows monthly average O_3 at Molteno and Goodwood as well as monthly average atmospheric pressure. The monthly average O_3 maximum occurs in October while the average monthly atmospheric pressure maximum occurs in July. Figures 4.39 and 4.41 suggest that the mechanism driving seasonal changes in O_3 at these sites is neither temperature nor atmospheric pressure related. The influences of $\Delta T / \Delta Z$ (i.e. change of temperature with height, which is an

indicator of inversion conditions (when positive) and thus atmospheric stability) and the wind regime are worthy of further investigation to explain this cycle.
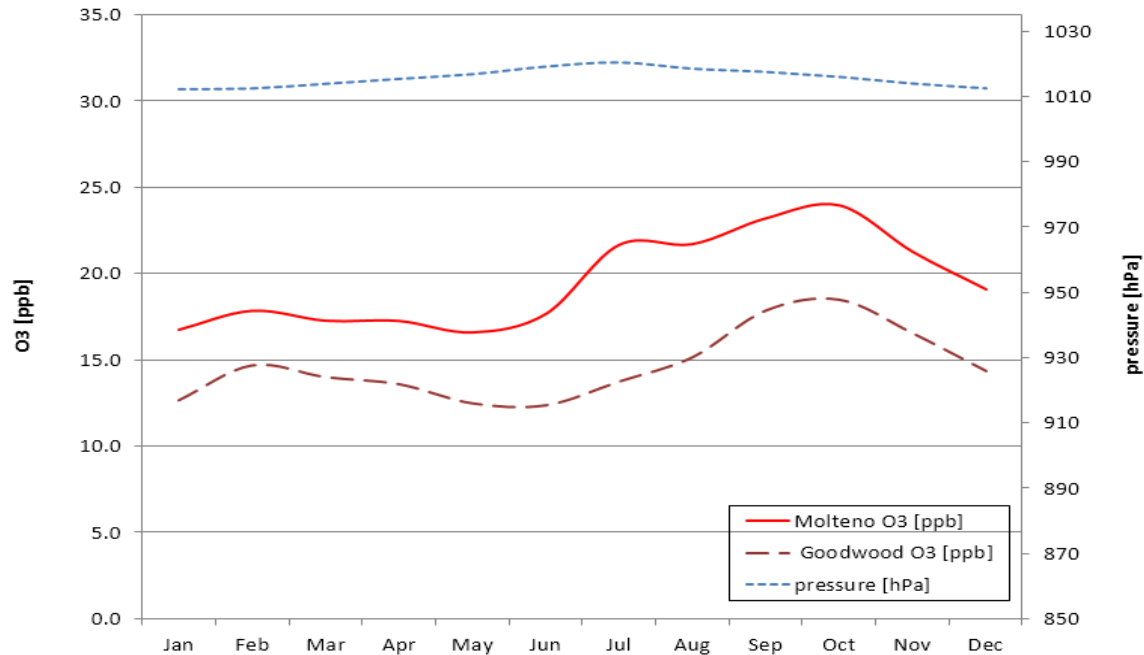
Figure 4.43: Monthly average atmospheric pressure at Cape Town and monthly average O_3 at Molteno and Goodwood (2000 – 2006).

Figure 4.44 illustrates an inverse relationship between monthly average O_3 emissions and monthly average temperatures recorded at Goodwood from 2000 to 2006. The relationship between these variables is not significant at 95% confidence level (p = 0.925, r = 0.044, r^2 = 0.002) at this site. In summer months, higher temperatures are observed while higher O_3 averages are recorded in spring. Minima temperatures are observed in winter whereas lowest O_3 concentrations are recorded in summer. Therefore, there is no clear relationship between monthly average temperature and monthly average O_3. As indicated above, the observed O_3 maxima in spring is not related to temperature.
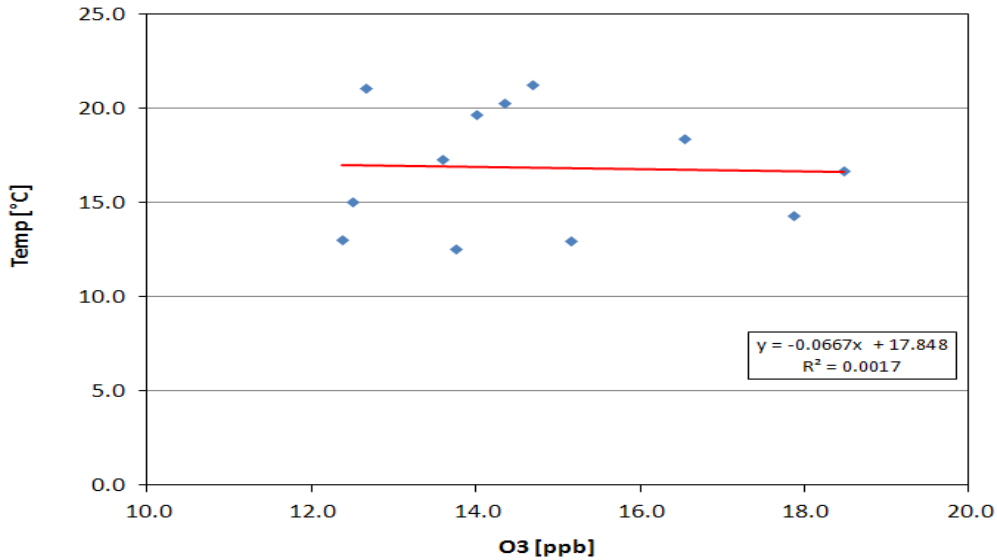
Figure 4.44: Correlation between monthly average O_3 and temperature at Goodwood (2000 – 2006).

Figure 4.45 illustrates monthly average O_3 concentrations and atmospheric pressure at Molteno from 2002 to 2007. A positive relationship between temperature and pressure is observed. However, the relationship between these variables is not significant at 95% confidence level (p = 0.432, r = 0.4, r^2 = 0.16). Pressure maxima occur in winter months whereas O_3 maxima occur in spring. The literature suggest higher levels of O_3 are expected under high pressure meteorological conditions, but the timing of the O_3 maximum at Molteno does not coincide with high atmospheric pressure.
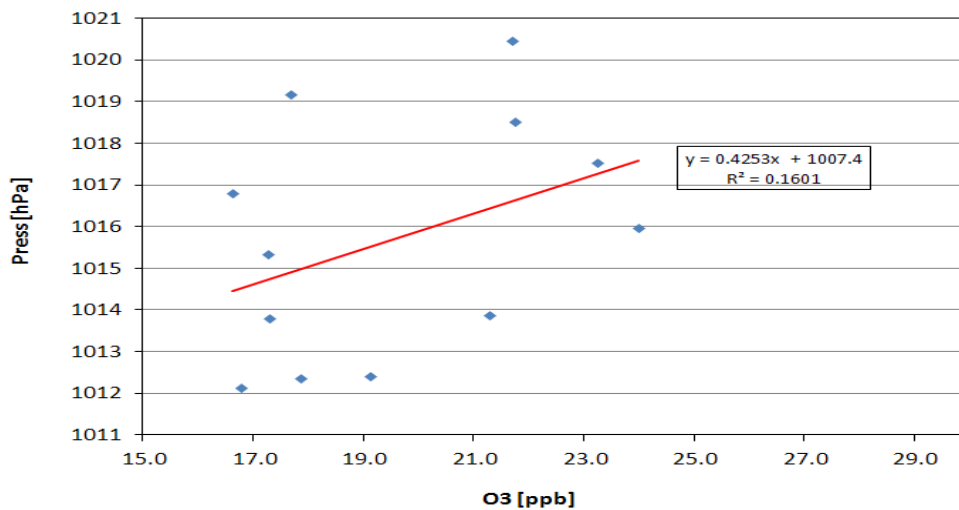
Figure 4.45: Correlation between monthly average O_3 and pressure at Molteno (1997 – 2007).

Figure 4.46 illustrates the relationship between monthly average O_3 concentrations and pressure at Goodwood from 2000 to 2006. The relationship between these variables is not significant at the 95% confidence level. As discussed in section 4.3, Goodwood recorded O_3 maxima in spring and minima in summer. On the other hand, atmospheric pressure is lower in summer and higher in winter (June and July). Therefore, there is no significant relationship detected between O_3 concentrations and atmospheric pressure.
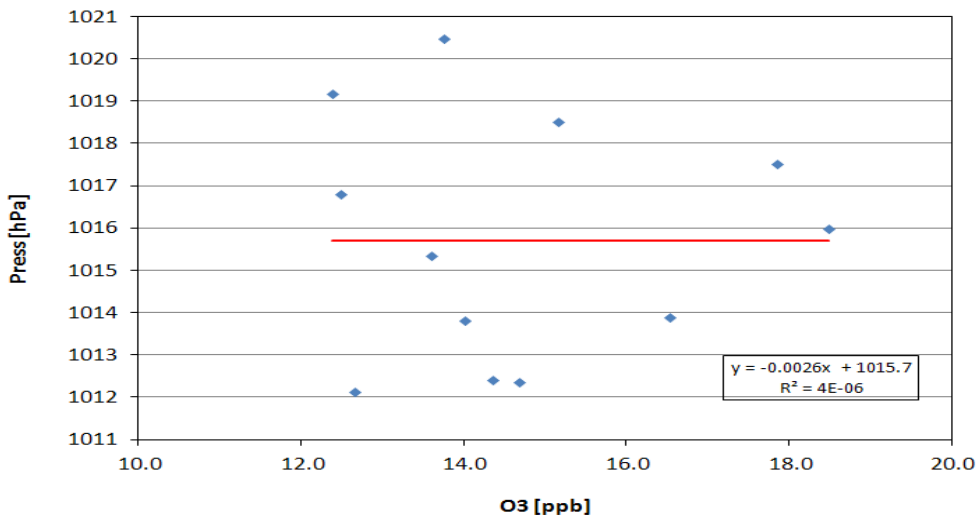
Figure 4.46: Correlation between monthly average O_3 and pressure at Goodwood (2000 – 2006).

Figure 4.47 illustrates a strong inverse relationship between monthly average NO_x concentrations at Goodwood and monthly average temperature experienced in Cape Town from 2000 to 2006. The relationship between NO_x and temperature is significant at the 95 % confidence interval (p = 0.031, r = -0.80, r^2 = 0.64). At Goodwood, the NO_x maxima are recorded in winter while minima are recorded in summer. Low temperatures are observed in winter and high temperatures are observed in summer. Therefore, the relationship between monthly NO_x averages and temperature is inversely proportional. The observed results of NO_x maxima in winter can be related to a number of factors as discussed above, including vehicular traffic increases in winter and increased fuel use for heating in winter.
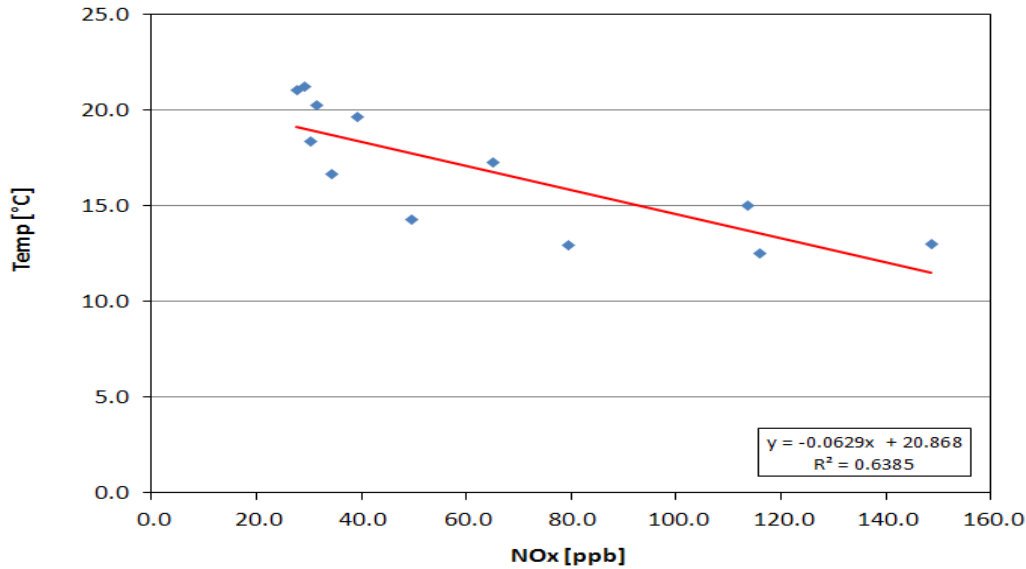
Figure 4.47: Correlation between monthly average NO_x and temperature at Goodwood (2000 – 2006).

4.8 Effect of wind speed on seasonal cycles

The O_3 data was filtered according to wind speed categories (less than 5 m/s, 5 to 10 m/s and 10-15 m/s) for SANAE (Figure 4.48), Cape Point background (Figure 4.49), Cape Point non-background (Figure 4.50), Molteno (Figure 4.51) and Goodwood (Figure 4.52). Monthly average O_3 then was calculated for each wind speed category for each month. A description of each site follows. These results are then interpreted at the end of the section.

Figure 4.48 illustrates O_3 concentrations as a function of wind speed at SANAE. The data can be summarized as follows:

An O_3 minimum of 16.18 ppb is observed in February while a maximum of 33.86 ppb is observed in July for wind speed less than 5 m/s. This results in a peak-to-peak value of 16.68 ppb. For wind speed between 5 to 10 m/s, an O_3 minimum of 16.22 ppb is observed in January while a maximum of 33.15 ppb is observed in July. This results in a peak-to-peak value of 16.93 ppb. Furthermore, an O_3 minimum of 16.39 ppb is observed in January while a maximum of 33.11 ppb is observed in July for wind speed between 10 to 15 m/s. This results in peak-to-peak value of 16.72 ppb.

Literature suggests that winds with lower speeds result in high NO_x concentration and low O_3 concentrations compared to winds with higher speeds. There is no clear relationship between

monthly O_3 averages and wind speed categories at SANAE, and this is likely to be related to the lack of NO_x pollution at SANAE.

Figure 4.48: Monthly average O_3 for specific wind speed categories at SANAE (2002 – 2009).

Figure 4.49 illustrates O_3 concentrations as a function of wind speed at Cape Point background. The data can be summarized as follows:

An O_3 minimum of 18.30 ppb is observed in January while a maximum of 28.77 ppb is observed in September. This results in a peak-to-peak value of 10.47 ppb. For wind speed between 5 to 10 m/s, an O_3 minimum of 17.97 ppb is observed in February while a maximum of 30.23 ppb is observed in August. This results in a peak-to-peak value of 12.26 ppb. Furthermore, an O_3 minimum of 16.94 ppb is observed in January while a maximum of 31.24 ppb is observed in July for wind speed between 10 to 15 m/s. This results in a peak-to-peak value of 14.29 ppb.

Although peak-to-peak values increase with increasing wind speed categories, only winter months show lower O_3 concentrations for winds with low speed. In other months there is no clear relationship between O_3 and wind speed. The observed O_3 relationship with wind speed in winter could be an artefact of the data filtering into background and non-background air masses.
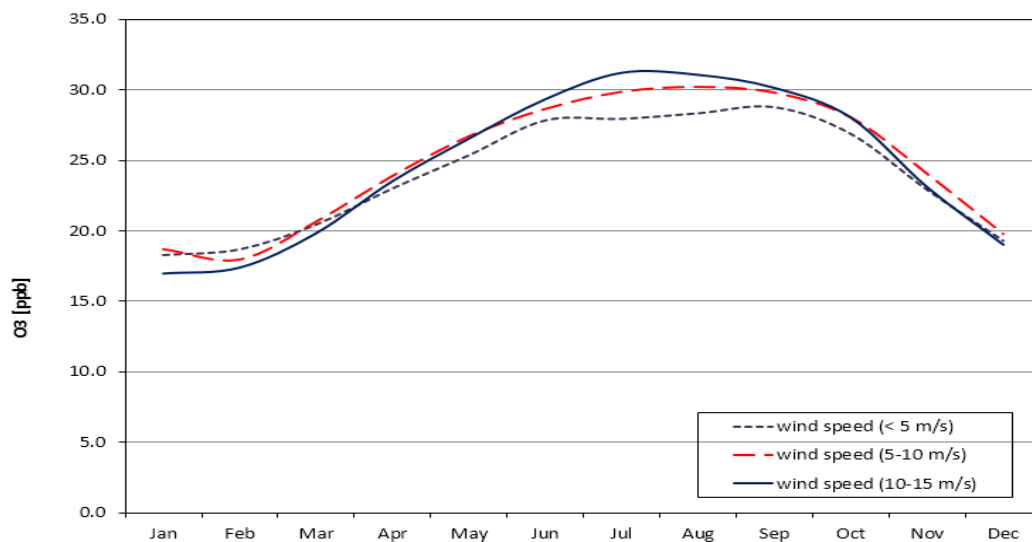
Figure 4.49: Monthly average O_3 for specific wind speed categories at Cape Point background station (1997 – 2009).

Figure 4.50 illustrates O_3 concentrations as a function of wind speed at Cape Point non-background. The data can be summarized as follows:

An O_3 minimum of 19.47 ppb is observed in January while a maximum of 28.49 ppb is observed in September. This results in a peak-to-peak value of 9.02 ppb. For wind speed between 5 to 10 m/s, an O_3 minimum of 20.73 ppb is observed in February while a maximum of 30.39 ppb is observed in October. This results in a peak-to-peak value of 9.66 ppb. Furthermore, An O_3 minimum of 16.82 ppb is observed in January while a maximum of 30.41 ppb is observed in August for wind speed between 10 to 15 m/s. This results in a peak-to-peak value of 13.59 ppb.

Although there is no clear relationship between O_3 and speed in winter, O_3 maximum is increasing with increasing wind speed while minimum is decreasing with increasing wind speed. This results in peak-to-peak values of 9.02 ppb, 9.66 ppb and 13.59 ppb for < 5 m/s, 5 – 10 m/s and 10 – 15 m/s respectively.
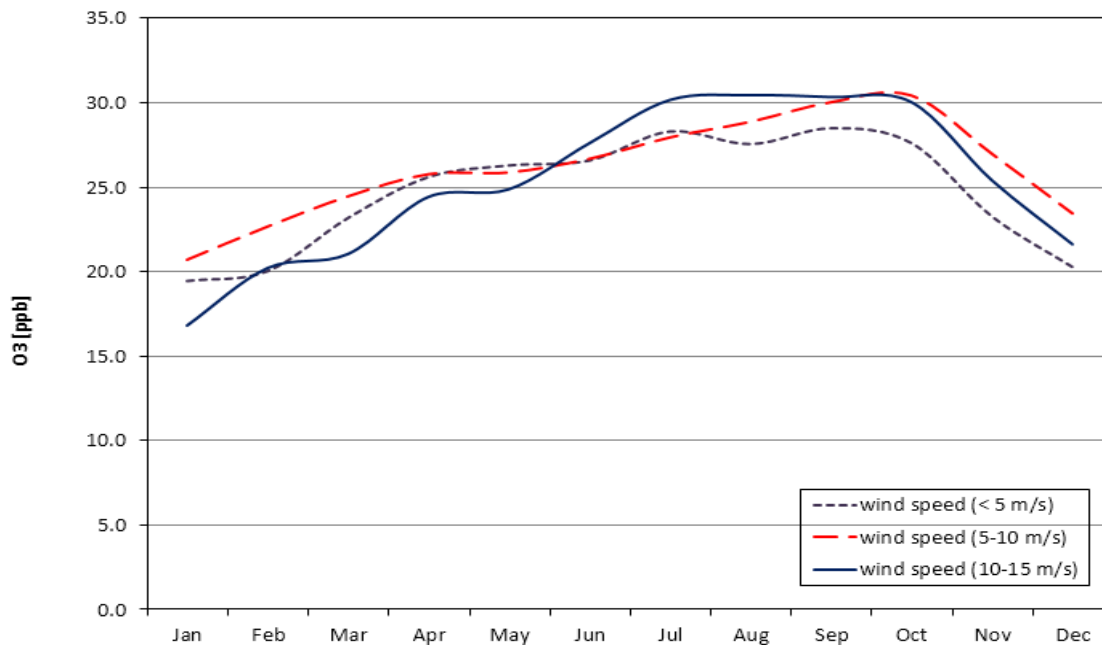
Figure 4.50: Monthly average O_3 for specific wind speed categories at Cape Point non-background (1997 – 2009).

Figure 4.51 illustrates O_3 concentrations as a function of wind speed at Molteno. The data can be summarized as follows:

An O_3 minimum of 13.49 ppb is observed in January while a maximum of 21.65 ppb is observed in October. This results in a peak-to-peak value of 8.16 ppb.

For wind speed between 5 to 10 m/s, an O_3 minimum of 17.88 ppb is observed in January while a maximum of 25.60 ppb is observed in October. This results in a peak-to-peak value of 7.71 ppb. Furthermore, an O_3 minimum of 18.10 ppb is observed in January while a maximum of 28.23 ppb is observed in September for wind speed between 10 to 15 m/s. This results in a peak-to-peak value of 10.14 ppb.

The relationship between monthly O_3 averages and wind speed in Figure 4.51 reflects theory (e.g. Dapeng *et al.*, 1996; Dabdub *et al.*, 1999; Rodriguez and Guerra, 2001) in that lower speeds occur with lower O_3 concentrations while higher wind speeds occur with higher O_3 concentrations. Lower wind speeds promote accumulation of NO_x and lower levels of O_3 because of O_3 titration by NO_x, on the other hand, higher wind speeds promote the transportation of air masses and result in lower O_3 concentrations.
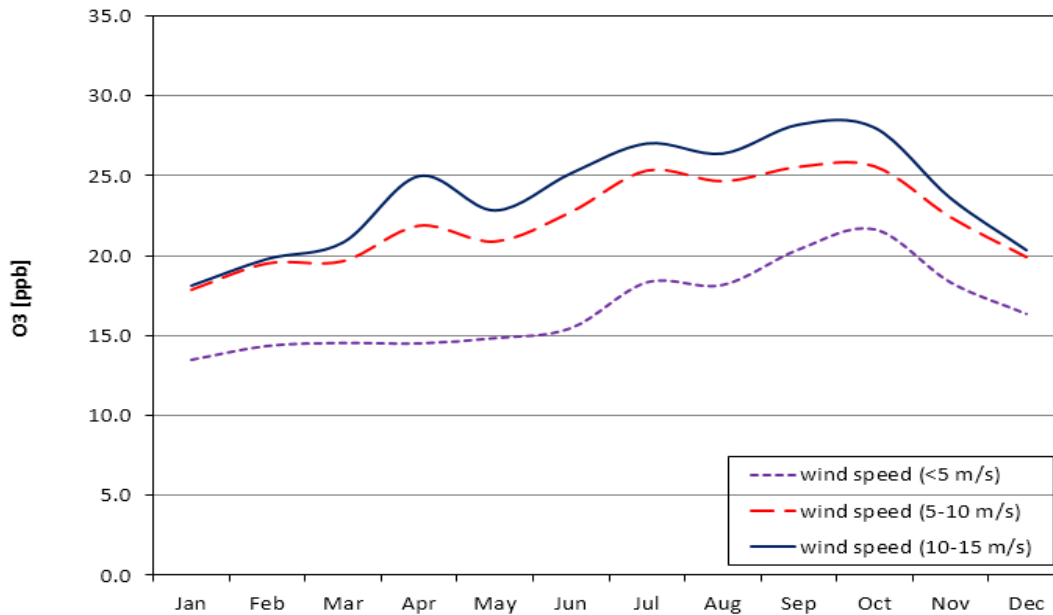
Figure 4.51: Monthly average O_3 for specific wind speed categories at Molteno (1997 – 2007).

Figure 4.52 illustrates O_3 concentrations as a function of wind speed at Goodwood. The data can be summarized as follows:

An O_3 minimum of 11.51 ppb is observed in January while a maximum of 15.90 ppb is observed in October for wind speed less than 5 m/s. This results in a peak-to-peak value of 4.39 ppb.

For wind speeds between 5 to 10 m/s, an O_3 minimum of 13.45 ppb is observed in January while a maximum of 21.21 ppb is observed in October. This results in a peak-to-peak value of 7.75 ppb. Furthermore, an O_3 minimum of 13.11 ppb is observed in January while a maximum of 23.11 ppb is observed in October for wind speed between 10 to 15 m/s. This results in peak-to-peak value of 10.00 ppb.

As discussed previously, winds with low speed result in high O_3 concentrations while high wind speed promoted low O_3 concentrations. Results in Figure 4.52 suggest that the relationship between wind speed and O_3 monthly averages is most clearly evident in stations located in urban areas (Molteno and Goodwood).
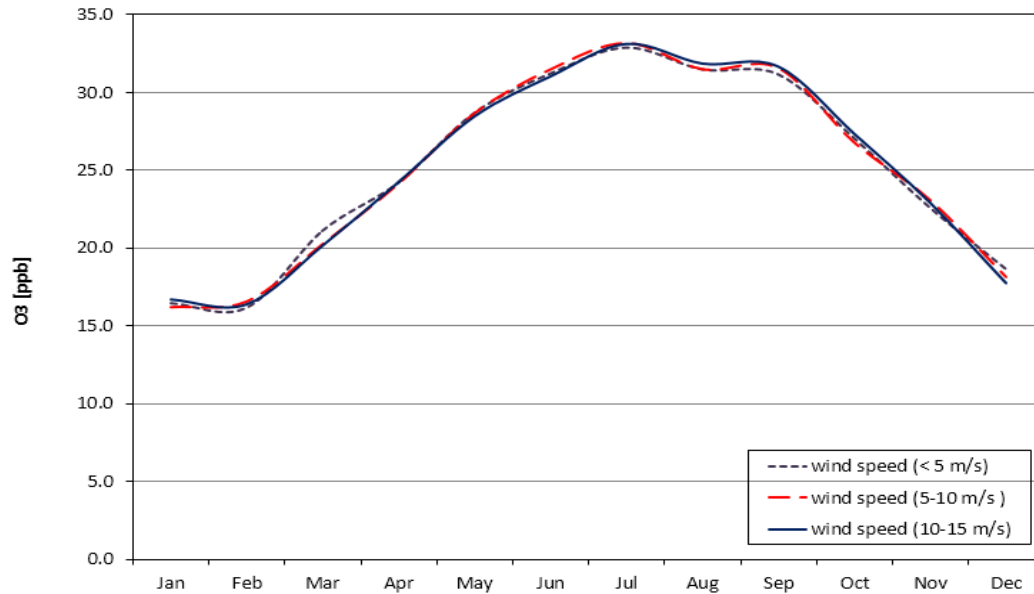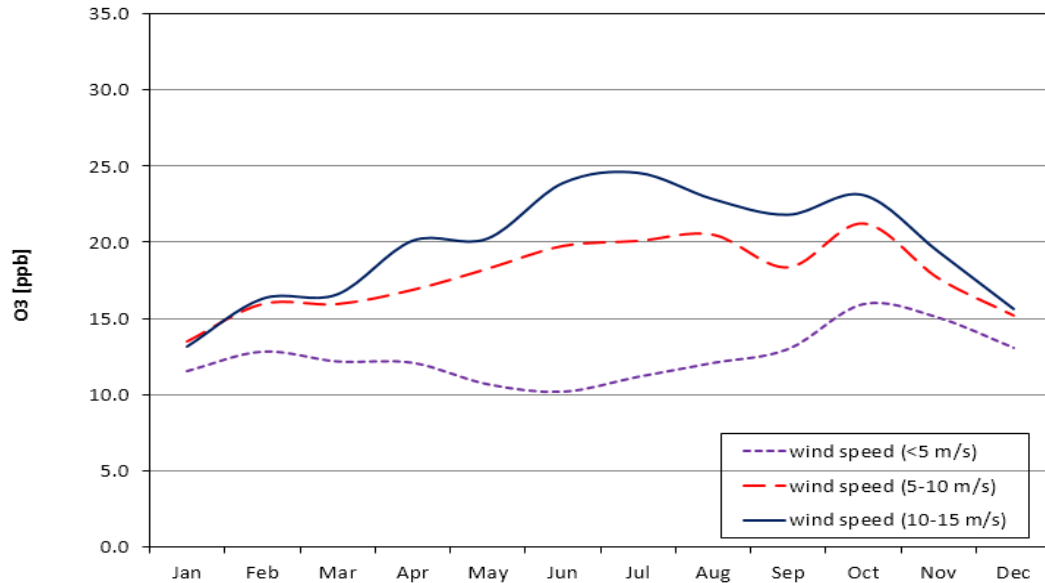
Figure 4.52: Monthly average O_3 for specific wind speed categories at Goodwood (2000 – 2006)

Figure 4.53 illustrates NO_x concentrations as a function of wind speed at Goodwood. The data can be summarized as follows:

A NO_x minimum of 15.00 ppb is observed in January while a maximum of 98.29 ppb is observed in June for wind speed less than 5 m/s. This results in a peak-to-peak value of 83.29 ppb. For wind speeds between 5 to 10 m/s, a NO_x minimum of 9.91 ppb is observed in January while a maximum of 23.55 ppb is observed in June. This results in a peak-to-peak value of 13.63 ppb. Furthermore, a NO_x minimum of 9.03 ppb is observed in January while a maximum of 28.91 ppb is observed in June for wind speed between 10 to 15 m/s. This results in a peak-to-peak value of 19.88 ppb.

With the exception of 5 – 10 m/s maximum, the observed results are in agreement with the findings reported in the literature (Dapeng *et al.*, 1996; Dabdub *et al.*, 1999; Rodriguez and Guerra, 2001), more especially in urban sites where NO_x levels are higher.

In summary, at Goodwood and Molteno, higher wind speed categories show lower O_3 concentrations while lower wind speed categories show higher O_3 concentrations. At SANAE and Cape Point the relationship between monthly O_3 averages and monthly speed averages is not clear.
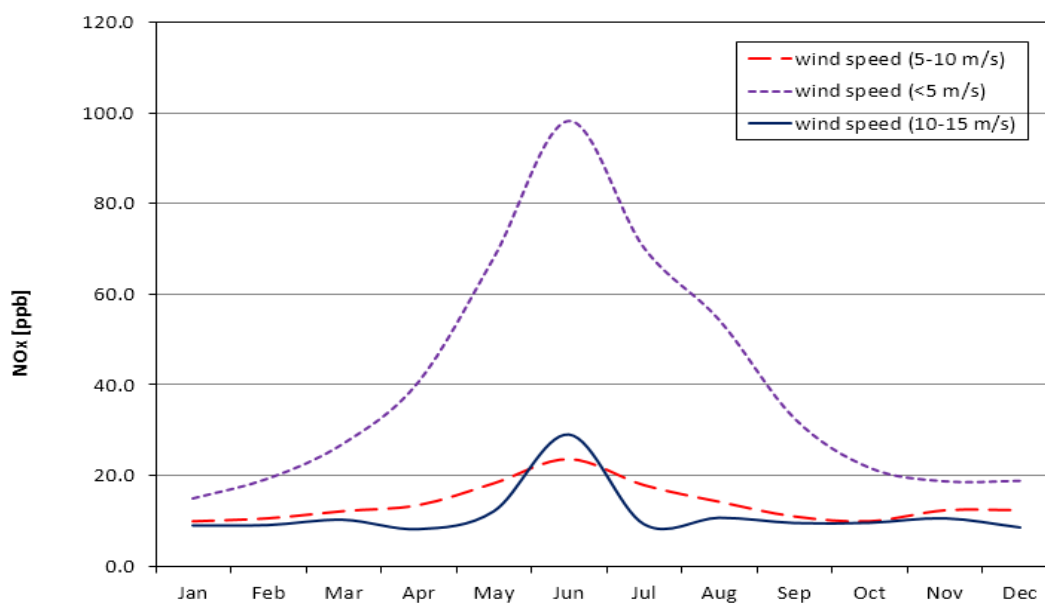
Figure 4.53: Monthly average NO$_x$ for specific wind speed categories at Goodwood (2000 – 2006).

4.9. Long Term Trends of O$_3$ at Various Sites

Monthly O$_3$ averages were calculated from the hourly dataset from 1997 to 2009. The figures below (Figure 4.54, 4.55, 4.56, 4.57 and 4.58) show the monthly average O$_3$ at SANAE, Cape Point background, Cape Point non-background, Molteno and Goodwood respectively. Twelve month moving averages were calculated to investigate trends. Visual analysis of the figures below indicates a general increase, decrease or stabilization in ozone concentrations. Slope (in ppb/yr) is reported for each station.

At SANAE (Figure 4.54) and Cape Point background (Figure 4.55) a clear seasonal cycle is evident with minima in summer and maxima in winter. SANAE shows a slight increasing trend of 0.11 ppb/yr from 2002 to 2009.
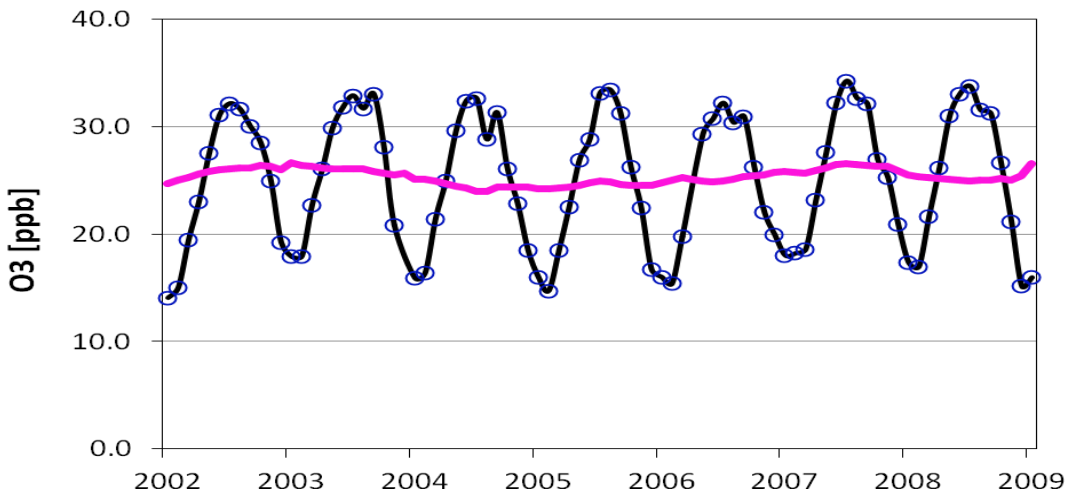
Figure 4.54: Trend in monthly average O_3 at SANAE with twelve month running average (2002-2009).

At Cape Point background (Figure 4.55) ozone levels are stable (an average trend of -0.02 ppb/yr) from 1997 to 2009. An increasing slope of 0.18 ppb/yr is calculated from 1997 to 2003 followed by stable levels (-0.02 ppb/yr) from 2004 to 2009. When calculating trends, it is important to calulate slope for years which show similar trend behaviour (increase, decrease or stabilization) so that changing trends are not averaged out over longer time periods.
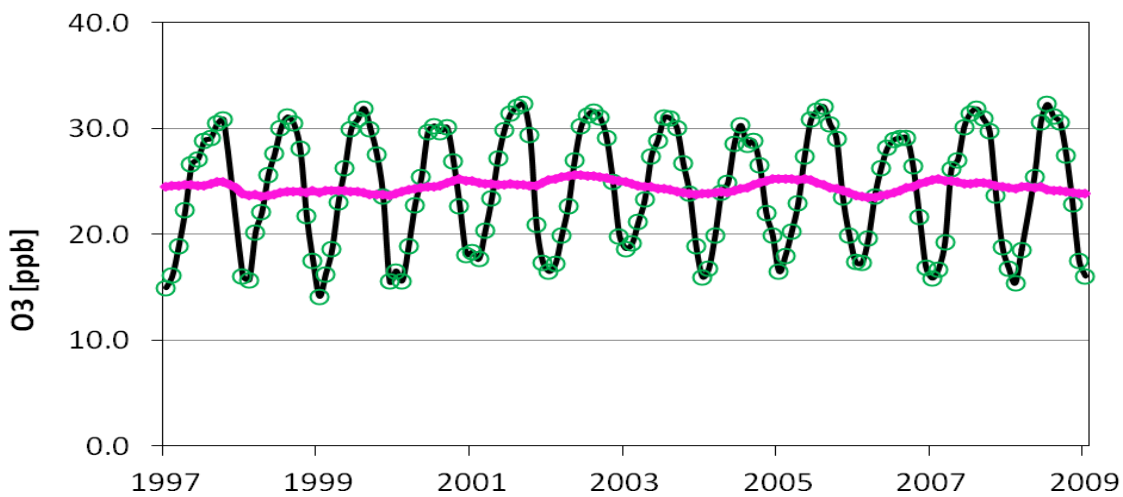
Figure 4.55: Trend in monthly average O_3 at Cape Point background station with twelve month running average (1997-2009).

At Cape Point non-background (Figure 4.56) a negative trend of -0.14 ppb/yr is observed from 1997 to 2009. An increasing trend of 1.76 ppb/yr is calculated from 1997 to 2000 followed by a negative trend of -0.10 ppb/yr from 2001 to 2009. At Cape Point non-background, Molteno and Goodwood, monthly O_3 averages show high variability. Molteno and Goodwood show more monthly O_3 variation compared to Cape Point non-background data. At SANAE and Cape Point background, there is a steady increase from January to June and steady decrease from July to December.
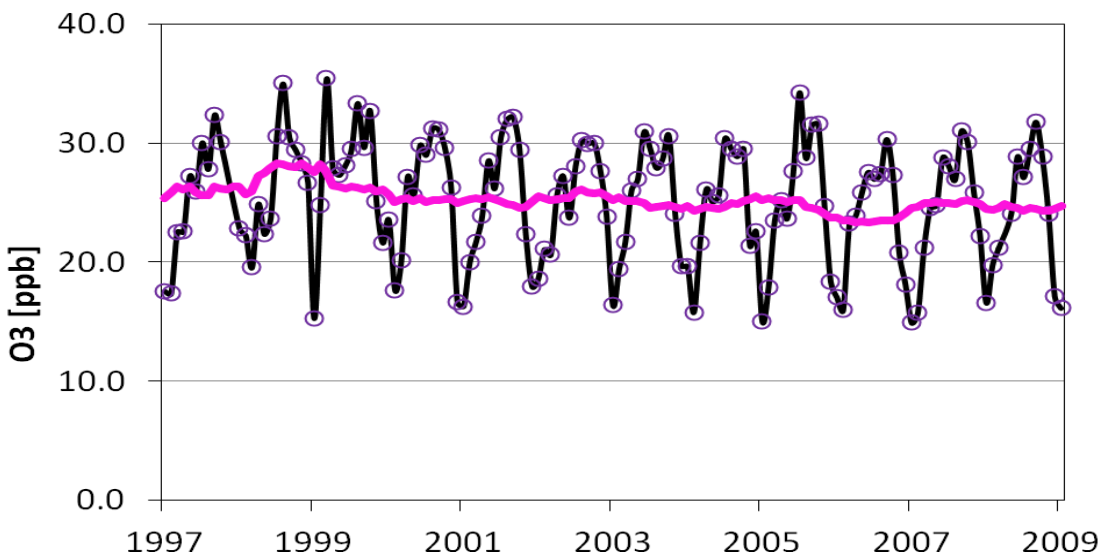
Figure 4.56: Trend in monthly average O_3 at Cape Point non-background with twelve month running average (1997-2009).

At Molteno (Figure 4.57) a negative trend of -0.46 ppb/yr is observed from 1997 to 2007. An increasing trend of 0.86 ppb/yr is observed from 1997 to 2000 followed by a negative trend of -0.44 ppb/yr from 2001 to 2007.
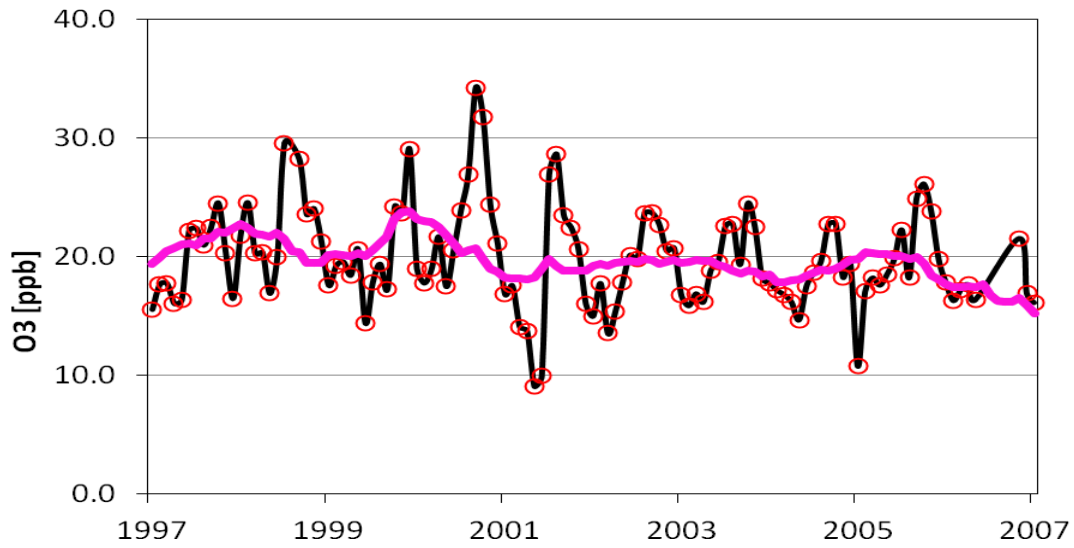
Figure 4.57: Trend in monthly average O_3 at Molteno with twelve month running average (1997-2007).

At Goodwood (Figure 4.58), an increasing O_3 trend of 0.16 ppb/yr is observed from 2000 to 2006. However, NO_x shows a negative trend during from 2000 to 2006 (Figure 4.59).
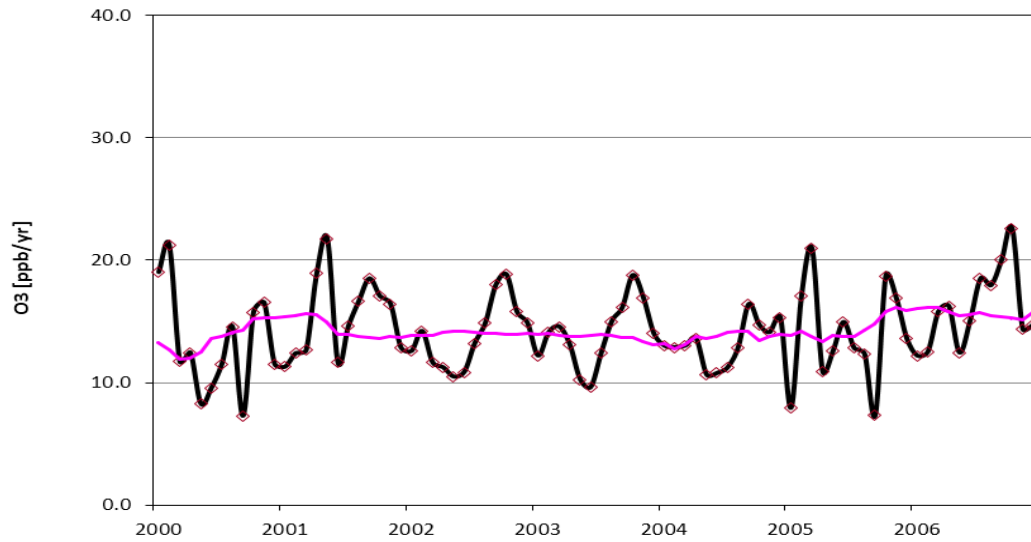
Figure 4.58: Trend in monthly average O_3 at Goodwood with twelve month running average (2000-2006).
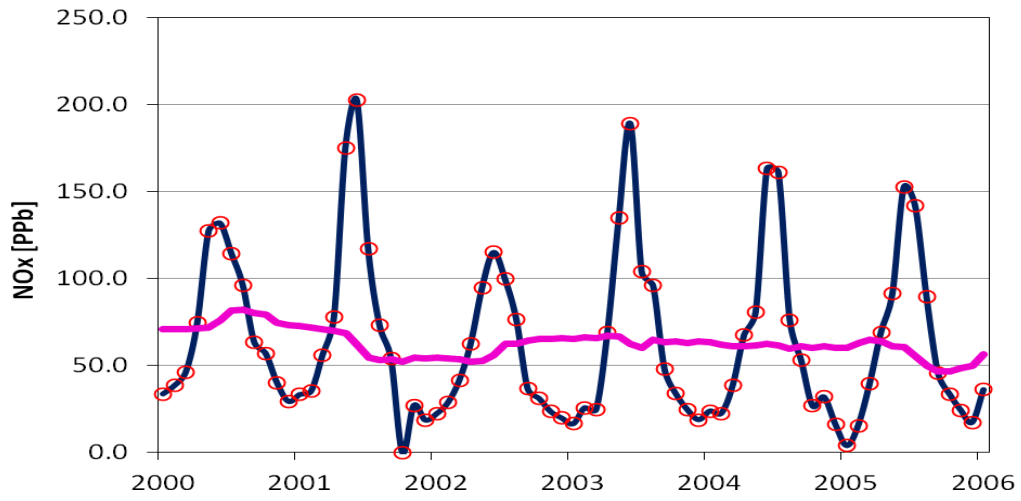
Figure 4.59: Trend in monthly average NO_x at Goodwood with twelve month running average (2000- 2006).

CHAPTER 5

SUMMARY AND CONCLUSIONS

5.1 Summary

This chapter summarizes the analysis of surface O_3 at SANAE (2002-2009), Cape Point background and Cape Point non-background (1997-2009), Molteno (1997-2007) and Goodwood (2000-2006). Diurnal and seasonal cycles, weekend effect and long term trends in these data were assessed.

At SANAE and Cape Point background, diurnal peak-to-peak values are lower relative to non-background stations. Goodwood shows a peak-to-peak value of 16.80 ppb while a peak-to-peak value of 12.16 ppb is recorded at Molteno. The Cape Point non-background station peak-to-peak value (6.00 ppb) is higher than the SANAE (0.24 ppb) and Cape Point non-background data (1.26 ppb) peak-to-peak values. The Cape Point non-background data resembles the Cape Town region (Molteno and Goodwood) with respect to diurnal and seasonal cycle trend but with lower diurnal variation. The correlation between Cape Point non-background O_3 and Molteno O_3 was not significant (p = 0.061, r = 0.732, r^2 = 0.54) at the 95% confidence level, but significant at the 90% confidence level. The correlation between Cape Point non-background and Goodwood was not significant at the 95% or 90% confidence level (p = 0.116, r = 0.647, r^2 = 0.42). The diurnal variation on weekends and weekdays showed higher peak-to-peak values on weekdays compared to weekends at Molteno and Goodwood. This is most likely due to the well-established 'weekend effect' in O_3 concentrations at urban stations associated with increased vehicular NO_x emissions during the week. This is supported by NO_x measurements at Goodwood.

Monthly average maxima of 33.20 ppb and 30.80 ppb were observed in winter at SANAE and Cape Point background respectively, while monthly average minima of 16.47 ppb and 16.43 ppb occurred during summer at SANAE and Cape Point background respectively. Monthly average peak-to-peak values are much lower in the Cape Town region (Molteno and Goodwood) relative to those observed at SANAE and Cape Point. At Molteno (16.62 ppb) and Goowood (12.38 ppb), monthly average minima are observed in winter, while monthly average maxima are observed in spring. These maxima do not coincide with NO_x or temperature extremes. The Cape

Point non-background data reveals a monthly average minimum of 17.69 ppb in summer and monthly average maximum of 30.24 ppb in spring.

The 'weekend effect' is clearly evident at Molteno and Goodwood but not at SANAE, Cape Point background and Cape Point non-background. On weekends, correlation between Molteno monthly average O_3 and Cape Point non-background monthly average O_3 is strong and significant at the 95% confidence level (p = 0.00, r = 0.80, r^2 = 0.64) while a non-significant correlation is observed between Goodwood monthly average O_3 and Cape Point non-background monthly average O_3 is observed on weekends (p = 0.191, r = 0.41, r^2 = 0.16). On weekdays, monthly averages NO_x is higher at Goodwood, particularly during the winter months (maximum in June), with a difference of 132.9 ppb observed between monthly NO_x maxima on weekends and monthly NO_x minima on weekdays.

Correlation results of monthly average O_3 with monthly average temperature and monthly average pressure show both significant and non-significant relationships. At SANAE, the correlation between monthly average temperature and monthly average O_3 is very strong and significant at the 95% confidence level (p = 0.00018, r = -0.958, r^2 = 0.918) but at Molteno (p = 0.407, r = -0.42, r^2 = 0.18) and Goodwood (p = 0.925, r = 0.044, r^2 = 0.002), the correlation between monthly average temperature and monthly average O_3 is not significant at the 95% confidence level. At SANAE, Molteno and Goodwood, the correlation between monthly average pressure and monthly average O_3 is not significant at the 95% confidence level however at Cape Point background the correlation is strong and significant at the 95% confidence level (p = 0.0000018, r = 0.94, r^2 = 0.89).

Pollution roses at Molteno and Goodwood show higher sectoral average O_3 concentrations during winds from the south-east and north-west relative to other sectors. However, NO_x pollution roses show lower concentrations from these sectors. Higher NO_x sectoral average concentrations are observed from east-north-east relative to other sectors. On the other hand, O_3 concentrations are lower during winds from the east-north-east relative to other sectors. These results show more O_3 titration by NO_x from east-north-east relative to other sectors. The observed maximum sectoral average NO_x concentrations are 34.53 ppb, 136.79 ppb, 132.70 ppb,

and 59.29 ppb during summer, autumn, winter and spring respectively. Generally, the maximum sectoral average NO_x originates from the north-east to east directions, and these high levels are associated with vehicular emissions. At SANAE, the minimum sectoral average is observed from the northern sector in spring with a difference of 8.00 ppb relative to the maximum sectoral average. At Cape Point non-background , the sectoral average minimum is observed from the northern sector (Cape Town region) in winter.

At Molteno and Goodwood, an increase in wind speed results in an increase in transportation of air masses, promoting lower levels of NO_x and higher levels of O_3. On the other hand, lower wind speeds promotes accumulation of NO_x and lower levels of O_3.

An increasing trend of 0.11 ppb/yr of O_3 is observed at SANAE from 2002 to 2009. At Cape Point background an increasing trend of 0.18 ppb/yr is observed from 1997 to 2003 followed by stable values (0.02 ppb/yr) from 2004 to 2009. On the other hand, Cape Point non-background shows an increasing trend of 0.21 ppb/yr from 1997 to 2000 followed by a negative trend of 0.12 ppb/yr from 2001 to 2009. Similary, Molteno shows an increasing trend of 0.86 ppb/yr from 1997 to 2000 followed by a negative trend of 0.42 ppb/yr from 2001 to 2007. The Goodwood trend deviates from that of Molteno and Cape Point non-background. A continous increase of 0.26 ppb/yr from 2000 to 2006 is recorded while the NO_x trend decreased by 2.56 ppb/yr for the same period.The observed O_3 trend increase in Goodwood suggests s decrease O_3 titration by NO_x

5.2 Final Comments

The diurnal cycle of O_3 and NO_x (Figure 4.4) at Goodwood can be subdivided as follows: (a) In the mornings, a NO_x peak was observed associated with morning traffic, (b) O_3 formation persists between 09:00 and 14:00, (c) afternoon NO_x accumulation occurs due to traffic peak, (d) balancing of NO_x and O_3 during night hours (19:00 to 05:00). Although the correlation between O_3 and NO_x was not significant, 32% of the variation in NO_x corresponds with the variation in O_3 concentrations at Goodwood. Trends at Cape Point background resemble those of SANAE while trends in Cape Point non-background are almost similar those of the Cape Town region. NO_x plays a crucial role in the O_3 diurnal cycle at Molteno and Goodwood; O_3 levels

were higher on weekends due to lower NO_x levels and lower during the week when vehicular emissions of NO_x levels were elevated.

The geographical location of stations play a crucial role in O_3 concentrations for both short and long term trends. At SANAE and Cape Point background stations, monthly average maxima occur in winter while at Molteno and Goodwood monthly average maxima occur in spring (October or November). Even though the monthly average NO_x and the monthly average O_3 correlation was not significant ($p = 0.202$, $r = 0.501$, $r^2 = 0.255$) at 95% confidence interval, 25.5% of the variation in NO_x corresponds with the variation of O_3. Molteno and Goodwood are affected more by NO_x fluctuations than SANAE and Cape Point.

The 'weekend effect' on O_3 is more evident at Molteno and Goodwood than at SANAE and Cape Point. Current results indicate higher O_3 concentrations on weekends in all the seasons for both stations (Molteno and Goodwood). Although the monthly average correlation between O_3 and monthly average NO_x at Goodwood is not significant, 19.5% of the variation in NO_x corresponds with the variation of O_3 in weekdays relative to only 0.27% on weekends.

Wind speed is important for the interpretation of transportation of pollutants from one region to another. An assessment of NO_x concentrations at different wind speed categories at Goodwood revealed that winds with lower speeds (less than 5m/s) result in higher concentrations of NO_x relative to higher wind speeds (between 10 to 15 m/s). Current findings show lower monthly O_3 averages at higher wind speeds at Molteno and Goodwood. On the other hand, winds with high wind speed show low NO_x concentrations and high O_3 concentrations. At SANAE, Cape Point background and non-background stations there is no significant relationship between monthly O_3 averages and wind speed.

Cape Point background shows a similar long-term O_3 trend to that at SANAE, while Cape Point non-background station reflects the Molteno trend. Goodwood shows increase in O_3 while NO_x concentrations decreased. It is tentatively suggested that Goodwood is a VOC sensitive station but due to the lack of VOC measurements at the station, further investigation needs to be done at a later time when this data is available.

5.3 Limitations of the Study

Nitrogen oxides and other O_3 precursor measurements are critical to understand surface O_3 changes (seasonal fluctuations and long term trends). The absence of NO_x measurents at Molteno during the period of study limits the conclusions that can be drawn from the observed O_3 trends.

5.4 Recommendations

A trend comparison using SANAE data and other polar stations (e.g. Neumayer and South Pole) is recommeneded since the data used by Helming *et al* (2007) was not adequate to investigate long term trends at SANAE.

Cape Point is less impacted by human activities than the Cape Town stations due to prevailing south-westerly winds (from the Atlantic ocean). The observed increasing trend at Cape Point background O_3 is not related to air masses from Cape Town region. Further investigation is required to find out if the observed trend stabilization from 2004 to 2009 is a regional, hemisphical or global phenomenon.

It is further recommended that analyses of O_3 concentrations are conducted at other sites in the Cape Town region (stations under Cape Town provincial government) to allow for further investigation the underlying mechanism involved for spring O_3 maximum. Upper air data temperature data could be useful for determining whether the observed phenomenon is linked to temperature inversions.

To further undertand the decreasing O_3 trend at Molteno and Cape Point non-background data, more detailied investigation and increased monitoring of O_3 precursors is necessary. More work remains to be done in the characterization of regional and hemispheric O_3 trends.

References

Aghedo, A. M., Schultz, M. G. and Rast, S. (2007). The influence of African air pollution on regional and global tropospheric ozone. *Atmospheric Chemistry and Physics* 7, 1193–1212.

Akimoto, H. (2003). Global air quality and pollution. *Science* 302, 1716-1719.

Andreae, M. O. and Merlet, P. (2001). Emission of trace gases and aerosols from biomass burning. *Global Biogeochemical Cycles* 15 (4), 955.

Andreae, M. O. (1991). Biomass burning: Its history, use, and distribution and its impact on environmental quality and global climate, in: Levine, J. (ed.): *Global biomass burning: Atmospheric, climatic, and biospheric implications*, Massachusetts Institute of Technology (MIT) Press, Cambridge, London, 3-21.

Ashmore, R. M. (2005). Assessing the future global impacts of ozone on vegetation. *Plant, Cell and Environment Journal* 28, 949-964.

Ayers, G. P., Granek, H. and Boers, R. (1997). Ozone in the marine boundary layer at Cape Grim: model simulation. *Journal of Atmospheric Chemistry* 27, 179–195.

Baker, A. K., Beyersdorf, A. J., Doezema, L. A., Katzenstein, A., Meinardi, S., Simpson, I. J., Blake, D. R. and Rowland, F. S. (2008). Measurements of nonmethane hydrocarbons in 28 United States cities. *Atmospheric Environment* 42, 170-182.

Barrie, L. A., Bottenheim, J. W., Rasmussen, R. A., Schnell, R. C. and Crutzen, P. J. (1988). Ozone destruction and photochemical reactions at polar sunrise in the lower Arctic troposphere. *Nature* 334, 138–141.

Bhattacharya, S. C. and Salam, P. A. (2002). Low greenhouse gas biomass options for cooking in the developing countries. *Biomass and Bioenergy 22,* 305 – 317.

Benkovitz, C. M., Scholtz, M. T., Pacyna, J., Tarrason, L., Dignon, J., Voldner, E. C., Spiro, P. A., Logan, J. A. and Graedel. T. E. (1996). Global gridded inventories of anthropogenic emissions of sulfur and nitrogen. *Journal of Geophysics Research* 101, 29239-29253.

Bertman, S. B. and Roberts J. M. (1991). A PAN analog from isoprene photo-oxidation. *Geophysical Research Letters* 18, 1461-1464.

Bluestein, H. B. (1993). Synoptic-Dynamic Meteorology in Midlatitudes. Observations and Theory of Weather Systems 2. Oxford University Press, New York, United States of America, 594.

Boersma, K. F., Eskes, H. J., Meijer, E. W. and Kelder, H. M. (2005). Estimates of lightning NOx production from GOME satellite observations. *Atmospheric Chemistry and Physics* 5 (2), 2311–2331.

Bottenheim, J. W., Gallant, A. G. and Brice, K. A. (1986). Measurements of NOy species and O3 at 821 N latitude. *Geophysical Research Letters* 13, 113–116.

Bottenheim, J. W., Sirios, A., Brice, K .A. and Gallant, A. J. (1994). Five years of continuous observations of PAN and ozone at a rural location in eastern Canada. *Journal of Geophysical Research 99,* 5333-5352.

Bradley, K. S., Stedman, D. H. and Bishop, G. A. (1999). A global inventory of carbon monoxide emissions from motor vehicles, Chemosphere. *Global Change Science* 1, 65-72.

Brewer, A. W. (1949). Evidence for a world circulation provided by the measurements of helium and water vapour distribution in the stratosphere. *Quarterly Journal of the Royal Meteorological Society* 75 (326), 351–363.

Brioude, J., Cammas, J. P. and Cooper, O. R. (2006). Stratospheretroposphere exchange in a summertime extratropical low: Analysis. *Atmospheric Chemistry and Physics* 6, 2337–2353. DOI 10.5194/acp-6- 2337-2006.

Brooker, F. L. (2009). The ozone component of global change: potential effects on agricultural and horticultural plant yield, product quality and interactions with invasive species. *Journal of Integrative Plant Biology* 51, 337-351.

Brunke E. G., Mkololo, T., Labuschagne, C. and Scheel, H. E. (2011, September). Ozone Observations at Cape Point (1983-2010) (paper presented at South African Society for Atmospheric Sciences Conference, Pretoria).

Brunke, E. G. and Scheel, H. E. (1998). Surface ozone measurements at Cape Point (341S, 181E), Bojkov, R. D. and Visconti, G. (eds), '*Atmospheric Ozone', Proceedings of the XVIII Quadrennial Ozone Symposium*, L'Aquila, Italy, 12–21 September 1996', pp. 331–334.

Brunke, E. G., Labuschagne, C., Parker, B. and Whittlestone, S. (2004). Baseline air mass selection at Cape Point, South Africa: application of ^{222}Rn and other filter criteria to CO_2. *Atmospheric Environment* 38, 5693-5702.

Brunke E. G, Mkololo, T., Labuschagne, C. and Scheel, H. E. (2009, September).*Analyses of Ozone from three air intake heights at Cape Point* (poster presented at SASAS Conference, Cape Town).

Buzcu, B. and Fraser, M. P. (2006). Source Identification and apportionment of Volatile Organic Compounds in Houston, T X. *Atmospheric Environment* 40, 2385 - 2400.

Calatayud, V., Cervero, J., Calvo, E., Garcia-Breijo, F. J., Reig-Arminana, J. and Sanz, M. J. (2011). Responses of evergreen and deciduous Quercus species to enhanced ozone levels. *Environmental Pollution* 159 (1), 55-63.

Canadell, J. G., Raupach, M. R. and Houghton, R. A. (2008). Anthropogenic CO2 emissions in Africa. *Biogeosciences* 6, 463–468.

Chapman, S. (1930). On ozone and atomic oxygen in the upper atmosphere. *Philosophical Magazine* 10, 369-383.

Choi, Y., Wang, Y. H., Zeng, T., Martin, R. V., Kurosu, T. P. and Chance, K. (2005). Evidence of lightning NOx and convective transport of pollutants in satellite observations over North America. *Geophysical Research Letters* 32 (L02805). DOI 10.1029/2004GL021436.

Cotter, E. S. N., Jones, A. E. and Wolff, et al. (2003). What controls photochemical NO and NO_2 production from Antarctic snow? Laboratory investigation assessing the wavelength and temperature dependence. *Journal of Geophysical Research* 108 (D4), 4147. DOI 10.1029/2002JD002602.

Crutzen, P. J. (1973). A discussion of the chemistry of some minor constituents in the stratosphere and troposphere. *Pure and Applied Geophysics* 106, 108-1385.

Crutzen, P. J. (1974). Photochemical reaction initiated by and influencing ozone in unpolluted tropospheric air. *Tellus* 26, 45-55.

Crutzen, P. J. and Andreae, M. O. (1990). Biomass burning in the tropics: impact on atmospheric chemistry and biogeochemical cycles. *Science* 250, 1669–1678.

Cui, J., Sprenger, M., Staehelin, J., Siegrist, A., Kunz, M., Henne, S. and Steinbacher, M. (2009). Impact of stratospheric intrusions and intercontinental transport on ozone at Jungfraujoch in 2005: Comparison and validation of two Lagrangian approaches. *Atmospheric Chemistry and Physics* 9, 3371–3383.

Dabdub, D., Dehaan, L. L. and Seinfield, J. H. (1999). Analysis of ozone in the San Joaquin Valley of Califonia. *Atmospheric Environment* 33, 2501-2514.

Danielsen, E. F. (1968). Stratospheric-tropospheric exchange based on radioactivity, ozone and potential vorticity. *Journal of Atmospheric Science* 25, 502–518.

Dapeng, X. U., Yap, D. and Taylor, P. A. (1996). Meteologically adjusted ground level ozonetrends in Ontario. *Atmospheric Environment* 30 (7), 1117-1124.

Darrall, N. M. (1989). The effect of air pollutants on physiological processes in plants. P*lant, Cell and Environment* 12, 1-30.

Debaje, S. B. and Kakade, A. D. (2006). Weekend ozone effect over rural and urban site in India. *Aerosol and Air Quality Research* 6, 322–333.

Delmas, R. A., Druilhet, A., Cros, B., Durand, P., Delon, C., Lacaux, J. P., Brustet, J. M., Serca, D., Affre, C., Guenther, A., Greenberg, J., Baugh, W., Harley, P., Klinger, L., Ginoux, P., Brasseur, G., Zimmerman, P. R., Gregoire, J. M., Janodet, E., Tournier, A., Perros, P., Marion, T., Gaudichet, A., Cachier, H., Ruellan, S., Masclet, P., Cautenet, S., Poulet, D., Biona, C. B., Nganga, D., Tathy, J. P., Minga, A., Loemba-Ndembi, J. and Ceccato, P. (1999). Experiment for Regional Sources and Sinks of Oxidants (EXPRESSO). An overview, *Journal of Geophysical Research* 104, 30 609– 30 624.

Delon, C., Galy-Lacaux, C., Boone, A., Liousse, C., Serc¸a, D., Adon, M., Diop, B., Akpo, A., Lavenu, F., Mougin, E. and Timouk, F. (2009). Atmospheric nitrogen budget in Sahelian dry savannas. *Atmospheric Chemistry and Physics Discussion* 9, 14189–14233.

Derwent, R. G. (1995). The estimation of global warming potentials for a range of radiatively active gases. In non-CO2 Greenhouse Gases, Vann Ham, J., Janssen L. J. H. M. and Swart, R. J.(eds), pp. 289-299. Kluwer, Dordrecht.

Domine, F. and Shepson, P. B. (2002). Air snow interactions and atmospheric chemistry. *Science* 297 (5586), 1506-1510.

Domine, F., Albert, M., Huthwelker, T., Jacobi, H.W., Kokhanovsky, A., Lehning, M., Picard, G. and Simpson, W.R. (2008). Snow physics as relevant to snow photochemistry. *Atmospheric Chemistry and Physics*, 8, 171-208.

Domine, F., Albert, M., Huthwelker, T., Jacobi, H. W., Kokhanovsky, A., Lehning, M., Picard, G. and Simpson, W. R. (2008). Snow physics as relevant to snow photochemistry, *Atmospheric Chemistry and Physics*, 8 (2), 171-208.

Edwards, D. P., Lamarque, J. F., Attie, J. L., Emmons, L. K., Richter, A., Cammas, J. P., Lyjak, L. V., Francis, G. L., Gille, J. C. and Drummond, J. R. (2003). Tropospheric ozone over the tropical Atlantic: A satellite perspective. *Journal of Geophysical Research* 108 (D8), 4237. DOI 10.1029/2002JD002927.

Elkus, B. and Wilson, K. R. (1977). Photochemical air pollution: weekend-weekday differences. *Atmospheric Environment* 11, 509-515.

Fenneteaux, I., Colin, P., Etienne, A., Boudries, H., Dutot, A. L., Perros, P. E. and Toupance, G. (1999). Influence of continental sources on oceanic air composition at the eastern edge of the North Atlantic, TOR 1992-1995. *Journal of Atmospheric Chemistry* 32, 233-280.

Finkelstein, J, N. and Johnston, C. J. (2004). Enhanced sensitivity of the postnatal lung to environmental insults and oxidant stress. *Pediatrics* 113, 1092-1096.

Finnan, J. M., Burke, J. I. and Jones, M. B. (1997). An evaluation of indices that describe the impact of ozone on the yield of spring wheat (Triticum aestivum L.). *Atmospheric Environment* 31, 2685–93.

Fiore, A. M., West, J. J., Horowitz, L. W., Naik, V. and Schwarzkopf, M. D. (2008). Characterizing the tropospheric ozone response to methane emission controls and the benefits to climate and air quality. *Journal of Geophysical Research* 113 (D08307). DOI 10.1029/2007JD009162.

Fiscus, E. L., Booker, F. L. and Burkey, K. O. (2005). Crop responses to ozone: uptake, modes of action, carbon assimilation and partitioning. *Plant, Cell and Environment* 28, 997-1011.

Fishman, J., Fakhruzzamen, K., Cros, B. and Nganga, D. (1991). Identification of widespread pollution in the Southern Hemisphere deduced from satellite analyses. *Science* 252, 1693-1696.

Fishman, J., Ramanathan, V., Cruttzen, P. J. and Liu, S. C. (1979a). Tropospheric ozone and climate. *Nature* 282, 818-820.

Fishman, J., Watson, C. E., Larsen, J. C. and Logan, J. A. (1990). Distribution of tropospheric ozone determined from satellite data. *Journal of Geophysical Research* 95 (D4), 3599-3617.

Fumagalli, I., Gimeno, B. S., Velissariou, D., Mills, G., De Temmerman, L. and Fuhrer, J. (2001). Evidence of ozone-induced adverse effects on Mediterranean vegetation. *Atmospheric Environment* 35, 2583-2587.

Ganzeveld, L., Helming, D., Fairall, C. W., Hare, J. and Pozszer, A. (2009). Atmosphere-ocean ozone exchange- A global modeling study of biogeochemical, atmosphere and water-side turbulence dependencies. *Global Biogeochemical Cycles* 23 (GB4021). DOI 10.1029/2008BG003301.

Gimeno, B. S., Peñuelas, J., Porcuna, J. L. and Reinert, R. A. (1995). Biomonitoring ozone phytotoxicity in eastern Spain. *Water Air and Soil Pollution* 85, 1521-1526.

Grewe, V., Brunner, D., Dameris, M., Grenfell, J. L., Hein, R., Shindell, D. and Staehelin, J. (2001). Origin and variability of upper tropospheric nitrogen oxides and ozone at northern midlatitudes. *Atmospheric Environment* 35, 3421-3433.

Haagen-Smit, A. J. (1952). Chemistry and physiology of Los Angeles smog. *Industrial and Engineering Chemistry* 44, 1342–1346.

Han, S., Bian, H., Feng, Y., Liu, A., Li, X., Zeng, F. and Zhang, X. (2011). Analysis of the Relationship between O3, NO and NO2 in Tianjin, China. *Aerosol and Air Quality Research* 11, 128–139.

Hao, W. M. and Liu, M. H. (1994). Spatial and temporal distribution of tropical biomass burning. *Global Biogeochemical Cycles* 8, 495–503.

Hayes, F., Mills, G., Harmens, H. and Norris, D. (2007). Evidence of widespread ozone damage to vegetation in Europe (1990-2006). ICP-Vegetation report. Centre for Ecology and Hydrology. 58. http://icpvegetation.ceh.ac.uk/Reports/Evidence_Report.pdf.

Hayes, F., Williamson, J. and Mills, G. (2012). Ozone pollution affects flower numbers and timing in a simulated BAP priority calcareous grassland community. *Environmental Pollution* 163, 40-47.

Helmig, D., Oltmans, S. J., Carlson, D., Lamarquec, J. F., Jones, A., Labuschagne, C., Anlauf, K. and Hayden, K. (2007). A review of surface ozone in the polar regions. *Atmospheric Environment.* DOI 10.1016/j.atmosenv.2006.09.053.

Holton, J. R. (1992). An Introduction to Dynamic Meteorology, pp. 511, Elsevier, New York, United States of America.

Holton, J. R., Haynes, P. H., McIntyre, M. E., Douglass, A. R., Rood, R. B. and Pfister, L. (1995). Stratosphere-troposphere exchange. *Reviews of Geophysics* 33 (4), 403–439.

Honrath, R. E., Peterson, M. C., Guo, S., Dibb, J. E., Shepson, P. B. and Cambell, B. (1999). Evidence of NOx production within or upon ice particles in the Greenland snowpack. *Geophysical Research Letters* 26 (6), 695-698.

Intergovernmental Panel on Climate Change, Climate Change (2001). The Scientific Basis – Contribution of Working Group I to the Third Assessment Report of the Intergovernmental Panel on Climate Change, Houghton, J. T., Ding, Y., Griggs, D. J., Noguer, M., van der Linden, P. J., Dai, X., Maskell, K. and Johnson, C. A. (eds), pp. 881, Cambridge University Press, New York.

Intergovernmental Panel on Climate Change, Climate Change (2007). The Physical Science Basis, Summary for Policymakers – Contribution of Working Group I to the Fourth Assessment Report of the Intergovernmental Panel on Climate Change, Cambridge University Press, New York.

Jaffe, D. A., Parrish, D., Goldstein, A., Price, H. and Harris, J. (2003). Increasing backgroundozone during spring on the west coast of North America. *Journal of Geophysical Research* 30 (12), 1613. DOI 10.1029/2003GL017024.

Janach, W. E. (1989). Surface ozone: trend details, seasonal variations, and interpretation. *Journal of Geophysical Research* 94, 18289-18295.

Jenkin, M. E., Davies, T. J. and Stedman, J. R. (2002). The Origin and Day-of-Week Dependence of Photochemical Ozone Episodes in the UK. *Atmospheric Environment* 36, 999–1012.

Jourdain, L., Worden, H. M., Worden, J. R., Bowman, K., Li, Q., Eldering, A., Kulawik, S. S., Osterman, G., Boersma, K. F., Fisher, B., Rinsland, C. P., Beer, R. and Gunson, M. (2007). Tropospheric vertical distribution of tropical Atlantic ozone observed by TES during the northern African biomass burning season. *Geophysical Research Letters* 34 (L04810). DOI 10.1029/2006GL028284.

Jury, M., Tegen, A., Ngeleza, E. and Du Toit, M. (1990). Winter air pollution episodes over Cape Town. *Boundary Layer Meteorology* 53, 1 - 20.

Kaleschle, L., Hollwedel, J., Richter, A., Burrows, J., Afe, O., Heygster, G., Notholt, J., Roscoe, H. K., Wolff, E. W. and Yang, X. (2005). Boundary-layer ozone loss near the poles—why spring and not autumn? *Geophysical Research Abstracts* EGU (7), 04916.

Kinney, P. L., Thurston, G, D. and Raizenne, M. (1996). The effects of ambient ozone on lung function in children: A reanalysis of six summer camp studies. *Environmental Health Perspectives* 104 (2), 170-174.

Kirkman, G. A., Piketh, S. l., Andreae, M. O., Annegarn, H. l. and Helas, G. (2000). Distribution of aerosols, ozone and carbon monoxide over southern Africa. *South African Journal of Science* 96, 423-431.

Kruger, A. C., Goliger, A. M., Retief, J. V. and Sekele, S. (2010). Strong wind climatic zones in South Africa. *Wind and Structures* 13 (1), 37-55.

Labrador, L. J., von Kuhlmann, R. and Lawrence, M. G. (2005). The effects of lightning-produced NOx and its vertical distribution on atmospheric chemistry: sensitivity simulations with MATCHMPIC. *Atmospheric Chemistry and Physics* 5, 1815–1834.

Labuschagne, C., Brunke, E. G., Parker, B. and Weller, R. (2003, October). Comparison of first surface ozone measurements from IV, Antarctica with adjacent Neumayer station. (Paper presented at South African Society for Atmospheric Sciences—Nineteenth Annual Conference, Pretoria).

Labuschagne, C., Brunke, E. G. and Scheel, H. E. (2001, October). Long-term observations of trace gases at Cape Point (Paper presented at National Association for Clean Air Conference, Port Elizabeth, South Africa).

Lacis, A. A., Wuebbles, D. J. and Logas, J. A. (1990). Radiative forcing of climate by changes in the vertical distribution of ozone. *Journal of Geophysical Research* 95, 9971-9981.

Lelieveld, J. and Dentener, F. J. (2000). What controls tropospheric ozone? *Journal of Geophysical Research* 105, 3531-3551.

Lemieux, P. M., Lutes, C. C. and Santoianni, D. A. (2004). Emission of organic air toxics from open burning, A Comprehensive review progress in Energy and combustion. *Science* 30, 1-32.

Levy, H. (1971). Normal atmosphere: Large radical and formaldehyde concentrations predicted. *Science* 173, 141–143.

Liu, S. C. M., Trainer, F. C., Fehsenfeld, D. D., Parrish, E. J., Williams, D. W., Fahey, G., Hubler, and Murphy, P. C. (1987). Ozone Production in the Rural Troposphere and the Implications for Regional and Global Ozone Distributions. *Journal of Geophysical. Research* 92, 4191-4207.

Liu, S. and Ridley, B. (1999). Tropospheric ozone. Brasseur, G. P., Orlando, J. J., Tyndall, G. S. (eds), Atmospheric Chemistry and Global Change. Oxford University Press, Oxford, pp. 465–485.

Logan, J. A. (1985). Tropospheric ozone: seasonal behavior, trends, and anthropogenic influence. *Journal of Geophysical Research* 90 (D6), 10463-10482.

Logan, J. A. (1999). An analysis of ozonesonde data for the troposphere: recommendations for testing 3-D models and development of a gridded climatology for tropospheric ozone. *Journal of Geophysical Research* 104, 16115-16149.

Ludwig, J., Meixner, F. X., Vogel, B. and Forstner, J. (2001). Soil-air exchange of nitric oxide: An overview of processes, environmental factors and modeling studies. *Biogeochemistry* 52, 225–257.

Lyons, T., Ploch, M., Turcsany, E. and Barnes, J. (2000). Extracellular antioxidants: a protective screen against ozone? Environmental Pollution and Plant Responses, pp. 183-201, Lewis Publishers, Boca Raton, London, New York, Washington.

Martin, R. V., Sauvage, B., Folkins, I., Sioris, C. E., Boone, C., Bernath, P. and Ziemke, J. (2007). Space-based constraints on the production of nitric oxide by lightning. *Journal of Geophysical Research: Atmospheres* 112 (D09309). DOI 10.1029/2006JD007831.

Marufu, L., Dentener, F., Lelieveld, J., Andreae, M. O. and Helas, G. (2000). Photochemistry of the African troposphere: influence of biomass-burning emissions. *Journal of Geophysical Research* 105 (14), 513–14 530.

Monks, P. S., Carpenter, L. C., Penkett, S. A., Ayers, G. P., Gillett, R. W., Galbally, I. E. and Meyer, C. P. (1998). Fundamental ozone photochemistry in the remote marine boundary: the SOAPEX experiment, measurement and theory. *Atmospheric Environment* 32 (21), 3647-3664.

Morgan, P. B., Mies, T. A., Bollero, G. A., Nelson, R. L. and Long, S. P. (2006). Season-long elevation of ozone concentration to projected 2050 levels under fully open-air conditions substantially decreases the growth and production of soybean. *New Phytologist* 170, 333–343.

National Research Council (1999). Ozone-Forming Potential of Reformulated Gasoline. National Academy Press, Washington.

Newell, R. E. (1963). Transfer through the tropopause and within the stratosphere. *Quarterly Journal of the Royal Meteorological Society* 89 (380), 167–204.

Nightingale, P. D. and Liss, P. S. (2003). Gases in Seawater, In the Oceans and Marine Geochemistry, Elderfield, H. (eds), 3 (6), 49–82.

Olivier, J. G. J. and Berdowski, M. (2001). Global emissions sources and sinks, in The Climate System, Berdowski, J. Guicherit, R. and Heij, B. J. (eds), 33-78.

Olivier, J. G. J., Bouwman, A. F., Vander Maas, C. W. M., Berdowski, J. J. M., Veldt, C., Bloos, J. P. J., Visschedijk, A. J. H., Zandveld, P. Y. J. and Haverlag, J. L. (1996). Description of EDGAR Version 2.0. A set of global emission inventories of greenhouse gases and ozone-depleting substances for all anthropogenic and most natural sources on a per country basis and on 1x1 grid. Report of the RIVM Technical (771060 002) and TNO-MEP (R96/119). National Institute of Public Health and the Environment, Bilthoven.

Oltmans, S. J. and Komhyr, W. D. (1986). Surface ozone distributions and variations from 1973-1984 measurements at the NOAA geophysical monitoring for climatic change baseline observations. *Journal of Geophysical Research* 91, 5229-5236.

Oltmans, S. J. and Levy II, H. (1994). Surface ozone measurements from the global network. *Atmospheric Environment* 28, 9-24.

Paakkonen, E., Metsarinne, S., Holopainen, T. and Karenlampi, L. (1995b). The ozone sensitivity of birch (Betula pendula) in relation to the developmental stage of leaves. *New Phytologist* 132, 145-154.

Palacios-Orueta, A., Parra, A., Chuvieco, E. and Carmona-Moreno, C. (2004). Remote sensing and geographic information systems methods for global spatiotemporal modeling of biomass burning emissions: Assessment in the African continent. *Journal of Geophysical Research* 109, (D14S09). DOI 10.1029/2004JD004734.

Paoletti, E., Contran, N., Bemasconi, P., Gunthrardt-Georg, M. S. and Vollenweider, P. (2009). Structural and physiological responses to ozone in Manna ash (Fraxinus omus L.) leaves of seedlings and mature trees under controlled and ambient conditions. *Science of the Total Environment* 407 (5), 1631-1643.

Penuelas, J., Ribas, A., Gimeno, B. S. and Filella, I. (1999). Dependence of ozone biomonitoring on meteorological conditios of different sites in Catalonia (N.E. Spain). *Environmental Monitoring and Assessment* 56, 221-224.

Pickering, K. E., Wang, Y. S., Tao, W. K., Price, C. and Muller, J. F. (1998). Vertical distributions of lightning NOx for use in regional and global chemical transport models. *Journal of Geophysical Research: Atmospheres* 103, 31 203–31 216.

Pochanart, P., Hirokawa, J., Kajii, Y., Akimoto, H. and Nakao, M. (1999). The influence of regional scale anthropogenic activity in Northeast Asia on seasonal variations of surface ozone and carbon monoxide observed at Oki. Japan. *Journal of Geophysical Research* 104, 3621–3631.

Pretzsch, H. and Dieler, J. (2011). The dependency of the size-growth relationship of Norway spruce (*Picea abies* [L.] Karst.) and European beech (*Fagus sylvatica* [L.]) in forest stands on long-term site conditions, drought events, and ozone stress. *Trees-Structure and Function* 25, 355-369.

Price, C., Penner, J. and Prather, M. (1997). NOx from lightning. Global distribution based on lightning physics. *Journal of Geophysical Research: Atmospheres* 102, 5929–5941.

Pudasainee, D., Sapkota, B., Shrestha, M. L., Kaga, A., Akira Kondo, A. and Inoue, Y. (2006). Ground level ozone concentrations and its association with NOx and meteorological parameters in Kathmandu valley, Nepal. *Atmospheric Environment* 40, 8081–8087.

Pulikesi, M., Baskaralingam, P., Rayudu, V. N., Elango, D., Ramamurthi, V. and Sivanesan, S. (2006). Surface ozone measurements at urban coastal site Chennai, in India. *Journal of Hazardous Materials* B137, 1554–1559.

Raghunandan, A., Mahumane, G. and Diab, R. (2007). Elevated ozone events over Johannesburg based on analysis of tropospheric ozone partial columns. *Research Letters*, *South African Journal of Science* 103, 248-252.

Ramanathan, V. and Dickinson, R. E. (1979). The role of stratospheric ozone in the zonal and seasonal radiation energy balance of the earth troposphere system. *Journal of the Atmospheric Sciences* 36, 1084-1104.

Richards, B. L., Middleton, J. T. and Hewitt, W. B. (1958). Air pollution with relation to agronomic crops: V. Oxidant stipple of grape. *Agronomy Journal* 50, 559-561.

Rodriguez, S. and Guerra, J. C. (2001). Monitoring of ozone in a marine environment in Tenerife (Canary Islands). *Atmospheric Environment* 135, 1829-1841.

Sadanaga, Y., Shibata, S., Hamana, M., Takenaka, N. and Bandow, H. (2008). Weekday/Weekend Difference of Ozone and its Precursors in Urban Areas of Japan, Focusing on Nitrogen Oxides and Hydrocarbons. *Atmospheric Environment* 42, 4708–4723.

Sadanaga, Y., Sengen, M., Takenaka, N. and Bandow, H. (2012). Analyses of the Ozone Weekend effect in Tokyo, Japan: Regime of Oxidant (O3 + NO2) Production. *Aerosol Air Quality Research* 12, 161–168.

Schumann, U. and Huntrieser, H. (2007). The global lightning-induced nitrogen oxides source. *Atmospheric Chemistry and Physics* 7, 3823–3907.

Science Policy Report (2008). Ground level ozone in the 12st century: future trends, impacts and policy implications. The Royal Society, ISBN: 978-0-85403-713-1.

Seiler, W. and Crutzen, P. (1990). Estimates of gross and net fluxes of carbon between the biosphere and the atmosphere from biomass burning. *Climatic Change* 2, 207–247.

Seinfeld, J. H. and Pandis, S. N. (1998). From Air Pollution to Climate Change. *Atmospheric Chemistry and Physics*. Wiley and Sons, New York.

Seinfeld, J. H. and Pandis, S. N. (2006). From Air Pollution to Climate Change. *Atmospheric Chemistry and Physics*. John Willey and Sons, New Jersey.

Shepson, P., Matrai, P., Barrie, L. and Bottenheim, J. (2003). Ocean–atmosphere–sea ice–snowpack interactions in the Arctic, and global change. *Arctic Interactions* 84 (EOS), 349–355.

Shindell, D. T., Faluvegi, G. and Bell, N. (2003). Preindustrial-to-present-day radiative forcing by tropospheric ozone from improved simulations with the GISS chemistry climate GCM. *Atmospheric Chemistry and Physics* 3, 1675-1702. DOI 10.5194/acp-3-1675-2003.

Shutters, S. T. and Balling Jr., R. C. (2006). Weekly periodicity of environmental variables in Phoenix, Arizona. *Atmospheric Environment* 40, 304– 310.

Sillman, S. (1999). The relation between ozone, NOx and hydrocarbons in urban and polluted rural environments. *Atmospheric Environment* 33, 1821-1845.

Simpson, D., Guenther, A., Hewitt, C. N. and Steinbrecher, R. (1995). Biogenic emissions in Europe: estimates and uncertainties. *Journal of Geophysical Research* 100 (D11), 22875-22890.

Sirois, A. and Bottenheim, J. W. (1995). Use of backward trajectories to interpret the 5-year record of PAN and O3 ambient air concentrations at Kejimkujik National Park, Nova Scotia. *Journal of Geophysical Research* 100, 2867-2881.

Solberg, S., Krognes, T., Stordal, F., Hov, O., Beine, H. J., Jaffe, D. A., Chemitshaw, K. C. and Penkett, S. A. (1997). Reactive nitrogen compounds at Spitsbergen in the Norwegian Arctic. *Journal of Atmospheric Chemistry* 28, 113-123.

Sorteberg, A., Hov, O., Solberg, S., Torseth, K., Areskoug, H., Ferm, M., Granby, K., Lattila, H., Persson, K. and Sompson, D. (1998). Gaseous and particulate oxidized and reduced nitrogen species in the atmospheric boundary layer in Scandinavia in spring. *Journal of Atmospheric Chemistry* 30, 241-271.

Swamy, Y. V., Venkanna, R., Nikhil, G. N., Chitanya, D. N. S. K., Sinha, P. R., Ramakrishna, M. and Rao, A. G. (2012). Impact of Nitrogen Oxides, Volatile Organic Compounds and Black Carbon on Atmospheric Ozone Levels at a Semi-Arid Urban Site in Hyderabad. *Aerosol and Air Quality Research* 12, 662–671. DOI 10.4209/aaqr.2012.01.0019.

Tarasova, O. A. and Karpetchko, A. Y. (2003). Accounting for local meteorological effects in the ozone time-series of Lovozero (Kola Peninsula). *Atmospheric Chemistry Physics Discussion* 3, 655–676.

The World Fact Book- CIA (2007), Air Pollution by photochemical oxidants. United States Central Intelligence Agency, Colbeck, I. and Mackenzie, A. R. (eds). *Elsevier, Amsterdam* 232.

Thompson, A. M., Doddridge, B. G., Witte, J. C., Hudson, R. D., Luke, W. T., Johnston, J. E., Johnston, B. J., Oltmans, S. J. and Weller, R. (2000). A tropical Atlantic paradox: Shipboard and

satellite views of a tropospheric ozone maximum and wave-one in January–February 1999. *Geophysical Research Letters* 27, 3317–3320.

Thompson, A. M., Witte, J. C., Hudson, R. D., Guo, H., Herman, J. R. and Fujiwara, M. (2001). Tropical tropospheric ozone and biomass burning. *Science* 291, 2128–2132.

Tie, X., Zhang, R., Brasseur, G. and Lei, W. (2002). Global NOx Production by Lightning. *Journal of Atmospheric Chemistry* 43, 61-74.

Treshow, M. and Stewart, D. (1973). Ozone sensitivity of plants in natural communities. *Biology and Conservation* 5 (3), 209-214.

Tyson, P. D., Kruger, F. J. and Louw, C. W. (1988). Atmospheric pollution and its implications in the Eastern Transvaal Highveld, South African National Scientific Programmes, Report of the Foundation for Research and Development (150), Pretoria, 39.

Van der A, R. J., Eskes, H. J., Boersma, K. F., van Noije, T. P. C., van Roozendael, M., De Smedt, I., Peters, D. H. M. U. and Meijer, E. W. (2008). Trends, seasonal variability and dominant NOx source derived from a ten year record of NO2 measured from space. *Journal of Geophysics Research* 113, (D04302). DOI 10.1029/2007JD009021.

Van der Werf, G. R., Randerson Collatz, G. J. and Giglio, L. (2003). Carbon emission from fires in 30 tropical and subtropical ecosystems. *Global Change Biology* 9, 547–562.

Van der Werf, G. R., Randerson, J. T., Giglio, L., Collatz, G. J., Kasibhatla, P. S. and Arellano Jr., A. F. (2006). Interannual variability in global biomass burning emissions from 1997 to 2004. *Atmospheric Chemistry and Physics* 6, 3423–3441.

Vingarzan, R. (2004). A review of surface ozone background levels and trends. *Atmospheric Environment* 38, 3431- 3442.

Volz, A. and Kley, D. (1988). Evaluation of the Montsouris series of ozone measurements made in the nineteenth century. *Nature* 332, 240-242.

Wallington, T. J., Sullivan, J. L. and Hurley, M. D. (2008). Emissions of CO2, CO, NOx, HC, PM, HFC-134a, N2O and CH4 from the global light duty vehicle fleet. *Meteorologische Zeitschrift* 17 (2), 109-116.

Walton, N. (2005). Characterisation of Cape Town Brown Haze. MSc Dissertation, University of Witwatersrand.

Wang, Y., Jacob, D. J. and Logan, J. A. (1998). Global simulation of tropospheric O3-NOx-hydrocarbon chemistry. Origin of tropospheric ozone and effects on non-methane hydrocarbons. *Journal of Geophysical Research* 103 (10), 757–768.

Warneke, C., McKeen, S. A., de Gouw, J. A., Goldan, P. D., Kuster, W. C., Holloway, J. S., Williams, E. J., Lerner, B. M., Parrish, D. D., Trainer, M., Fehsenfeld, F. C., Kato, S., Atlas, E. L., Baker, A. and Blake, D. R. (2007). Determination of urban volatile organic compound emission ratios and comparison with an emissions database. *Journal of Geophysical Research* 112 (D10S47). DOI 10.1029/2006JD007930.

Weller, R., Jones, A. E., Wille, A., Jacobi, H. W., McIntyre, H. P., Sturges, W. T., Huke, M. and Wagenbach, D. (2002). Seasonality of reactive nitrogen oxides (NOy) at Neymayer stations, Antarctica. *Journal of Geophysical Research* 107 (D23), 4673, DOI 10.1029/2002JD002495.

West, J. J., Fiore, A. M., Naik, V., Horowitz, L. W., Schwarzkopf, M. D. and Mauzerall, D. L. (2007a). Ozone air quality and radiative forcing consequences of changes in ozone precursor emissions. *Geophysical Research Letters* 34 (L06806). DOI 10.1029/2006GL029173.

Wichmann, J. (2006). Seasonal inter-site correlation among air pollution monitoring sites in Cape Town, Dissertation, University of Pretoria.

Wicking-Baird, M. C., de Villiers, M. G and Dutkiewicz R. K. (1997). Cape Town Brown Haze Study. Report of Energy Research Institute (182), Cape Town.

Wild, O., Prather, M. J. and Akimoto, H. (2001). Indirect long-term global radiative cooling from NO_x emissions. *Geophysical Research Letters* 28, 1719–1722.

Wittig, V. E., Ainsworth, E. A., Naidu, S. L., Karnosky, D. F. and Long, S. P. (2009). Quantifying the impact of current and future tropospheric ozone on tree biomass, growth, physiology and biochemistry: a quantitative meta-analysis. *Global Change Biology* 15, 396-424.

Zachariasse, M., van Velthoven, P. F. J., Smit, H. G. J., Lelieveld, J., Mandal, T. K. and Kelder, H. (2000). Influence of stratosphere-troposphere exchange on tropospheric ozone over the tropical Indian Ocean during the winter monsoon. *Journal of Geophysical Research* 105 (15), 403- 416.

Zhang, R. Y., Tie, X. X. and Bond, D. W. (2003). Impacts of anthropogenic and natural NOx sources over the U.S. on tropospheric chemistry. *Proceedings of the National Academy of Sciences of the United States of America* 100, 1505–1509.

Zunckel, M., Raghunandan, A., Venjonoka, K., Pienaar, J .J., Snow, N., Brunke, E. G., Bundi, P. and van Tienhoven, M. A. (2004). Surface Ozone over southern Africa: Synthesis of monitoring results during the CAPIA project. *Atmospheric Environment* 38, 36, 6142.

http://earthobservatory.nasa.gov/IOTD/view.php?id=9060.

http://web1.capetown.gov.za/web1/NewCityAirpol/.

http://web1.capetown.gov.za/web1/NewCityAirpol/monsites.asp.

http://www.crh.noaa.gov/lmk/soo/presentations/Lightning_WFO_LMK.pdf.

http://www.ecophotoexplorers.com/antarcticastations.asp#map1.

http://www.epa.gov/climateleadership/documents/resources/mobilesource_guidance.pdf.

http://www.gfdl.noaa.gov/brian-magi-homepage.

http://www.grabovrat.com/mapsViews/mapsViews80.html.

http://www.sanap.org.za/sanap SANAE/SANAE life at base.html.

http://www.scar.org/information.

http://www.srh.noaa.gov/jetstream/global/jet.htm.

http://www.unece.org/fileadmin/DAM/env/lrtap/ExecutiveBureau/Air.Pollution%20Studies.No.1
6.Hemispheric%20Transport.pdf.